

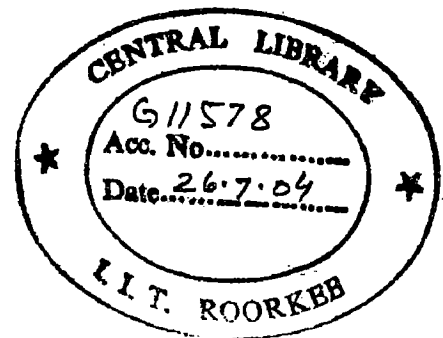
DESIGN OF DEPRESSED WEIR ON PERMEABLE FOUNDATION WITH A DOWNSTREAM CONCRETE CUTOFF

A DISSERTATION

*Submitted in partial fulfillment of the
requirements for the award of the degree*
of
MASTER OF TECHNOLOGY
in
**WATER RESOURCES DEVELOPMENT
(CIVIL)**

By

GIR BAHADUR K.C.



WATER RESOURCES DEVELOPMENT TRAINING CENTRE
INDIAN INSTITUTE OF TECHNOLOGY ROORKEE
ROORKEE - 247 667 (INDIA)
JUNE, 2004

11

CANDIDATE'S DECLARATION

I hereby declare that the dissertation titled "**DESIGN OF DEPRESSED WEIR ON PERMEABLE FOUNDATION WITH A DOWNSTREAM CONCRETE CUTOFF**" which is being submitted in partial fulfillment of the requirement for the award of Degree of **Master of Technology in Water Resources Development** at Water Resources Development Training Center (WRDTC), Indian Institute of Technology, Roorkee is an authentic record of my own work carried out during the period of 1-06-2003 to 30-06-2004 under the supervision and guidance of **Dr. G.C. Mishra, Professor**, WRDTC IIT, Roorkee.

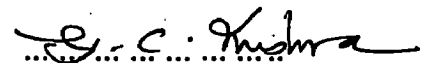
I have not submitted the matter embodied in this dissertation for the award of any other degree.

Place: Roorkee.

Dated: 30-6-2004


.....
Gir Bahadur K.C.

This is to certify that the above statement made by the candidature is correct to the best of my knowledge.



Dr. G.C. Mishra

Professor, WRDTC

IIT, Roorkee

Roorkee-247667, (India)

ACKNOWLEDGEMENT

I take this opportunity to express my profound sense of gratitude and grateful regards to **Dr. G.C. Mishra**, Professor, WRDTC, Indian Institute of Technology, Roorkee for his intelligent, endowed and inspiring guidance, constant encouragement and persuasion and ceaseless help during the period of preparing this dissertation work.

I am greatly thankful to **Prof. U.C. Chaube** Prof.& Head of WRDTC, IIT Roorkee for extending various facilities in completion of this dissertation.

I am also grateful to the staff of WRDTC who extended all cooperation whenever required. I am thankful to all the staffs of computer lab and computer center for helping me in analyzing the data through computer. I am also thankful to the Librarians for providing help in time.

I wish to express my thanks to Department of Irrigation, Ministry of Water Resources, His Majesty's Government of Nepal for giving me an opportunity to undergo M.Tech. Course at IIT Roorkee.

I cannot forget to express my profound gratitude and indebtedness to my parents. I, also wish to record my love and affection to my wife Parbata K.C. and my kids who extended their full moral support and encouraged me throughout the course of my study.

It would be unworthy, if I don't express my cordial thanks to my friend Mr. Tek Bahadur Karki for his suggestion and guidance in running the program and all my friends of the class who help in preparing this work.

Financial assistance provided by Govt. of India under ITEC program during the M.Tech. Course in WRD (civil) at IIT Roorkee is also highly acknowledged.

Place: Roorkee

Gir Bahadur K.C.

Dated: JUNE-2004

SYNOPSIS

A weir is constructed across a river to divert flow into a man made channel satisfying all possibilities of surface and sub-surface flow considerations. The surface flow consideration decides the crest level, downstream floor length, minimum depth of cutoff /sheet pile for the upstream and downstream end of floor. The maximum depth of cutoff/sheet pile depends upon the design flood. The effect of sub-surface flow is considered in respect of the uplift pressures of the percolating water acting on the bottom of the floor and the exit gradient and hence safety of the structure against piping. The total weir floor length is determined in relation to the downstream cutoff/sheet pile depth in order to satisfy exit gradient criteria. These parameters, cutoff/sheet pile depths and floor length, govern the uplift pressure at different points under the floor. These uplift pressures are counter acted by the floor thickness.

Structures built on pervious soil, little resistance may be offered by the soil and percolation may reach the downstream toe of the structure without any substantial loss of head. In such situation the percolating water may carry soil particles with it and thus undermine the structure. This is called piping. The sub-soil flow below weirs along with the hydraulic gradients and uplift-pressures has been widely recognised as the determining factor in the design of a weir on permeable foundation after the classic experiments that have been carried out by Lt. Col.Clibborns, Principal Thomson Engineering College, Roorkee, to Khanki weir in 1895, with a tube 36.6m long and 8.6m diameter filled with Khanki sand. These experiments confirmed the accuracy of Darcy's law regarding subsoil flow except under high heads. As a result of Col.Clibborns experiments in 1902, the hydraulic gradient theory came to be generally accepted in India.

Later Bligh (1907) went a step forward and presumed that the percolation water creeps along the contact of base profile of the structure with subsoil and losses head in proportion to the creep distance.

E.W. Lane (1935), after analyzing a large number of dams and weirs both with failures and non failures, brought out deficiencies in Bligh theory .He propounded a new theory on statistical basis which is known as Lane's weighted creep theory.

Investigations carried out by Dr.A.N.Khosla on the then existing weirs led to the rational solution to the problem of sub-surface flow at the Punjab Irrigation Research Institute.

The results have been published in publication No.12 of CBIP (Central Board of Irrigation and Power) India, NewDelhi.

These developments took place with special reference to weirs on permeable foundations but are applicable to all hydraulic structures on alluvial soils.

Weirs on permeable foundation are designed to safeguard against uplift pressure and piping. The flow characteristics are determined assuming the flow to be two dimensional and steady. For non-homogeneous sub-soil, numerical method is used to solve the two dimensional equation satisfying the boundary conditions.

For homogeneous, isotropic soil, the Laplace equation can be solved analytically using conformal mapping technique.

Using the Schwartz-Christoffel conformal mapping technique, Khosla et.al. (1936) have obtained analytical solutions for a stepped weir with a sheet pile provided at the step, resting on a homogeneous, isotropic porous medium of infinite depth. They have neglected the depression so as to reduce the number of vertices to arrive at a simple solution and suggested a correction factor to account for the depression.

Present study is undertaken to find an analytical solution which can quantify uplift pressure below the floor of depressed weir with downstream concrete cutoff and to prepare a comprehensive comparison of the values of uplift pressure with that obtained, by using the equation of Khosla et.al.(1936) in case of sheet pile. It is also expected to see the effects due to increase in the thickness of concrete cutoff. The comparison is to be carried for weirs with depression and with cutoff at various positions. It is proposed to compare for the following hydraulic structures:

- I. Depressed weir with concrete cutoff downstream.
- II. Depressed weir with concrete cutoff upstream.
- III. Depressed weir with concrete cutoff positioned at various options.

In this dissertation, an analytical solution for the flow around a depressed weir with a concrete cutoff at the downstream end, upstream end and cutoff position at different options has been obtained using the Schwartz-Christoffel conformal mapping technique where many non linear equations are derived.

Since the integrals are improper, Gaussian-Quadrature method of substitution has been used to remove the singularities of the integrals. Newton Raphson technique has been used to find the solution. The solution of Jacobian Matrix is done by using FORTRAN program.

From the study it is found that:

- 1) It is possible to solve two dimension flow under a hydraulic structure which has more number of vertices. Solution to flow under a depressed weir with concrete cutoff has been given. The conformal mapping transformation parameters have been computed conveniently using Newton-Raphson technique.
- 2) Khosla's approximate correction to account for depression may lead to uneconomical and unsafe design. Using the solution given in this study uplift pressure can be computed exactly at any point.
- 3) A depression on downstream is more advantageous than that in upstream side; a depressed floor acts as a sheet pile and controls the exit gradient.

Contents	PageNo
CANDIDATE'S DECLARATION	i
ACKNOWLEDGEMENT	ii
SYNOPSIS	iii
CONTENTS	vi
LIST OF TABLES	viii
LIST OF FIGURES	xi
LIST OF SYMBOLS	xv
CHAPTER 1	1
Introduction	1
1.1 General	1
1.2 Background	3
1.3 Need for further studies	4
1.4 Scope of present study	4
1.5 Objectives of Present Study	4
CHAPTER 2	6
Literature Review	6
2.1 General	6
2.2 Approximate Method for Accounting Depression:	6
2.3 Condition and Methods of Conformal Transformation	8
2.4 Analytical Method for Accounting Depression	9
2.5 Conclusion	9
CHAPTER 3	10
Analysis	10
3.1 General	10
3.2 Statement of the Problem	10
3.3 Analysis	10
3.3.1 Weir with downstream concrete cutoff.	10
3.3.2 Weir with an upstream concrete cutoff.	15
3.3.3 Weir with cutoff at any position along the floor	18
3.3.4 Mapping of w - plane onto lower half of t - plane:	23

Contents	PageNo
3.4 The Pressure Distribution	25
3.5 The Exit Gradient	27
CHAPTER 4	29
Tabulation and Plotting of Results	29
4.1 Depressed Weir With Concrete Cutoff Downstream	29
4.2 Depressed Weir With Concrete Cutoff Upstream	46
4.3 Comparison in the Potential Variation (Weir with cutoff at any position along the floor) with the sheet pile.	58
4.4 Exit Gradient Curves for Different Cases	67
CHAPTER 5	75
Results, Discussion and Conclusion	75
5.1 Variation of Potential Distribution with Concrete Cutoff toe	75
5.2 Variation of Potentials Distribution with Concrete Cutoff Upstream	78
5.3 Potential variation at the key points for the depressed weir with Concrete cutoff at different points of the floor	81
5.4 Exit Gradient	87
5.5 Conclusion	88
Appendix-I	90
Appendix- II	94
Appendix-III	96
References	

List of Tables	Page No.
1. Table 4.1.1 Variation of potential distribution with increasing thickness of cutoff for depressed weir with concrete cutoff (d/s)	29
2. Table 4.1.2 Variation of potential distribution with increasing thickness of cutoff for depressed weir with concrete cutoff (d/s)	31
3. Table 4.1.3 Variation of potential distribution with increasing thickness of cutoff for depressed weir with concrete cutoff (d/s)	33
4. Table 4.1.4 Potential distribution with increasing cutoff depth of depressed weir with concrete cutoff (d/s)	35
5. Table 4.1.5 Potential distribution with increasing cutoff depth of depressed weir with concrete cutoff (d/s)	37
6. Table 4.1.6 Potential distribution with increasing cutoff depth of depressed weir with concrete cutoff (d/s)	38
7. Table 4.1.7 Variation of potential distribution with increasing depression for depressed weir with d/s concrete cutoff	40
8. Table 4.1.8 Variation of potential distribution with increasing depression for depressed weir with concrete cutoff (d/s)	41
9. Table 4.1.9 Potential variation at the key point with increasing u/s and d/s depression respectively	43
10. Table 4.2.1 Variation of potential distribution with increasing thickness of cutoff for depressed weir with concrete cutoff (u/s)	46
11. Table 4.2.2 Variation of potential distribution with increasing thickness of cutoff for depressed weir with concrete cutoff (u/s)	48
12. Table 4.2.3 Variation of potential distribution with increasing depth of cutoff for depressed weir with concrete cutoff (u/s)	50
13. Table 4.2.4 Variation of potential distribution with increasing depression for depressed weir with u/s concrete cutoff	52
14. Table 4.2.5 Variation of potential distribution with increasing depression for depressed weir with u/s concrete cutoff	53
15. Table 4.2.6 Potential variation at the key point with increasing u/s and	55

d/s depression respectively

16. Table 4.3.1 Potential variation at point 'D' for different case B/S=5,30 and B/T=10	58
17. Table 4.3.2 Potential variation at point 'F' for different case B/S=5,30 and B/T=10	59
18. Table 4.3.3 Potential variation at point 'G' for different case B/S=5,30 and B/T=10	61
19. Table 4.3.4 Potential variation at point 'D' for different case B/S=5,30 and B/T=20	62
20. Table 4.3.5 Potential variation at point 'F' for different case B/S=5,30 and B/T=20	64
21. Table 4.3.6 Potential variation at point 'G' for different case B/S=5,30 and B/T=20	65
22. Table 4.4.1 Exit Gradient calculation equal depression u/s and d/s	67
23. Table 4.4.2 Exit Gradient Calculation for Unequal Depression u/s and d/s	71
24. Table 5.1.1 Variation in ϕ_D and ϕ_E with variation of T/B concrete cutoff d/s	75
25. Table 5.1.2 Variation ϕ_D and ϕ_E with variation of S/B concrete cutoff d/s	76
26. Table 5.1.3 Variation in ϕ_D and ϕ_E with variation of D/B concrete cutoff d/s	77
27. Table 5.1.4 Variation in ϕ_D and ϕ_E with variation of D₁/B and D₂/B concrete cutoff d/s	78
28. Table 5.2.1 Variation in ϕ_D and ϕ_E with variation of T/B concrete cutoff u/s	79
29. Table 5.2.2 Variation in ϕ_D and ϕ_E with variation of S/B concrete cutoff u/s	79
30. Table 5.2.3 Variation in ϕ_D and ϕ_E with variation of D/B concrete cutoff u/s	80
31. Table 5.2.4 Variation in ϕ_D and ϕ_E with variation of D₁/B and D₂/B concrete cutoff u/s	80
32. concrete cutoff u/s	
33. Table 5.3.1 Deviation in % for Φ_D with respect to Khosla's values	82

34. Table 5.3.2 Deviation in % for Φ_G with respect to Khosla's values	83
35. Table 5.3.3 Differences in velocity potential Φ_D, Φ_F and Φ_G with changing cutoff position from upstream end of floor to downstream end of floor for $B/S=5,30$ and $B/T=10,20$.	83
36. 5.3.4 Floor length with respect to equal depression	88
37. Table 5.3.5 Floor length with respect to unequal depression	88

List of Figures	Page No.
1. Figure 1.5.1 Depressed weir with concrete cutoff downstream	5
2. Figure 1.5.2 Depressed weir with concrete cutoff upstream	5
3. Figure 1.5.3 Depressed weir with concrete cutoff positioned at various options	5
4. Figure 1.5.4 Depressed weir without concrete cutoff	5
5. Figure 2.1.1 Two dimensional steady of flow	6
6. Figure 2.2.1 Depressed weir	7
7. Figure 3.3.1 a) Physical Domain in z-plane for downstream concrete cutoff	11
8. Figure 3.3.1 (b) Physical Domain Mapped onto t-plane boundaries for d/s cutoff	11
9. Figure. 3.3.2(a) Physical Domain in z-plane for u/s cutoff	14
10. Figure 3.3.2(b) : Physical Domain Mapped onto t-plane boundaries for u/s cutoff	15
11. Figure. 3.3.3 (a) Physical Domain in z-plane for varying cutoff position	18
12. Figure 3.3.3 (b) : Physical Domain Mapped onto t-plane boundaries for varying cutoff position	18
13. Figure 3.3.4 (a) ω -plane for variation of cutoff position	23
14. Fig 3.3.4 (b) ω -plane for downstream cutoff	25
15. Figure 4.1.1 (a) Variation of ϕ_D with increasing cutoff thickness (d/s)	30
16. Figure 4.1.1 (b) Variation of ϕ_E with increasing cutoff thickness (d/s)	30
17. Figure 4.1.2 (a) Variation of ϕ_D with increasing cutoff thickness (d/s)	32
18. Figure 4.1.2 (b) Variation of ϕ_E with increasing cutoff thickness (d/s)	32
19. Figure 4.1.3 (a) Variation of ϕ_D with increasing cutoff thickness (d/s)	34
20. Figure 4.1.3 (b) Variation of ϕ_E with increasing cutoff thickness (d/s)	35
21. Figure 4.1.4 (a) Variation of ϕ_D with increasing cutoff depth (d/s)	36
22. Figure 4.1.4 (b) Variation of ϕ_E with increasing cutoff depth (d/s)	36
23. Figure 4.1.5 (a) Variation of ϕ_D with increasing cutoff depth (d/s)	37
24. Figure 4.1.5 (b) Variation of ϕ_E with increasing cutoff depth (d/s)	38
25. Figure 4.1.6 (a) Variation of ϕ_E with increasing cutoff depth (d/s)	39
26. Figure 4.1.6 (b) Variation of ϕ_D with increasing cutoff depth (d/s)	39
27. Figure 4.1.7(a) Variation of ϕ_D with increasing depression	40

28. Figure 4.1.7(b) Variation of ϕ_E with increasing depression	41
29. Figure 4.1.8 (a) Variation of ϕ_D with increasing depression	42
30. Figure 4.1.8 (b) Variation of ϕ_E with increasing depression	42
31. Figure 4.1.9 (a) Variation of ϕ_D with increasing u/s depression	44
32. Figure 4.1.9 (b) Variation of ϕ_D with increasing d/s depression	44
33. Figure 4.1.9 (c) Variation of ϕ_E with increasing u/s depression	45
34. Figure 4.1.9 (d) Variation of ϕ_E with increasing d/s depression	45
35. Figure 4.2.1(a) Variation of ϕ_D with increasing cutoff thickness (u/s)	47
36. Figure 4.2.1(b) Variation of ϕ_E with increasing cutoff thickness (u/s)	47
37. Figure 4.2.2 (a) Variation of ϕ_D with increasing cutoff depth (u/s)	49
38. Figure 4.2.2 (b) Variation of ϕ_E with increasing cutoff depth (u/s)	49
39. Figure 4.2.3 (a) Variation of ϕ_D with increasing cutoff depth (u/s)	51
40. Figure 4.2.3 (b) Variation of ϕ_E with increasing cutoff depth (u/s)	51
41. Figure 4.2.4(a) Variation of ϕ_D with increasing depression	52
42. Figure 4.2.4(b) Variation of ϕ_E with increasing depression	53
43. Figure 4.2.5(a) Variation of ϕ_D with increasing depression	54
44. Figure 4.2.5(b) Variation of ϕ_E with increasing depression	54
45. Figure 4.2.6 (a) Variation of ϕ_D with increasing u/s depression	56
46. Figure 4.2.6 (b) Variation of ϕ_E with increasing u/s depression	56
47. Figure 4.2.6 (c) Variation of ϕ_E with increasing d/s depression	57
48. Figure 4.2.6 (d) Variation of ϕ_E with increasing d/s depression	57
49. Figure 4.3.1 (a) Variation of ϕ_D at B/S=5 and B/T=10 for different cases	58
50. Figure 4.3.1 (b) Variation of ϕ_D at B/S=30 and B/T=10 for different cases	59
51. Figure 4.3.2 (a) Variation of ϕ_F at B/S=5 and B/T=10 for different cases	60
52. Figure 4.3.2 (b) Variation of ϕ_F at B/S=30 and B/T=10 for different cases	60
53. Figure 4.3.3 (a) Variation of ϕ_G at B/S=5 and B/T=10 for different cases	61
54. Figure 4.3.3 (b) Variation of ϕ_G at B/S=30 and B/T=10 for different cases	62
55. Figure 4.3.4 (a) Variation of ϕ_D at B/S=5 and B/T=20 for different cases	63

	Page No.
56. Figure 4.3.4 (b) Variation of ϕ_D at B/S=30 and B/T=20 for different cases	63
57. Figure 4.3.5 (a) Variation of ϕ_F at B/S=5 and B/T=20 for different cases	64
58. Figure 4.3.5 (b) Variation of ϕ_F at B/S=30 and B/T=20 for different cases	65
59. Figure 4.3.6 (a) Variation of ϕ_G at B/S=5 and B/T=20 for different cases	66
60. Figure 4.3.6 (b) Variation of ϕ_G at B/S=30 and B/T=20 for different cases	66
61. Figure 4.4.1 (a) Exit Gradient Curve for D/S=0.20 and T/S=0.20	68
62. Figure 4.4.1 (b) Exit Gradient Curve for D/S=0.20 and T/S=0.60	69
63. Figure 4.4.1 (c) Exit Gradient Curve for D/S=0.40 and T/S=0.20	69
64. Figure 4.4.1 (d) Exit Gradient Curve for D/S=0.40 and T/S=0.60	70
65. Figure 4.4.1 (e) Exit Gradient Curve for D/S=0.60 and T/S=0.20	70
66. Figure 4.4.1 (f) Exit Gradient Curve for D/S=0.80 and T/S=0.80	71
67. Figure 4.4.2 (a) Exit Gradient Curve for D₁/S=0.40, D₂/S=0.10 and T/S=0.20	72
68. Figure 4.4.2 (b) Exit Gradient Curve for D₁/S=0.40, D₂/S=0.10 and T/S=0.40	72
69. Figure 4.4.2 (c) Exit Gradient Curve for D₁/S=0.60, D₂/S=0.10 and T/S=0.40	73
70. Figure 4.4.2 (d) Exit Gradient Curve for D₁/S=0.10, D₂/S=0.60 and T/S=0.40	73
71. Figure 4.4.2 (e) Exit Gradient Curve for D₁/S=0.10, D₂/S=0.60 and T/S=0.60	74
72. Exit Gradient Curve (sheet pile)	74
73. Figure 5.1.1 Depressed weir with concrete cutoff downstream	75
74. Figure 5.2.1 Depressed weir with concrete cutoff upstream	78
75. Figure 5.3.1 Variation of concrete cutoff at different point of the horizontal floor	81
76. Figure 5.3.2 Variation of sheet pile at different point of the horizontal floor	81
77. Figure 5.3.3 Variation of Potential difference Φ_G for constant cutoff thickness with variation of cutoff depth	85
78. Figure 5.3.4 Variation of Potential difference Φ_D for constant cutoff thickness with variation of cutoff depth	86
79. Figure 5.3.5 Variation of Potential difference Φ_F for constant cutoff thickness with variation of cutoff depth	87

List of Figures**Page No.**

-
- | | |
|---|----|
| 80. Figure A-1 Streamlines for flat base weirs on surface | 91 |
| 81. Figure A-2 Physical domain in Z -plane | 91 |
| 82. Figure A-3 Physical domain mapped on t -plane | 92 |

List of Symbols

d/s =Downstream

u/s=Upstream

ϕ_C = Velocity Potential at point C

ϕ_D = Velocity Potential at point D

ϕ_E = Velocity Potential at point E

ϕ_F = Velocity Potential at point F

ϕ_G = Velocity Potential at point G

M, N, M_1, N_1 Complex constants B =Length of horizontal floor

T = Thickness of cutoff

S =Depth of cutoff

D =Depression

D_1 =u/s depression

D_2 =d/s depression

h =Difference of u/s and d/s water level

i = Complex imaginary number

γ_w =Unit weight of water

P_C =Pressure at point C

P_D =Pressure at point D

P_E =Pressure at point E

P_F =Pressure at point F

P_G =Pressure at point G

I_E =Exit gradient

K =Hydraulic conductivity

ϕ = Velocity potential function

ψ =Stream function

CHAPTER 1

INTRODUCTION

1.1 General

The art of constructing weir across rivers to divert the flow for irrigation purpose is quite old. Some weirs constructed in 19th century are still serving their purpose, while some have been renovated or reconstructed. In such structures the water way was generally kept equal to the width of the river. History of these works indicates that their maintenance was generally problematic due to shoaling formation on the upstream and meandering of the river. On such works a complex river training works got developed, which suggests that an artificial narrowing of waterway can be done with advantage. It was also felt that it would improve the performance of the barrage and was adopted at works constructed during 20th century.

However, too much narrowing of water way may not be desirable and economical as a high afflux can lead to deep cistern with heavy excavation and long afflux bunds. Thus there is clear need to evolve a methodology to determine optimal waterway.

On the basis of such experience on existing works some guidelines have been laid to fix the waterway of weirs and barrages such as:

- i) Lacey's waterway = $4.83Q^{1/2}$ m where Q is design discharge in cumecs
- ii) Discharge intensity of 30 to 32 cumecs/m for boulder reaches
- iii) Discharge intensity of 22 to 27 cumecs/m for alluvial reaches

From the sub-surface flow, there are two forces that weirs have to withstand, firstly, the residual pressure, which will tend to lift up the weir floor if the weight on the latter is less than the upward pressure of water at that point, and secondly, the pressure gradient or the force of water acting along the direction of flow. This latter is of no moment except at the tail end where the water emerges from the sub-soil. If at this end upward force of water is in excess of the restraining force of the sub-soil, viz, weight, internal friction, etc., the surface soil will be lifted up followed by progressive disruption of that further down. This may result in undermining of the foundation soil and ultimate failure of the structure.

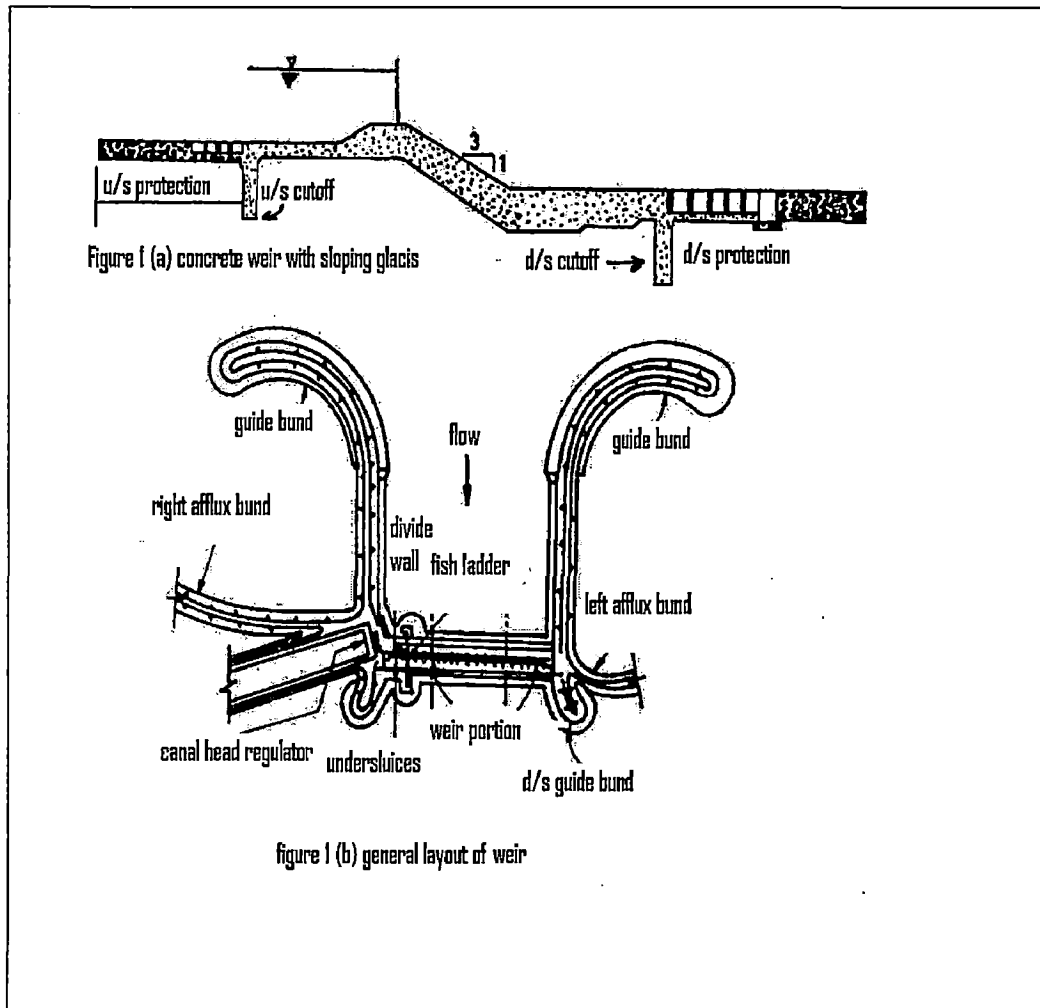


Figure 1.1 Typical drawing of a weir

The two essentials to be considered in weir design, therefore, are:

- i) Residual head or uplift pressure on the weir floor
- ii) Exit gradients

These two essentials are inter-connected. For any given foundation profile of a weir in a given class of soil, there will be a definite distribution of pressure and a definite exit gradient. To safeguard against undermining, the exit gradient must not be allowed to exceed a certain safe limit, generally $1/5$ to $1/7$. The uplift pressure must be kept as low as possible, consistent with safety at the exit, so as to keep the floor thickness at a minimum. Since ancient times in irrigation engineering, weirs remain as the most extensively used control structures for the diversion of flow and flow measurement. Though the types and shapes of weirs differ from place to place, depending on the available materials for construction, sub-soil condition and hydrology of the river, they are provided with one or more sheet piles when constructed in alluvial soils. Weirs are designed to satisfy the

surface and subsurface flow considerations. Where as the surface flow considerations decide the crest level, down stream floor length and minimum depths of upstream and downstream sheet-pile/cut-off, the sub-surface flow considerations at the maximum ponding condition require more attention to protect the structure against heaving, roofing, piping and uplift. The parameters i.e. sheet-pile depth and floor length influence the uplift pressure at different points under the floor. The uplift pressures are counteracted by the floor thickness. A weir generally consists of either a horizontal or sloping floor with sheet piles.

The sheet-pile/cutoff in the upstream is provided to reduce the uplift pressures under the floor and to cutoff the seepage-lines through permeable upper layers where as the provision of a down stream sheet-pile/cutoff raises the uplift pressures under the floor. A downstream sheet-pile/cutoff is necessary from scour consideration as well as to keep the exit gradient below the safe limit. This helps in mitigating the piping below the floor. The depression of the floor can replace the need of a sheet pile/cutoff to certain extent.

1.2 Background

The sub-soil flow below weirs along with the hydraulic gradients and uplift-pressures has been widely recognized as the determining factor in the design of a weir on permeable foundation after the classic experiments that have been carried out by Col.Clibborns, Principal of Thomson Civil Engineering College, Rookies in connection with the failure of Khanki Weir, in India during 1895-97. It was then concluded and accepted eventually by all over that the subject of subsurface flow is more complex than what the Bligh's creep theory indicated.

In 1936 Rai Bahadur A.N.Khosla, ISE presented a note on the observations and records of pressures below works on permeable foundations in publication No.8 of Central Board of Irrigation and Power.

Khosla et.al have analysed the flow under a stepped weir considering it to be resting on the surface of a porous medium of infinite depth. They have presented design charts, which are extensively used by the field engineers.

1.3 Need for further studies

As Khosla's concept of barrage or weir design for subsurface flow (Khosla et.al.1936) is based on the assumption that the thickness of floor is negligible and it is resting on the surface, the values of uplift pressure thus obtained refer to the bottom level of the floor,

where in practice; structures are somewhat depressed into, acting as foundation. In fact, in order to achieve a tractable analytical solution, the depression of the hydraulic structure has been neglected. With such assumptions, four extra vertices, which should take part in the conformal transformation, are reduced and some part of the seepage head is lost through the foundation depth. To remove the difference due to floor thickness, a correction factor is applied to the uplift pressure obtained from Khosla's equation. This factor is being computed by interpolation assuming that, there occurs a linear variation in the pressure along the upstream or downstream sheet-pile length.

1.4 Scope of present study

The present study is done to analyse the flow under a depressed weir with downstream concrete cutoff, using the conformal mapping technique. The aim of this investigation is to determine designs, which will ensure absolute safety with utmost economy.

1.5 Objectives of Present Study

Present study is undertaken to find an analytical solution which can quantify uplift pressure below the floor of depressed weir with downstream concrete cutoff and to prepare a comprehensive comparison of the values of uplift pressure with that obtained, by using the equation of Khosla et.al.(1936). It is also expected to see the effects due to increase in the thickness of concrete cutoff. The comparison is to be carried for weirs with depression and with cutoff at various positions. It is proposed to compare for the following hydraulic structures:

- I. Depressed weir with concrete cutoff downstream. (Figure 1.5.1)
- II. Depressed weir with concrete cutoff upstream. (Figure 1.5.2)
- III. Depressed weir with concrete cutoff positioned at various options. (Figure 1.5.3)
- IV. Depressed weir without concrete cutoff (Figure 1.5.4)

Use of conformal mapping technique generally results in multivariable non-linear equations. The non-linear equations are proposed to be solved by Newton-Raphson technique. Then the uplift pressure distribution at the key points and exit gradients are determined.

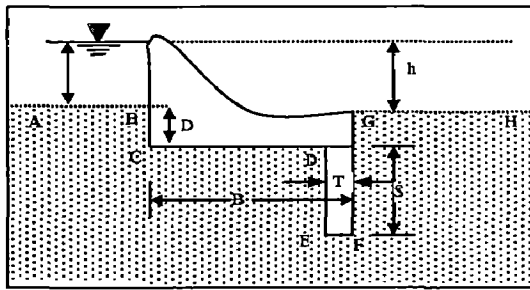


Figure 1.5.1 Depressed weir with concrete cutoff downstream.

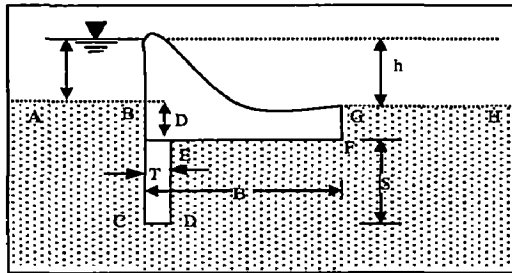


Figure 1.5.2 Depressed weir with concrete cutoff upstream

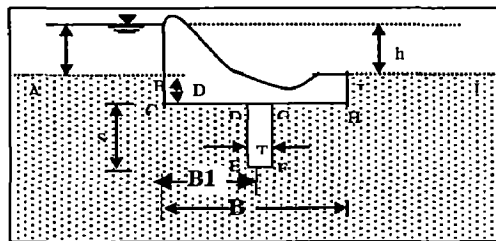


Figure 1.5.3 Depressed weir with concrete cutoff positioned at various options

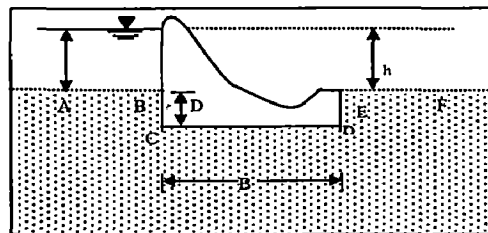


Figure 1.5.4 Depressed weir without concrete cutoff

CHAPTER 2

LITERATURE REVIEW

2.1 General

Kholsa et.al. (1936) found solutions to two-dimensional steady flow under a number of simple profiles of weirs resting on a homogeneous and isotropic soil of infinite depth using the Schwarz-Christoffel conformal transformation technique. Pressure heads; at key points (C, D, and E as shown in Figure.2.1) in excess of the hydrostatic head at the downstream boundary have been presented as a percentage of the seepage head in the form of charts, which are widely in use for the sub surface design of hydraulic structure. Khosia et.al. have neglected the depth of depression to reduce the number of vertices taking part in the conformal mapping. By reducing the number of vertices it was possible to carryout the integration required in solving the transformation. Numerical integration is necessary in case of structures having vertices more than three.

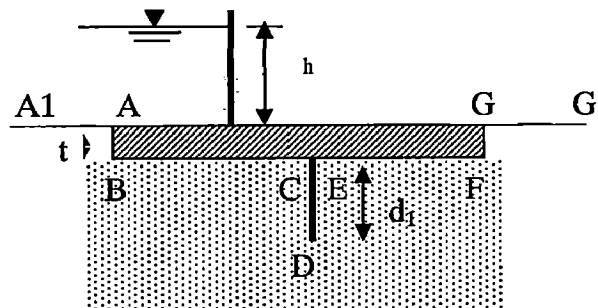


Figure 2.1 Two dimensional steady of flow

2.2 Approximate Method for Accounting Depression:

In Khosla's method of analysis, the excess pressure head has been derived, assuming that the thickness of floor is negligible and the structure is resting on the surface. As the foundation has some thickness, a part of the seepage head is lost along the foundation depth, which has to be accounted for.

To account for the head lost along the floor thickness, Khosia et.al. has suggested a correction. This is being computed by interpolation under the assumption that, the variation of hydraulic head is linear along the sheet-pile depth and the rate of variation is equal to the variation along the depth of depression. The correction for accounting depression for a flat-based weir proposed by them is as follows:

The correction for pressure head at point C in Figure.2.1 is $\left(\frac{\phi_C - \phi_D}{d_1}\right)t_{\min}$ which is subtracted from the value of ϕ_C . The correction for pressure head at the point 'E' is $\left(\frac{\phi_D - \phi_E}{d_1}\right)t_{\min}$ which is added to the value of ϕ_E , where ϕ_C , ϕ_D and ϕ_E are the pressure heads at points C, D and E respectively which have been obtained by neglecting the depression and using conformal mapping.

It may be noted here that the nature of dissipation of head along the depth of depression and sheet-pile are not similar. Because, at point A. the flow velocity is finite, where as, at point C the velocity is zero. Therefore, the corrections proposed by Khosia need an investigation.

Now a days, it is possible to carryout numerical integration and solve non-linear equations easily using computers. So instead of applying a correction factor as proposed by Khosla, in this dissertation, a solution has been given accounting floor thickness below the ground level for direct computation of the uplift pressure.

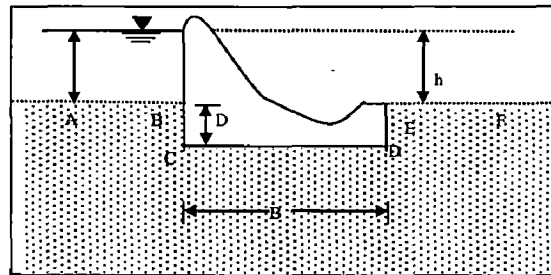


Figure 2.2.1 Depressed weir

Khosla has also suggested an empirical formula¹ for computation of uplift pressure under a flat bottom depressed weir, the type shown in Fig.2.2.1. The formula is based on tests conducted on a scale model. The empirical formula is

$$\phi'_D = \phi_D - \frac{2}{3}(\phi_C - \phi_D) + \frac{3}{\alpha^2}$$

in which ϕ_D and ϕ_C are pressures at D and C corresponding to figure.2.1 for which Khosla et.al. have given analytical solution. The parameter α is equal to B/D . ϕ'_D is the pressure at point D in figure 2.2.1.

Using the conformal mapping technique, Malhotra (1962) has given solution for flow under a depressed hydraulic structure having two sheet-piles one at each end. Safety against piping for depressed structure can be investigated using Lane's weighted creep theory (Lane,1935).

However no analytical solution are available for stepped-depressed weir.

2.3 Condition and Methods of Conformal Transformation

It is important to ascertain whether conformal transformation is indeed possible in all the foundation problems, with which we may eventually be confronted in practice. Apart from this, it is essential to know whether every particular transformation problem in hand admits of one solution only, or several such conditions.

Both question were dealt with in 1851 by Reiman in the following manner: Suppose we have a zone, or region, the boundaries of which are formed by a number of analytical curves (which includes, in this case straight lines as well).Reiman proved that such a zone can be conformally transformed into another one which is delimited by a circle; also, that this solution will be unique, provided that:

- (a) one point inside the first zone, and another one on its boundary, correspond respectively to a point inside the circle and second point on its periphery; or alternatively,
- (b) Three points taken in the same consecutive order, on the circle, represent three points on the original boundary.

Reiman's proof includes both the direct and the converse problems, ie. Transformation of surface delimited by analytical curves into that of circle, and vice versa. Thus , using the circle as an intermediate operation, areas circumscribed by analytical curves can always be transformed conformally from one into another, provided the conditions (a) and (b) are satisfied.

2.4 Analytical Method for Accounting Depression:

Pavlovsky (1922) has given solution to a flat bottomed depressed weir using Scwartz-christoffel transformation. Analytical solutions for the uplift pressure under the floor and the maximum exit gradient have been given.

Confomal mapping technique has been applied to compute uplift pressure and exit gradient for a flat depressed structure with two symmetrical row of piling on a permeable soil of infinite depth (Harr,1962). The solution has been given for structure on foundation of finite depth by Filchakov (Polubarinova-Kochina.1962). The analytical solution is not tractable as it contains elliptic integral of third kind.'

2.5 Conclusion

Analytical solution for a weir with concrete cutoff is not available. Analytical solution for flat-bottomed depressed floor resting on a soil of finite depth is available. However uplift pressure, exit gradient cannot be computed easily as the derived equations are highly non-linear and contain elliptic integral of third kind. Solution to flow under structure having vertices more than three can be obtained using conformal mapping and applying Newton-Raphson technique for solving the non-linear equation.

CHAPTER 3

ANALYSIS

3.1 General

Weirs on permeable foundation are designed to safeguard against uplift pressure and piping. The flow characteristics are determined assuming the flow to be two dimensional and steady. For non-homogeneous sub-soil, numerical method is used to solve the two dimensional equation satisfying the boundary conditions.

$$\frac{\partial}{\partial x}\{-k(x, y)\frac{\partial h}{\partial x}\} + \frac{\partial}{\partial y}\{-k(x, y)\frac{\partial h}{\partial y}\} = 0$$

For homogeneous, isotropic soil, the governing equation is the Laplace equation, which can be solved analytically using conformal mapping technique.

Using the Schwartz-Christoffel conformal mapping technique, Khosla et.al. (1936) have obtained analytical solutions for a stepped weir with a sheet pile provided at the step, resting on a homogeneous, isotropic porous medium of infinite depth. They have neglected the depression so as to reduce the number of vertices to arrive at a simple solution and suggested a correction factor to account for the depression. In this thesis, an analytical solution for the flow around a depressed weir with a concrete cutoff at the downstream end has been obtained using the Schwartz-Christoffel conformal mapping technique.

3.2 Statement of the Problem

The depressed weir with concrete cutoff either at down stream end or upstream end or at any position is analysed. The total width of floor including thickness of cutoff is 'B'. The depth of the cutoff is 'S' and thickness of cutoff is "T". The depth of depression of the floor at the upstream and down stream floor is "D". The heights of water above the upstream and downstream bed can be considered h_1 and h_2 respectively where as for maximum exit gradient the value of h_2 is assumed to be zero and the difference in the total heads between the upstream and downstream is h . It is required to find the pressure distribution along the impervious base BCDEFG of the structure and exit gradient along the downstream boundary.

3.3 Analysis

3.3.1 Weir with down stream concrete cutoff

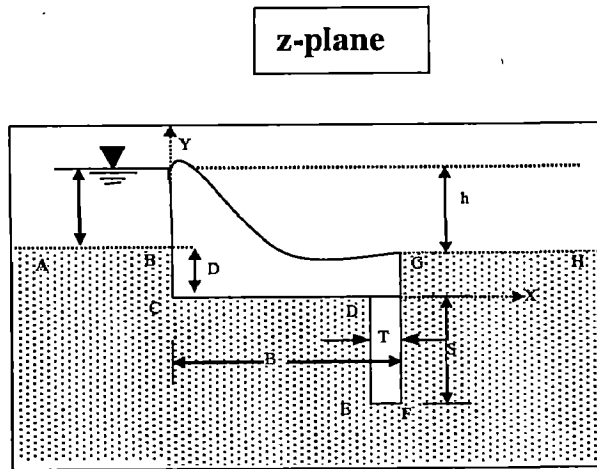


Figure 3.3.1 (a) Physical Domain in z-plane
t-plane

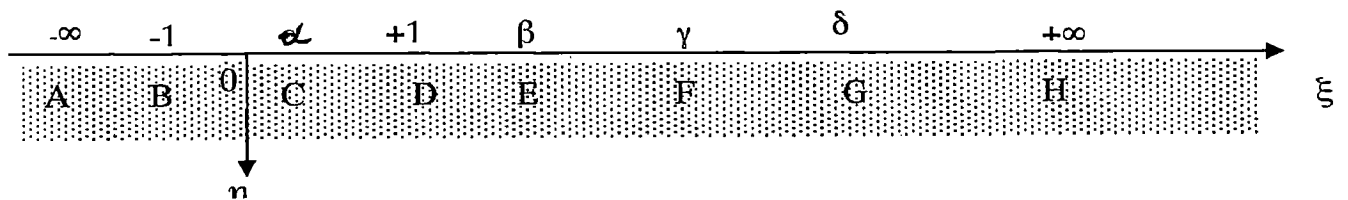


Figure 3.3.1 (b) : Physical Domain Mapped onto t-plane boundaries

The conformal mapping of the flow domain in z-plane onto the lower half of the auxiliary t-plane is given by:

$$z = M \int \frac{\sqrt{(t-\alpha)(\beta-t)(\gamma-t)}}{\sqrt{(1-t^2)(\delta-t)}} dt + N \quad (3.3.1)$$

The vertices A, B, C, D, E, F, G, H being mapped onto $-\infty, -1, \alpha, 1, \beta, \gamma, \delta$ and $+\infty$ respectively in the t-plane. M and N are complex constants to be determined. The constant N is governed by the lower limit of integration. To find the constants M and N, and the relationship between the transformation parameters and dimension of the structure integration between consecutive vertices are to be carried out.

(a). Integration between vertices C and D ($\alpha \leq t \leq 1$)

For point C, $t = \alpha$, and $z = 0$

For point D, $t = +1$ and $z = B-T$

Applying these conditions

$$B-T = M \int_{\alpha}^1 \frac{\sqrt{(t-\alpha)(\beta-t)(\gamma-t)}}{\sqrt{(1-t^2)(\delta-t)}} dt + 0$$

$$B-T = MI_1,$$

$$\text{where } I_1 = \int_{\alpha}^1 \frac{\sqrt{(t-\alpha)(\beta-t)(\gamma-t)}}{\sqrt{(1-t^2)(\delta-t)}} dt$$

$$\boxed{M = \frac{B-T}{I_1}}$$

(3.3.2)

(b) Integration between vertices D and E $(1 \leq t \leq \beta)$

For vertex D, $t=1$ and $z = B-T$

For vertex E, $t=\beta$ and $z=B-T-iS$

Applying these relations

$$B-T-iS = M \int_1^{\beta} \frac{\sqrt{(t-\alpha)(\beta-t)(\gamma-t)}}{\sqrt{(1-t^2)(\delta-t)}} dt + B-T$$

$$-iS = \frac{M}{i} \int_1^{\beta} \frac{\sqrt{(t-\alpha)(\beta-t)(\gamma-t)}}{\sqrt{(t^2-1)(\delta-t)}} dt$$

$$S = MI_2$$

$$\text{where } I_2 = \int_1^{\beta} \frac{\sqrt{(t-\alpha)(\beta-t)(\gamma-t)}}{\sqrt{(t^2-1)(\delta-t)}} dt$$

$$\frac{S}{B-T} = \frac{I_2}{I_1}$$

$$\boxed{F_1 = \frac{S}{B-T} - \frac{I_2}{I_1} = 0}$$

(3.3.3)

(c) Integration between vertices E and F $(\beta \leq t \leq \gamma)$

For vertex E, $t=\beta$ and $z=B-T-iS$

For F, $t=\gamma$ and $z=B-iS$

Applying these conditions

$$B-iS = M \int_{\beta}^{\gamma} \frac{\sqrt{(t-\alpha)(t-\beta)(\gamma-t)}}{\sqrt{(t^2-1)(\delta-t)}} dt + B-T-iS$$

$$T = M \int_{\beta}^{\gamma} \frac{\sqrt{(t-\alpha)(t-\beta)(\gamma-t)}}{\sqrt{(t^2-1)(\delta-t)}} dt = M I_3$$

$$\text{where } I_3 = \int_{\beta}^{\gamma} \frac{\sqrt{(t-\alpha)(t-\beta)(\gamma-t)}}{\sqrt{(t^2-1)(\delta-t)}} dt$$

$$\frac{T}{B-T} = \frac{I_3}{I_1}$$

$$\boxed{F_2 = \frac{T}{B-T} - \frac{I_3}{I_1} = 0}$$

(3.3.4)

(d) Integration between vertices F and G ($\gamma \leq t \leq \delta$)

For vertex F, $t=\gamma$ and $z=B-iS$

For vertex G, $t=\delta$ and $z=B+iD$

$$B+iD = Mi \int_{\gamma}^{\delta} \frac{\sqrt{(t-\alpha)(t-\beta)(t-\gamma)}}{\sqrt{(t^2-1)(\delta-t)}} dt + B-iS$$

$$D+S = MI_4, \text{ where } I_4 = \int_{\gamma}^{\delta} \frac{\sqrt{(t-\alpha)(t-\beta)(t-\gamma)}}{\sqrt{(t^2-1)(\delta-t)}} dt$$

$$\frac{D+S}{B-T} = \frac{I_4}{I_1}$$

$$\boxed{F_3 = \frac{D+S}{B-T} - \frac{I_4}{I_1} = 0}$$

(3.3.5)

(e) Integration between vertices B and C ($-1 \leq t \leq \alpha$)

For vertex B, $t=-1$ and $z=iD$

For vertex C, $t=\alpha$ and $z=0$

Applying these conditions

$$0 = M \int_{-1}^{\alpha} i \frac{\sqrt{(\alpha-t)(\beta-t)(\gamma-t)}}{\sqrt{(1-t^2)(\delta-t)}} dt + iD$$

$$-D = M \int_{-1}^{\alpha} \frac{\sqrt{(\alpha-t)(\beta-t)(\gamma-t)}}{\sqrt{(1-t^2)(\delta-t)}} dt$$

Substitute $t=-\tau$ then $dt=-d\tau$

For $t=-1, \tau=1$ and $t=\alpha, \tau=-\alpha$

$$D = M \int_1^{-\alpha} \frac{\sqrt{(\alpha+\tau)(\beta+\tau)(\gamma+\tau)}}{i \sqrt{(\tau^2-1)(\delta+\tau)}} d\tau$$

$$D = M \int_{-\alpha}^1 \frac{(\pm i) \sqrt{(\alpha+\tau)(\beta+\tau)(\gamma+\tau)}}{\sqrt{(1-\tau^2)(\delta+\tau)}} d\tau$$

$$\frac{D}{B-T} = \frac{I_5}{I_1},$$

$$\text{where } I_5 = \int_{-\alpha}^1 \frac{\sqrt{(\alpha+\tau)(\beta+\tau)(\gamma+\tau)}}{\sqrt{(1-\tau^2)(\delta+\tau)}} d\tau$$

$$F_4 = \frac{D}{B-T} - \frac{I_5}{I_1} = 0$$

(3.3.6)

The parameters α, β, γ and δ are to be found for known values of

$\frac{S}{B-T}, \frac{T}{B-T}, \frac{D+S}{B-T}, \frac{D}{B-T}$. From equation 3.3.2 to 3.3.6 which are the nonlinear equations.

3.3.2 Weir with an up stream concrete cutoff.

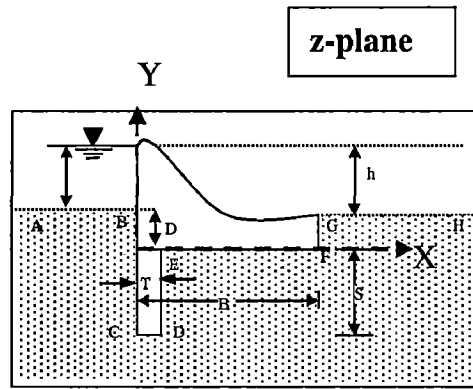


Figure. 3.3.2(a) Physical Domain in z-plane

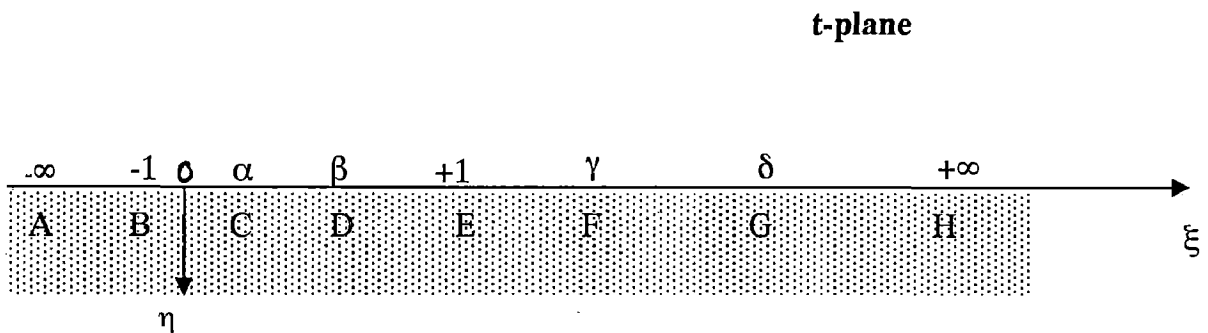


Figure 3.3.2(b) : Physical Domain Mapped onto t-plane boundaries

The conformal mapping of the flow domain in z-plane onto the lower half of the auxiliary t-plane is given by:

$$Z = M \int \frac{\sqrt{(t-\alpha)(\beta-t)(\gamma-t)}}{\sqrt{(1-t^2)(\delta-t)}} dt + N \quad (3.3.7)$$

the vertices A, B, C, D, E, F, G, H being mapped onto $-\infty, -1, \alpha, \beta, +1, \gamma, \delta$ and $+\infty$ respectively in the t-plane. M and N are complex constants to be determined. The constant N is governed by the lower limit of integration. To find the constants M and N, and the relationship between the transformation parameters and dimension of the structure, integration is carried out between consecutive vertices.

(a). Integration between vertices C and D ($\alpha \leq t \leq \beta$)

For point C, $t = \alpha$, and $z = -iS$ and

For point D, $t = \beta$ and $z = T - iS$

Applying these conditions

$$T - iS = M \int_{\alpha}^{\beta} \frac{\sqrt{(t-\alpha)(\beta-t)(\gamma-t)}}{\sqrt{(1-t^2)(\delta-t)}} dt - iS$$

$$T = M I_1,$$

$$\text{Where } I_1 = \int_{\alpha}^{\beta} \frac{\sqrt{(t-\alpha)(\beta-t)(\gamma-t)}}{\sqrt{(1-t^2)(\delta-t)}} dt$$

$$\boxed{M = \frac{T}{I_1}}$$

(3.3.8)

(b) Integration between vertices D and E ($\beta \leq t \leq 1$)

For vertex D, $t = \beta$ and $z = T - iS$

For vertex E, $t = 1$ and $z = T$

Applying these conditions

$$T = M i \int_{\beta}^1 \frac{\sqrt{(t-\alpha)(t-\beta)(\gamma-t)}}{\sqrt{(1-t^2)(\delta-t)}} dt + T - iS$$

$$S = M \int_{\beta}^1 \frac{\sqrt{(t-\alpha)(t-\beta)(\gamma-t)}}{\sqrt{(1-t^2)(\delta-t)}} dt = M I_2$$

$$\text{where } I_2 = \int_{\beta}^1 \frac{\sqrt{(t-\alpha)(\beta-t)(\gamma-t)}}{\sqrt{(1-t^2)(\delta-t)}} dt$$

Incorporating constant M

$$\frac{S}{T} = \frac{I_2}{I_1}$$

$$\boxed{F_1 = \frac{S}{T} - \frac{I_2}{I_1} = 0}$$

(3.3.9)

(c) Integration between vertices E and F ($1 \leq t \leq \gamma$)

For vertex E, $t = 1$ and $z = T$

For vertex F, $t = \gamma$ and $z = B$

Applying these conditions

$$B = M \int_1^\gamma \frac{\sqrt{(t-\alpha)(t-\beta)(\gamma-t)}}{\sqrt{(t^2-1)(\delta-t)}} dt + T$$

$$B-T = \frac{T}{I_1} \int_1^\gamma \frac{\sqrt{(t-\alpha)(t-\beta)(\gamma-t)}}{\sqrt{(t^2-1)(\delta-t)}} dt$$

$$\frac{B-T}{T} = \frac{I_3}{I_1}$$

$$\text{where } I_3 = \int_1^\gamma \frac{\sqrt{(t-\alpha)(t-\beta)(\gamma-t)}}{\sqrt{(t^2-1)(\delta-t)}} dt$$

$$\boxed{F_2 = \frac{B-T}{T} - \frac{I_3}{I_1} = 0}$$

(3.3.10)

(d) Integration between vertices F and G ($\gamma \leq t \leq \delta$)

For vertex F, $t=\gamma$ and $z=B$

For vertex G, $t=\delta$ and $z=B+iD$

Applying these conditions

$$B + iD = Mi \int_\gamma^\delta \frac{\sqrt{(t-\alpha)(t-\beta)(t-\gamma)}}{\sqrt{(t^2-1)(\delta-t)}} dt + B$$

$$D = \frac{T}{I_1} I_4$$

$$\text{where } I_4 = \int_\gamma^\delta \frac{\sqrt{(t-\alpha)(t-\beta)(t-\gamma)}}{\sqrt{(t^2-1)(\delta-t)}} dt$$

$$\boxed{F_3 = \frac{D}{T} - \frac{I_4}{I_1} = 0}$$

(3.3.11)

(e) Integration between vertices B and C ($-1 \leq t \leq \alpha$)

For vertex B, $t=-1$ and $z=iD$

For vertex C, $t=\alpha$ and $z=-iS$

Applying these conditions

$$-iS = M \int_{-1}^\alpha \frac{(\pm i) \sqrt{(\alpha-t)(\beta-t)(\gamma-t)}}{\sqrt{(1-t^2)(\delta-t)}} dt + iD$$

Substituting, $t=-\tau$, $dt=-d\tau$ and accordingly changing the limits of integration

$$-iS = M(\pm i) \int_{-\alpha}^1 \frac{\sqrt{(\alpha+\tau)(\beta+\tau)(\gamma+\tau)}}{\sqrt{(1-\tau^2)(\delta+\tau)}} d\tau + iD$$

$$D+S = \frac{T}{I_1} \int_{-\alpha}^1 \frac{\sqrt{(\alpha+\bar{\tau})(\beta+\bar{\tau})(\gamma+\bar{\tau})}}{\sqrt{(1-\bar{\tau}^2)(\delta+\bar{\tau})}} d\bar{\tau}$$

$$\frac{D+S}{T} = \frac{I_5}{I_1},$$

where $I_5 = \int_{-\alpha}^1 \frac{\sqrt{(\alpha+\tau)(\beta+\tau)(\gamma+\tau)}}{\sqrt{(1-\tau^2)(\delta+\tau)}} d\tau$

$$F_4 = \frac{S+D}{T} - \frac{I_5}{I_1} \quad (3.3.12)$$

The parameters α, β, γ and δ are to be found for known values of $\frac{S}{T}$,

$\frac{B-T}{T}$, $\frac{D}{T}$, $\frac{S+D}{T}$. from equation 3.4.2 to 3.4.6 which are the nonlinear equations.

3.3.3 Weir with a cutoff at any position along the floor

The solution to this problem will give solution for any position of a cutoff

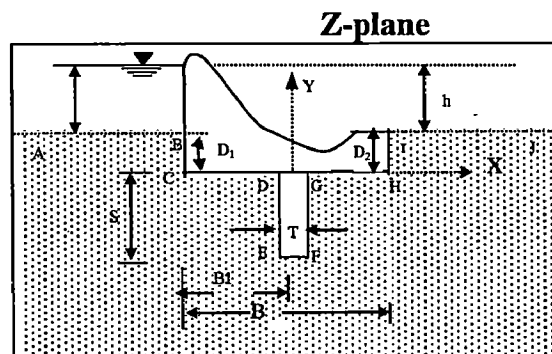


Figure. 3.3.3 (a) Physical Domain in z-plane

t-plane

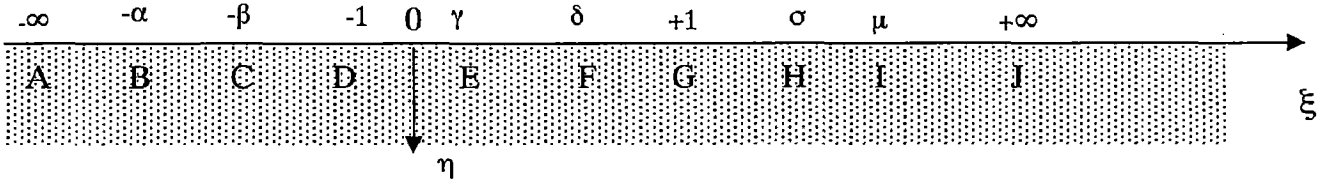


Figure 3.3.3 (b) : Physical Domain Mapped onto t-plane boundaries

The conformal mapping of the flow domain in z-plane onto the lower half of the auxiliary t-plane is given by:

$$z = M \int \frac{\sqrt{(\beta + t)(\delta - t)(t - \gamma)(\sigma - t)}}{\sqrt{(1 - t^2)(\alpha + t)(\mu - t)}} dt + N \quad (3.3.13)$$

The vertices A, B, C, D, E, F, G, H, I, j being mapped onto $-\infty, -\alpha, -\beta, -1, \gamma, \delta, +1, \sigma, \mu$ and $+\infty$ respectively in the t-plane. M and N are complex constants to be determined. The constant N is governed by the lower limit of integration. To find the constants M and N, and the relationship between the transformation parameters and dimension of the structure, integrations are carried out between consecutive vertices.

(a). Integration between vertices E and F ($\gamma \leq t \leq \delta$)

Applying the conditions

For vertex E, $t = \gamma$, and $z = -T/2 - iS$ and

For vertex F, $t = \delta$ and $z = T/2 - iS$

Applying these conditions

$$T/2 - iS = M \int_{\gamma}^{\delta} \frac{\sqrt{(\beta + t)(t - \gamma)(\delta - t)(\sigma - t)}}{\sqrt{(1 - t^2)(\alpha + t)(\mu - t)}} dt - T/2 - iS$$

$$T = MI_1$$

$$\text{where } I_1 = \int_{\gamma}^{\delta} \frac{\sqrt{(\beta + t)(t - \gamma)(\delta - t)(\sigma - t)}}{\sqrt{(1 - t^2)(\alpha + t)(\mu - t)}} dt$$

$$\boxed{M = \frac{T}{I_1}} \quad (3.3.14)$$

(b) Integration between vertices F and G ($\delta \leq t \leq 1$)

For vertex F, $t = \delta$ and $z = T/2 - iS$

For vertex G, $t = 1$ and $z = T/2$

Applying these conditions

$$\frac{T}{2} = Mi \int_{\delta}^1 \frac{\sqrt{(\beta+t)(t-\gamma)(t-\delta)(\sigma-t)}}{\sqrt{(1-t^2)(\mu-t)(\alpha+t)}} dt + \frac{T}{2} - iS$$

$$S = \frac{T}{I_1} \int_{\delta}^1 \frac{\sqrt{(\beta+t)(t-\gamma)(t-\delta)(\sigma-t)}}{\sqrt{(1-t^2)(\mu-t)(\alpha+t)}} dt$$

$$\frac{S}{T} = \frac{I_2}{I_1}$$

$$\text{where } I_2 = \int_{\delta}^1 \frac{\sqrt{(\beta+t)(t-\gamma)(t-\delta)(\sigma-t)}}{\sqrt{(1-t^2)(\mu-t)(\alpha+t)}} dt$$

$$\boxed{F1 = \frac{S}{T} - \frac{I_2}{I_1} = 0} \quad (3.3.15)$$

(C) Integration between vertices G and H ($1 \leq t \leq \sigma$)

For vertex G, $t=1$ and $z=T/2$

For vertex H, $t=\sigma$ and $z=B_2$

$$B_2 = M \int_1^{\sigma} \frac{\sqrt{(\beta+t)(t-\gamma)(t-\delta)(\sigma-t)}}{\sqrt{(t^2-1)(\mu-t)(\alpha+t)}} dt + \frac{T}{2}$$

$$\boxed{F2 = \frac{B_2}{T} - \frac{1}{2} - \frac{I_3}{I_1} = 0} \quad (3.3.16)$$

$$\text{where } I_3 = \int_1^{\sigma} \frac{\sqrt{(\beta+t)(t-\gamma)(t-\delta)(\sigma-t)}}{\sqrt{(t^2-1)(\mu-t)(\alpha+t)}} dt$$

(d) Integration between vertices H and I ($\sigma \leq t \leq \mu$)

For vertex H, $t=\sigma$ and $z=B_2$

For vertex I, $t=\mu$ and $z=B_2+iD_2$

Hence,

$$B_2 + iD_2 = \frac{iT}{I_1} \int_{\sigma}^{\mu} \frac{\sqrt{(\beta+t)(t-\gamma)(t-\delta)(t-\sigma)}}{\sqrt{(t^2-1)(\mu-t)(\alpha+t)}} dt + B_2$$

$$D_2 = \frac{T}{I_1} I_4$$

$$\text{where } I_4 = \int_{\sigma}^{\mu} \frac{\sqrt{(\beta+t)(t-\gamma)(t-\delta)(t-\sigma)}}{\sqrt{(t^2-1)(\mu-t)(\alpha+t)}} dt \quad \frac{D_2}{T} = \frac{I_4}{I_1}$$

$$\boxed{F_3 = \frac{D_2}{T} - \frac{I_4}{I_1} = 0} \quad (3.3.17)$$

(e) Integration between vertices D and E $(-1 \leq t \leq \gamma)$

For vertex D, $t = -1$ and $z = -T/2$

For vertex E, $t = \gamma$ and $z = -T/2 - iS$

$$-T/2 - iS = M(\pm i) \int_{-1}^{\gamma} \frac{\sqrt{(\beta+t)(\gamma-t)(\delta-t)(\sigma-t)}}{\sqrt{(1-t^2)(\alpha+t)(\mu-t)}} dt - T/2$$

Substituting $t = -\tau$, $dt = -d\tau$ and changing accordingly the limits of integration

$$S = \frac{T}{I_1} \int_{-\gamma}^1 \frac{\sqrt{(\beta-\tau)(\gamma+\tau)(\delta+\tau)(\sigma+\tau)}}{\sqrt{(1-\tau^2)(\alpha-\tau)(\mu+\tau)}} d\tau$$

$$\frac{S}{T} = \frac{I_5}{I_1}$$

$$\text{where } I_5 = \int_{-\gamma}^1 \frac{\sqrt{(\beta-\tau)(\gamma+\tau)(\delta+\tau)(\sigma+\tau)}}{\sqrt{(1-\tau^2)(\alpha-\tau)(\mu+\tau)}} d\tau$$

$$\boxed{F_4 = \frac{S}{T} - \frac{I_5}{I_1} = 0} \quad (3.3.18)$$

(f) Integration between vertices C and D $(-\beta \leq t \leq -1)$

For vertex C, $t = -\beta$ and $z = -B1$

For vertex D, $t = -1$ and $z = -T/2$

Hence,

$$-T/2 = M \int_{-\beta}^{-1} \frac{\sqrt{(\beta+t)(t-\gamma)(\delta-t)(\sigma-t)}}{\sqrt{(1-t^2)(\alpha+t)(\mu-t)}} dt - B_1$$

Substituting $t=-\tau$, $dt = -d\tau$ and changing accordingly the limits of integration

$$B_1 - \frac{T}{2} = \frac{T}{I_1} \int_1^\beta \frac{\sqrt{(\beta-\tau)(\gamma+\tau)(\delta+\tau)(\sigma+\tau)}}{\sqrt{(\tau^2-1)(\alpha-\tau)(\mu+\tau)}} d\tau$$

$$\frac{B_1}{T} - \frac{1}{2} = \frac{I_6}{I_1}$$

$$\text{where } I_6 = \int_1^\beta \frac{\sqrt{(\beta-\tau)(\gamma+\tau)(\delta+\tau)(\sigma+\tau)}}{\sqrt{(\tau^2-1)(\alpha-\tau)(\mu+\tau)}} d\tau$$

$$F_5 = \frac{B_1}{T} - \frac{1}{2} - \frac{I_6}{I_1} = 0$$

(3.3.19)

(g) Integration between vertices B and C ($-\alpha \leq t \leq -\beta$)

For vertex B, $t = -\alpha$ and $z = -B_1 + iD_1$

For vertex C, $t = -\beta$ and $z = -B_1$

Hence,

$$-B_1 = M \int_{-\alpha}^{-\beta} \frac{\sqrt{(\beta+t)(\gamma-t)(\delta-t)(\sigma-t)}}{\sqrt{(1-t^2)(\alpha+t)(\mu-t)}} dt - B_1 + iD_1$$

Substituting $t=-\tau$, $dt=-d\tau$, we get

$$\frac{D_1}{T} = \frac{I_7}{I_1}$$

$$\text{where } I_7 = \int_\beta^\alpha \frac{\sqrt{(\tau-\beta)(\gamma+\tau)(\delta+\tau)(\sigma+\tau)}}{\sqrt{(\tau^2-1)(\alpha-\tau)(\mu+\tau)}} d\tau$$

$$F_6 = \frac{D_1}{T} - \frac{I_7}{I_1} = 0$$

(3.3.20)

The parameters

$\alpha, \beta, \gamma, \delta, \mu$ and σ are to be found for known values of $\frac{S}{T}, \frac{B_2}{T}, \frac{D_2}{T}, \frac{B_1}{T}, \frac{D_1}{T}$.

From the six equations (3.3.15,3.3.16,3.3.17,3.3.18,3.3.19 and 3.3.20) which are nonlinear equations.

Newton Raphson technique has been used to find the solution and this has been explained in appendix. Using corresponding Jacobian matrix these nonlinear equations containing the six unknowns $\alpha, \beta, \gamma, \delta, \sigma$ and μ are expressed as

$$\begin{bmatrix} \frac{\partial F_1}{\partial \alpha} & \frac{\partial F_1}{\partial \beta} & \frac{\partial F_1}{\partial \gamma} & \frac{\partial F_1}{\partial \delta} & \frac{\partial F_1}{\partial \sigma} & \frac{\partial F_1}{\partial \mu} \\ \frac{\partial F_2}{\partial \alpha} & \frac{\partial F_2}{\partial \beta} & \frac{\partial F_2}{\partial \gamma} & \frac{\partial F_2}{\partial \delta} & \frac{\partial F_2}{\partial \sigma} & \frac{\partial F_2}{\partial \mu} \\ \frac{\partial F_3}{\partial \alpha} & \frac{\partial F_3}{\partial \beta} & \frac{\partial F_3}{\partial \gamma} & \frac{\partial F_3}{\partial \delta} & \frac{\partial F_3}{\partial \sigma} & \frac{\partial F_3}{\partial \mu} \\ \frac{\partial F_4}{\partial \alpha} & \frac{\partial F_4}{\partial \beta} & \frac{\partial F_4}{\partial \gamma} & \frac{\partial F_4}{\partial \delta} & \frac{\partial F_4}{\partial \sigma} & \frac{\partial F_4}{\partial \mu} \\ \frac{\partial F_5}{\partial \alpha} & \frac{\partial F_5}{\partial \beta} & \frac{\partial F_5}{\partial \gamma} & \frac{\partial F_5}{\partial \delta} & \frac{\partial F_5}{\partial \sigma} & \frac{\partial F_5}{\partial \mu} \\ \frac{\partial F_6}{\partial \alpha} & \frac{\partial F_6}{\partial \beta} & \frac{\partial F_6}{\partial \gamma} & \frac{\partial F_6}{\partial \delta} & \frac{\partial F_6}{\partial \sigma} & \frac{\partial F_6}{\partial \mu} \end{bmatrix} \begin{bmatrix} \nabla \alpha \\ \nabla \beta \\ \nabla \gamma \\ \nabla \delta \\ \nabla \sigma \\ \nabla \mu \end{bmatrix} = \begin{bmatrix} F_1(\alpha^*, \beta^*, \gamma^*, \delta^*, \sigma^*, \mu^*) \\ F_2(\alpha^*, \beta^*, \gamma^*, \delta^*, \sigma^*, \mu^*) \\ F_3(\alpha^*, \beta^*, \gamma^*, \delta^*, \sigma^*, \mu^*) \\ F_4(\alpha^*, \beta^*, \gamma^*, \delta^*, \sigma^*, \mu^*) \\ F_5(\alpha^*, \beta^*, \gamma^*, \delta^*, \sigma^*, \mu^*) \\ F_6(\alpha^*, \beta^*, \gamma^*, \delta^*, \sigma^*, \mu^*) \end{bmatrix}$$

In which $\alpha^*, \beta^*, \gamma^*, \delta^*, \sigma^*$ and μ^* are initial guess of the parameters. The integrals are improper; Method of substitution and then Gaussian Quadrature have been used to evaluate the integrals. The solution of Jacobian Matrix is done using a FORTRAN program. The FORTRAN program is listed in Appendix III.

3.3.4 Mapping of ω - plane onto lower half of t - plane:

The complex potential w is defined as

$$w = \phi + i\Psi \tag{3.3.21}$$

where ϕ = velocity potential function and ψ = stream function.

For Y-axis +ve upward, the velocity potential function ϕ is defined as

$$\phi = -k \left(\frac{P}{\gamma_w} + y \right) + c \tag{3.3.22}$$

The constant c is conveniently chosen as $k(h_2 + D_2)$, where h_2 is the depth of water and D_2 is the depth of depression, in the down stream side, p = water pressure, γ_w = unit weight of water, k = hydraulic conductivity.

Accordingly the velocity potential on downstream bed is zero and on upstream bed is $-kh$, where h is the hydraulic head difference causing flow. The complex potential, for the flow domain is shown in Figure 3.3.4(a), where $w = \phi + i\Psi$, and Ψ is stream function. So,

$$\phi = -k \left(\frac{p}{\gamma_w} + y \right) + k(D_2 + h_2) \quad (3.3.23)$$

The w -plane for the flow domain of Figure 3.3.3(a) is shown in Figure 3.4.

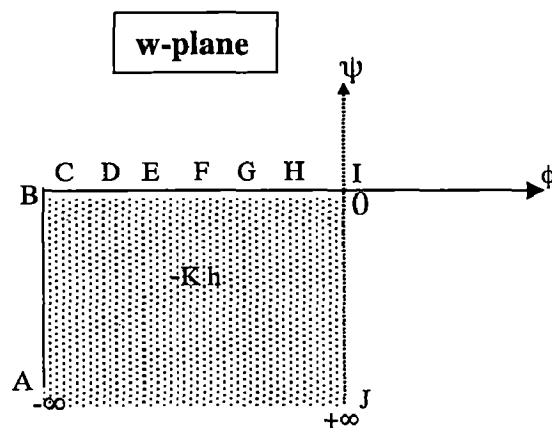


Figure 3.3.4 (a) w-plane for the flow domain of fig.3.3.3 (a)

Mapping of the complex potential plane onto the lower half t -plane is given by:

$$\frac{dw}{dt} = \frac{M_1}{\sqrt{(t + \alpha)(\mu - t)}}$$

$$w = M_1 \int \frac{dt}{\sqrt{(t + \alpha)(\mu - t)}} + N_1 \quad (3.3.24)$$

where M_1 and N_1 are complex constants.

With a substitution $t = \frac{1}{2}[\mu - \alpha + (\mu + \alpha)\sin \theta]$

$dt = \frac{1}{2}(\mu + \alpha)\cos \theta d\theta$, the integration reduces to

$$w = M_1 \sin^{-1} \left(\frac{2t + \alpha - \mu}{\alpha + \mu} \right) + N_1 \quad (3.3.25)$$

For the point I, $t = \mu$ and $w = \phi + i\psi = 0$,

$$\text{So } N_1 = -M_1 * \frac{\pi}{2}$$

$$w = M_1 \sin^{-1} \left(\frac{2t + \alpha - \mu}{\alpha + \mu} \right) - M_1 \frac{\pi}{2}$$

For the point B, $t = -\alpha$ and $w = -Kh$

$$\text{So } M_1 = \frac{Kh}{\pi}$$

$$\text{Thus we get } w = \frac{Kh}{\pi} \sin^{-1} \left(\frac{2t + \alpha - \mu}{\alpha + \mu} \right) - \frac{Kh}{2} \quad (3.3.26)$$

For the design purpose we need to know the pressure distribution acting along the various section of the structure and magnitude of the exit gradient. Now we have to find the potential at the key points B,C,D,E,F,G and H where stream function $\psi=0$. So $w=\phi$ along the impervious base of the structure. From equations (3.3.23) and (3.3.26)

$$-k \left(\frac{p}{\gamma_w} + y \right) + k(D_2 + h_2) = \frac{kh}{\pi} \sin^{-1} \left(\frac{2t + \alpha - \mu}{\alpha + \mu} \right) - \frac{kh}{2}$$

$$\frac{p}{\gamma_w h} = \frac{1}{2} - \frac{1}{\pi} \sin^{-1} \left(\frac{2t + \alpha - \mu}{\alpha + \mu} \right) + (D_2 + h_2 - y) \frac{1}{h} \quad (3.3.27)$$

This is the general equation for pressure distribution along the impervious floor for the case shown in Fig 3.3.3 (a).

3.4 The Pressure Distribution

Eq. (3.3.27) is the general equation for seepage pressure under the floor. To find the pressure at various points B,C,D,E,F,G,H and I, the ordinate of "y" from z-plane and the corresponding t from t-plane is to be entered in Eq. (3.3.27):

i). At point B ($y=D_1, t=-\alpha$, and

$$p_B = \gamma_w h_1 \quad (3.3.28)$$

ii) At point C $y=0, t=-\beta$,

$$\frac{p_C}{\gamma_w} = \frac{h}{2} - \frac{h}{\pi} \sin^{-1} \left(\frac{2\beta + \alpha - \mu}{\alpha + \mu} \right) + D_2 + h_2 \quad (3.3.29)$$

iii) At point D $y=0, t=-1$,

$$\frac{p_D}{\gamma_w} = \frac{h}{2} - \frac{h}{\pi} \sin^{-1} \left(\frac{-2 + \alpha - \mu}{\alpha + \mu} \right) + D_2 + h_2 \quad (3.3.30)$$

iv) At point E, $y=-S$, $t=\gamma$,

$$\frac{p_E}{\gamma_w} = \frac{h}{2} - \frac{h}{\pi} \sin^{-1} \left(\frac{2\gamma + \alpha - \mu}{\alpha + \mu} \right) + D_2 + S + h_2 \quad (3.3.31)$$

v) At point F $y=-S$, $t=\delta$,

$$\frac{p_F}{\gamma_w} = \frac{h}{2} - \frac{h}{\pi} \sin^{-1} \left(\frac{2\delta + \alpha - \mu}{\alpha + \mu} \right) + D_2 + S + h_2 \quad (3.3.32)$$

vi) At point G $y=0$, $t=+1$,

$$\frac{p_G}{\gamma_w} = \frac{h}{2} - \frac{h}{\pi} \sin^{-1} \left(\frac{2 + \alpha - \mu}{\alpha + \mu} \right) + D_2 + h_2 \quad (3.3.33)$$

vii) At point H $y=0$, $t=\sigma$,

$$\frac{p_H}{\gamma_w} = \frac{h}{2} - \frac{h}{\pi} \sin^{-1} \left(\frac{2\sigma + \alpha - \mu}{\alpha + \mu} \right) + D_2 \quad (3.3.34)$$

viii) At point I $y=D_2$, $t=\mu$

$$\frac{p_I}{\gamma_w} = h_2 \quad (3.3.35)$$

Similarly one can derive the equations for potential at different key points for the weir with the downstream cutoff Fig 3.3.1(a) and for the upstream cutoff Fig 3.3.2(a)

Now the w -plane for the down stream concrete cutoff with respect to Fig 3.3.1 (a) and 3.3.2 (a) will be as shown below:

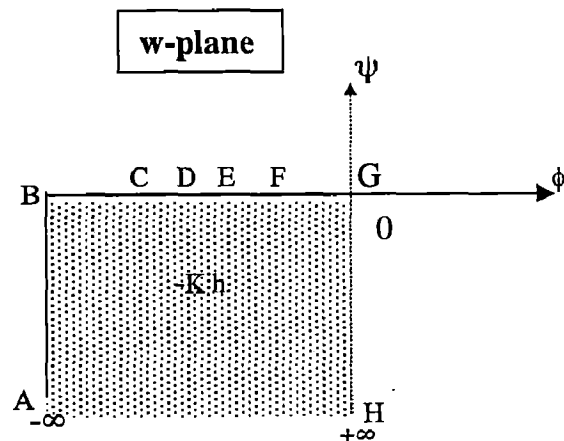


Figure 3.3.4 (b) w -plane for the flow domain of Fig.3.3.1 (a) and 3.3.2 (a)

The mapping of w-plane onto t-plane is given by

$$\frac{dw}{dt} = M_1 \frac{1}{\sqrt{(t+1)(\delta-t)}} \quad (3.3.36)$$

Following the preceding procedure, we get

$$w = \frac{Kh}{\pi} \sin^{-1} \left(\frac{2t+1-\delta}{1+\delta} \right) - \frac{Kh}{2} \quad (3.3.37)$$

The general equation for the potential distribution for a weir with down stream concrete cutoff is

$$\frac{p}{\gamma_w} = \frac{h}{2} - \frac{h}{\pi} \sin^{-1} \left(\frac{2t+1-\delta}{1+\delta} \right) - (h_2 + D) - y \quad (3.3.38)$$

For a weir with upstream concrete cutoff the general solutions for potential and pressure distribution are

$$w = \frac{kh}{\pi} \sin^{-1} \left(\frac{2t+\alpha-1}{1+\alpha} \right) \text{ and} \quad (3.3.39)$$

$$\frac{p}{\gamma_w} = \frac{h}{2} - \frac{h}{\pi} \sin^{-1} \left(\frac{2t+\alpha-1}{1+\alpha} \right) - (h_2 + D) - y \quad (3.3.40)$$

Pressures can be obtained at a point substituting the corresponding value of 't' and 'y' as described above.

3.5 The Exit Gradient

Since w is analytic, the differential

$$\frac{dw}{dz} = \frac{dw}{dx} = \frac{dw}{idy}$$

$$\frac{dw}{dx} = \frac{\partial}{\partial x} (\phi + i\psi) = \frac{\partial \phi}{\partial x} + i \frac{\partial \psi}{\partial x}$$

$$\frac{dw}{idy} = \frac{1}{i} \frac{\partial}{\partial y} (\phi + i\psi) = \frac{\partial \psi}{\partial y} - i \frac{\partial \phi}{\partial y}$$

$$\text{Hence, } \frac{dw}{dz} = u - iv \quad (3.3.41)$$

The downstream surface of the flow domain is horizontal. Hence $u=0$ and then

$$\frac{dw}{dz} = -iv = ikI_E$$

where I_E is the exit gradient

$$\text{or, } I_E = \frac{i}{K} \left(\frac{dw}{dt} * \frac{dt}{dz} \right) \quad (3.3.42)$$

3.5.1 Exit gradient for the weir with a downstream concrete cutoff

The flow domain is shown in Fig.3.3.1 (a)

$$I_E = \frac{1}{k} \left[\frac{kh}{\pi \sqrt{(t+1)(\delta-t)}} * \frac{\sqrt{(t^2-1)(\delta-t)}}{M \sqrt{(t-\alpha)(t-\beta)(t-\gamma)}} \right]$$

$$\text{where } M = \frac{S}{I_2}$$

For maximum exit gradient at $t=\delta$

$$I_E * \frac{S}{h} = \left[\frac{I_2}{\pi} * \frac{\sqrt{(\delta-1)}}{\sqrt{(\delta-\alpha)(\delta-\beta)(\delta-\gamma)}} \right] \quad (3.3.43)$$

$$\text{where } I_2 = \int_1^\beta \frac{\sqrt{(t-\alpha)(\beta-t)(\gamma-t)}}{\sqrt{(t^2-1)(\delta-t)}} dt$$

CHAPTER 4

TABULATION AND PLOTTING OF RESULTS

Numerical results for velocity potential distribution and exit gradient are obtained for different cases with the help of FORTRAN program. The calculated values are tabulated and plotted in the graph which are listed below:

4.1 Depressed Weir With Concrete Cutoff Downstream

Table 4.1.1 Variation of potential distribution with increasing thickness of cutoff for depressed weir with concrete cutoff (d/s)

D/B fixed, S/B varying										
D/B=0.05,S/B=0.05						Depressed weir with d/s concrete cutoff				
S.No.	T/B	$\Phi_C\%$	$\Phi_D\%$	$\Phi_E\%$	$\Phi_F\%$					
1	0.01	83.88	23.28272	19.78	15.57					
2	0.03	83.97	25.46648	22.57	15.11					
3	0.05	84.05	27.30124	24.71	14.9					
4	0.07	84.12	28.95087	26.55	14.77					
5	0.09	84.19	30.47798	28.22	14.68					
6	0.11	84.26	31.9159	29.77	14.61					
7	0.13	84.33	33.28531	31.22	14.56					
8	0.15	84.4	34.60022	32.61	14.51					
D/B=0.05,S/B=0.15						D/B=0.05,S/B=0.10				
S.No.	T/B	$\Phi_C\%$	$\Phi_D\%$	$\Phi_E\%$	$\Phi_F\%$	T/B	$\Phi_C\%$	$\Phi_D\%$	$\Phi_E\%$	$\Phi_F\%$
1	0.01	84.76	34.42492	26.88	22.43	0.01	84.32	29.49	23.76	19.38
2	0.03	84.88	36.13636	29.47	21.67	0.03	84.42	31.38	26.44	18.74
3	0.05	84.99	37.62973	31.43	21.28	0.05	84.52	33.01	28.48	18.42
4	0.07	85.09	39.0044	33.13	21.01	0.07	84.61	34.5	30.24	18.21
5	0.09	85.18	40.29911	34.66	20.8	0.09	84.69	35.89	31.83	18.06
6	0.11	85.28	41.53492	36.08	20.64	0.11	84.78	37.21	33.31	17.94
7	0.13	85.37	42.72511	37.42	20.51	0.13	84.86	38.47	34.7	17.84
8	0.15	85.46	43.87889	38.7	20.4	0.15	84.94	39.69	36.03	17.76

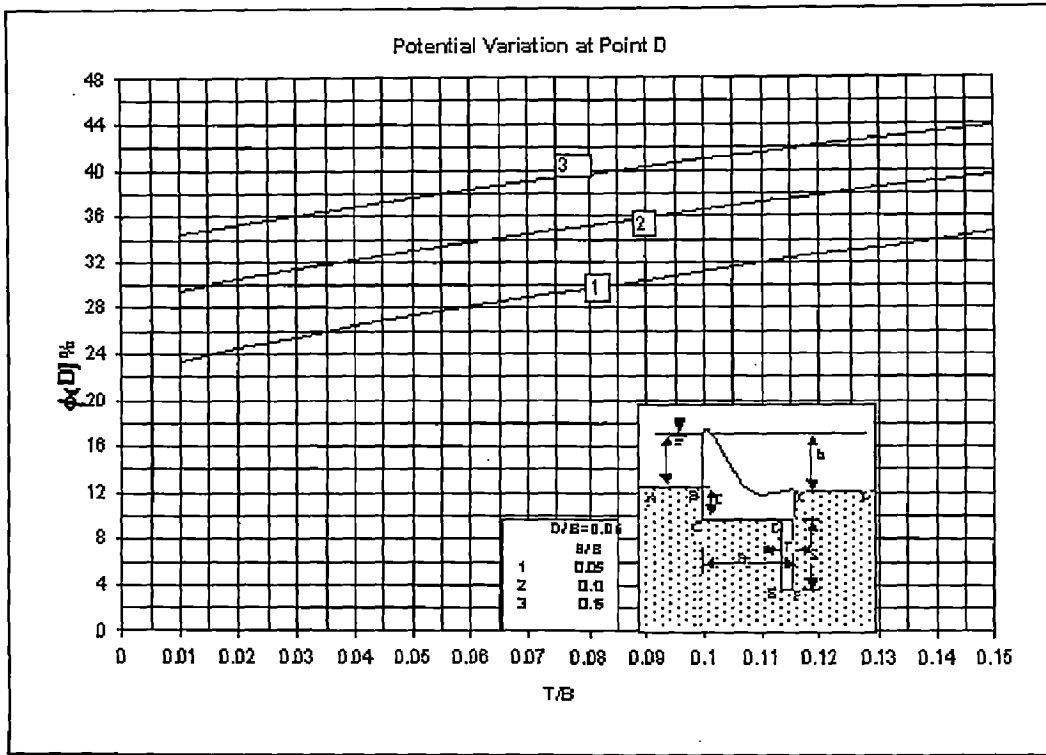


Figure 4.1.1 (a) Variation of ϕ_D with increasing cutoff thickness (d/s)

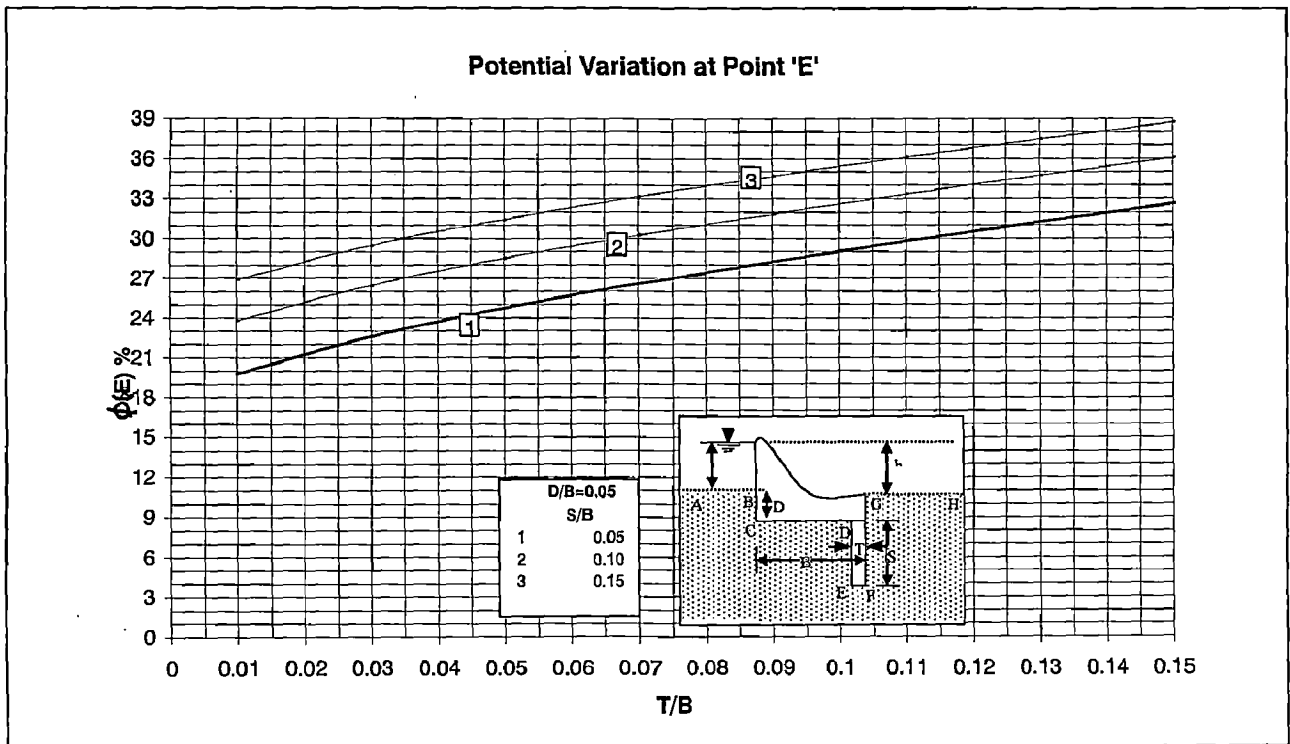


Figure 4.1.1 (b) Variation of ϕ_E with increasing cutoff thickness (d/s)

Table 4.1.2 Variation of potential distribution with increasing thickness of cutoff for depressed weir with concrete cutoff (d/s)

S/B fixed D/B varying									
S/B=.05,D/B=.02					S/B=.05,D/B=.06				
S.No.	T/B	$\Phi_C\%$	$\Phi_D\%$	$\Phi_E\%$	$\Phi_F\%$	$\Phi_C\%$	$\Phi_D\%$	$\Phi_E\%$	$\Phi_F\%$
1	0.01	87.75004	22.19153	18.39174	13.78046	83.01081	23.61907	20.19453	16.08962
2	0.02	87.78959	23.45061	20.06637	13.47753	83.06052	24.74883	21.6862	15.80341
3	0.03	87.8251	24.5645	21.44084	13.29919	83.10528	25.75419	22.91868	15.63262
4	0.04	87.85835	25.58706	22.65195	13.17565	83.14724	26.68106	24.01012	15.51328
5	0.05	87.89011	26.54394	23.7552	13.08286	83.18738	27.55132	25.0083	15.4231
6	0.06	87.92088	27.45016	24.78	13.00962	83.22624	28.37781	25.9386	15.35161
7	0.07	87.95089	28.31559	25.74433	12.94982	83.26416	29.16899	26.81647	15.29306
8	0.08	87.98036	29.14722	26.66017	12.89974	83.30139	29.93085	27.65224	15.24395
9	0.09	88.00941	29.95019	27.536	12.85701	83.3381	30.66783	28.45324	15.20201
10	0.1	88.03816	30.72849	28.37811	12.81998	83.37441	31.38334	29.22489	15.16566
11	0.11	88.06669	31.48526	29.19133	12.78749	83.41042	32.0801	29.97137	15.13378
12	0.12	88.09505	32.22306	29.97948	12.75871	83.44623	32.76034	30.696	15.10558
13	0.13	88.12331	32.94399	30.74561	12.73295	83.48188	33.42587	31.40141	15.08041
14	0.14	88.1515	33.64982	31.49224	12.70976	83.51746	34.07821	32.0898	15.05779
15	0.15	88.17967	34.34209	32.22151	12.68874	83.55299	34.7187	32.76301	15.03734
S/B=.05,D/B=.1					S/B=.05,D/B=.15				
S.No.	T/B	$\Phi_C\%$	$\Phi_D\%$	$\Phi_E\%$	$\Phi_F\%$	$\Phi_C\%$	$\Phi_D\%$	$\Phi_E\%$	$\Phi_F\%$
1	0.01	80.43277	24.82073	21.64195	17.85913	78.25401	26.06563	23.11003	19.61337
2	0.02	80.48658	25.86686	23.01697	17.58674	78.31049	27.03675	24.38155	19.35555
3	0.03	80.53512	26.80106	24.15751	17.42302	78.36152	27.90646	25.43961	19.1998
4	0.04	80.58065	27.66459	25.17058	17.30808	78.40942	28.71212	26.38174	19.09012
5	0.05	80.62423	28.47706	26.09936	17.22094	78.45527	29.4715	27.24727	19.00681
6	0.06	80.66643	29.25004	26.96675	17.15171	78.49966	30.19508	28.05701	18.94055
7	0.07	80.7076	29.99115	27.78673	17.09495	78.54298	30.88972	28.82365	18.88619
8	0.08	80.74802	30.70574	28.56861	17.0473	78.58549	31.56031	29.55568	18.84058
9	0.09	80.78786	31.39783	29.31902	17.00659	78.62738	32.21047	30.25909	18.80164
10	0.1	80.82726	32.07051	30.04286	16.97133	78.66881	32.84299	30.93834	18.76794
11	0.11	80.86633	32.72622	30.7439	16.94045	78.70988	33.46012	31.59688	18.73849
12	0.12	80.90517	33.36696	31.42511	16.91315	78.75068	34.06365	32.2374	18.7125
13	0.13	80.94384	33.99437	32.08891	16.88884	78.79129	34.65508	32.86209	18.68941
14	0.14	80.9824	34.60986	32.7373	16.86704	78.83178	35.23568	33.47275	18.66877
15	0.15	81.0209	35.2146	33.37191	16.84739	78.8722	35.80652	34.07089	18.65022

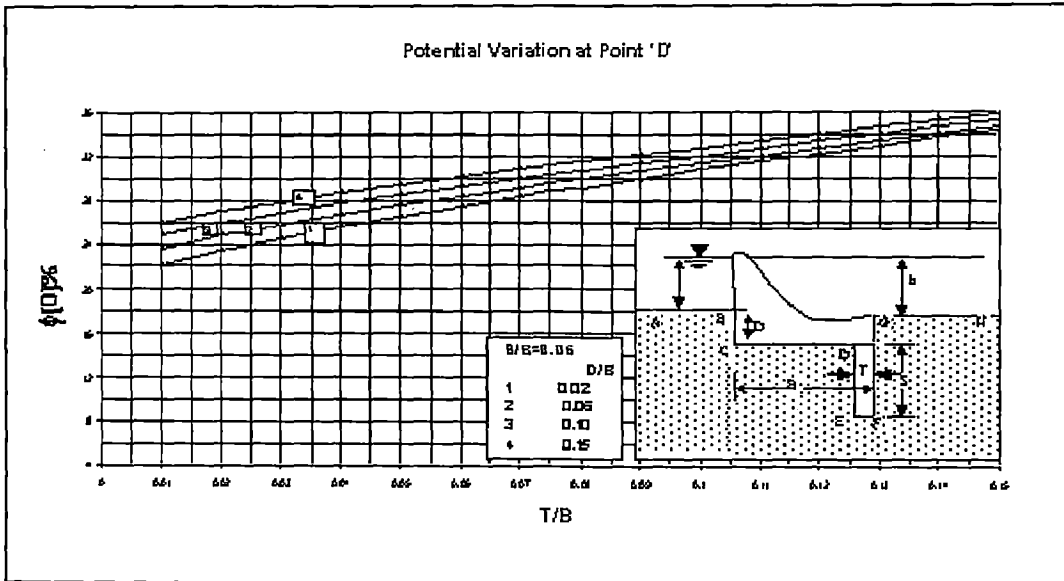


Figure 4.1.2 (a) Variation of ϕ_D with increasing cutoff thickness (d/s)

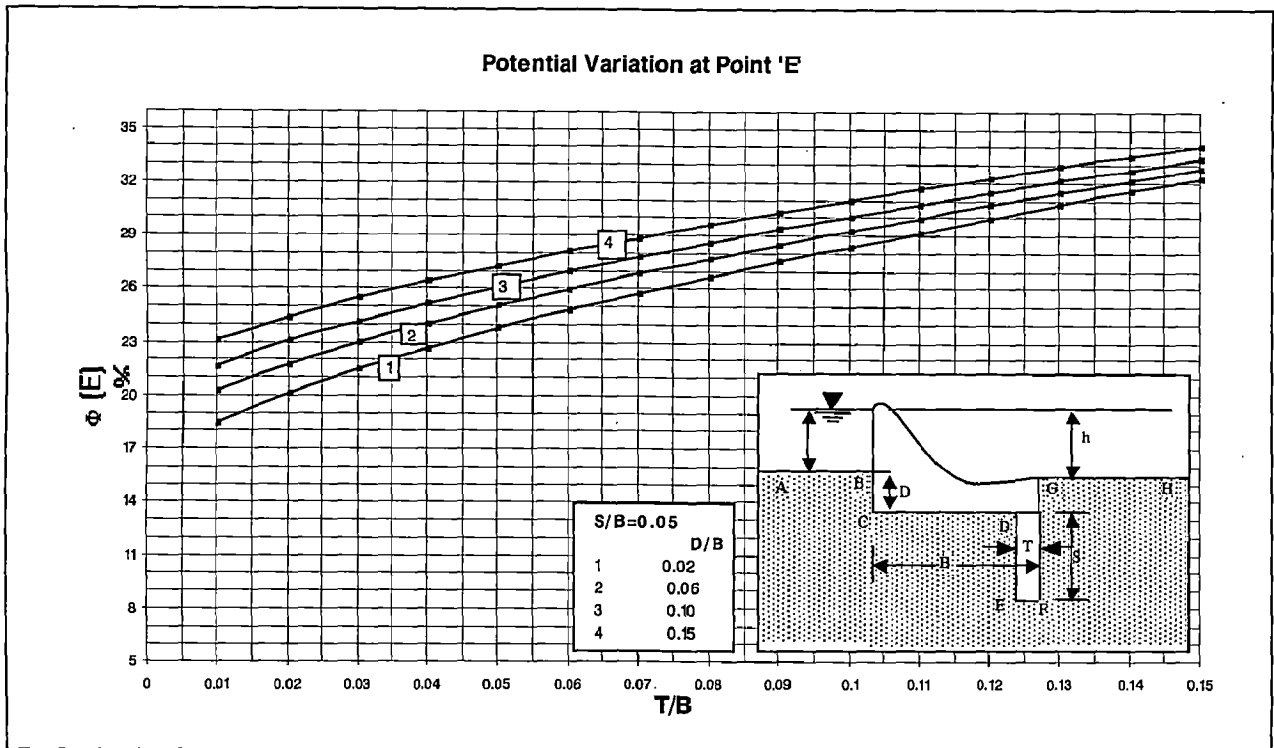


Figure 4.1.2 (b) Variation of ϕ_E with increasing cutoff thickness (d/s)

Table 4.1.3 Variation of potential distribution with increasing thickness of cutoff for depressed weir with concrete cutoff (d/s)

		S/B=0.12,D/B=0.02				S/B=0.12,D/B=0.06			
S.No.	T/B	$\Phi_C\%$	$\Phi_D\%$	$\Phi_E\%$	$\Phi_F\%$	$\Phi_C\%$	$\Phi_D\%$	$\Phi_E\%$	$\Phi_F\%$
1	0.01	88.27	31.31	24.42	19.71	83.64	31.7	25.32	20.99
2	0.02	88.32	32.32	25.97	19.26	83.71	32.64	26.74	20.57
3	0.03	88.36	33.24	27.23	18.98	83.76	33.48	27.91	20.3
4	0.04	88.4	34.09	28.35	18.78	83.81	34.28	28.94	20.11
5	0.05	88.44	34.9	29.37	18.61	83.86	35.03	29.88	19.95
6	0.06	88.48	35.67	30.31	18.48	83.91	35.75	30.76	19.83
7	0.07	88.52	36.41	31.2	18.37	83.96	36.44	31.59	19.72
8	0.08	88.56	37.14	32.05	18.27	84.01	37.12	32.38	19.63
9	0.09	88.59	37.84	32.86	18.19	84.05	37.77	33.13	19.55
10	0.1	88.63	38.52	33.64	18.11	84.1	38.41	33.86	19.48
11	0.11	88.66	39.19	34.4	18.05	84.14	39.03	34.57	19.41
12	0.12	88.7	39.84	35.13	17.99	84.19	39.65	35.25	19.36
13	0.13	88.73	40.48	35.84	17.93	84.23	40.25	35.92	19.3
14	0.14	88.77	41.11	36.53	17.88	84.28	40.84	36.57	19.25
15	0.15	88.8	41.73	37.21	17.83	84.32	41.43	37.2	19.21
		S/B=0.12,D/B=0.10				S/B=0.12,D/B=0.15			
S.No.	T/B	$\Phi_C\%$	$\Phi_D\%$	$\Phi_E\%$	$\Phi_F\%$	$\Phi_C\%$	$\Phi_D\%$	$\Phi_E\%$	$\Phi_F\%$
1	0.01	81.1	32.23	26.21	22.14	78.94	32.88	27.2	23.39
2	0.02	81.17	33.11	27.54	21.74	79.01	33.7	28.45	23.01
3	0.03	81.23	33.91	28.64	21.49	79.07	34.46	29.48	22.76
4	0.04	81.28	34.66	29.61	21.3	79.13	35.16	30.4	22.58
5	0.05	81.34	35.37	30.5	21.15	79.19	35.84	31.23	22.44
6	0.06	81.39	36.05	31.33	21.03	79.24	36.48	32.01	22.33
7	0.07	81.44	36.71	32.11	20.93	79.3	37.11	32.75	22.23
8	0.08	81.49	37.35	32.86	20.84	79.35	37.71	33.46	22.14
9	0.09	81.54	37.97	33.57	20.76	79.4	38.3	34.14	22.07
10	0.1	81.59	38.58	34.26	20.69	79.45	38.88	34.79	22
11	0.11	81.64	39.18	34.93	20.63	79.5	39.45	35.42	21.94
12	0.12	81.69	39.76	35.58	20.57	79.55	40	36.04	21.89
13	0.13	81.74	40.33	36.22	20.52	79.6	40.55	36.64	21.84
14	0.14	81.78	40.9	36.83	20.48	79.65	41.08	37.23	21.79
15	0.15	81.83	41.45	37.44	20.43	79.7	41.61	37.8	21.75

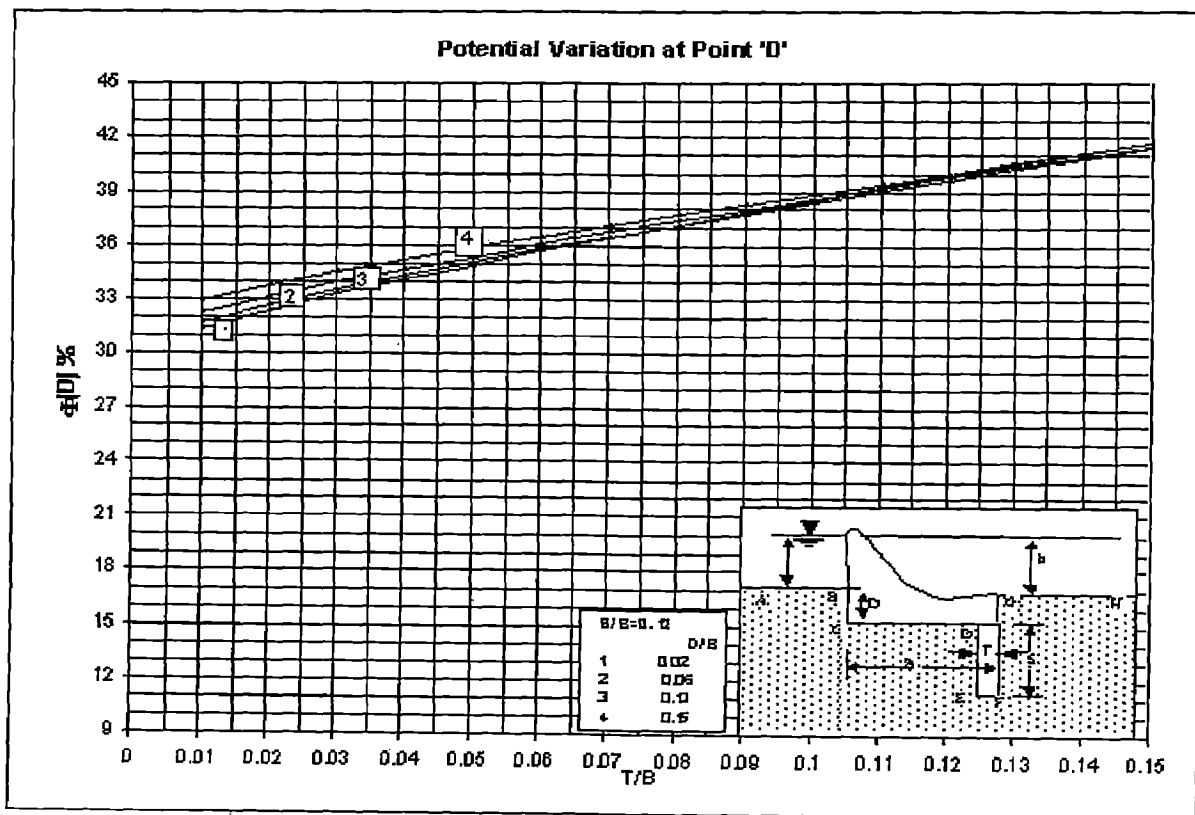


Figure 4.1.3 (a) Variation of ϕ_D with increasing cutoff thickness (d/s)

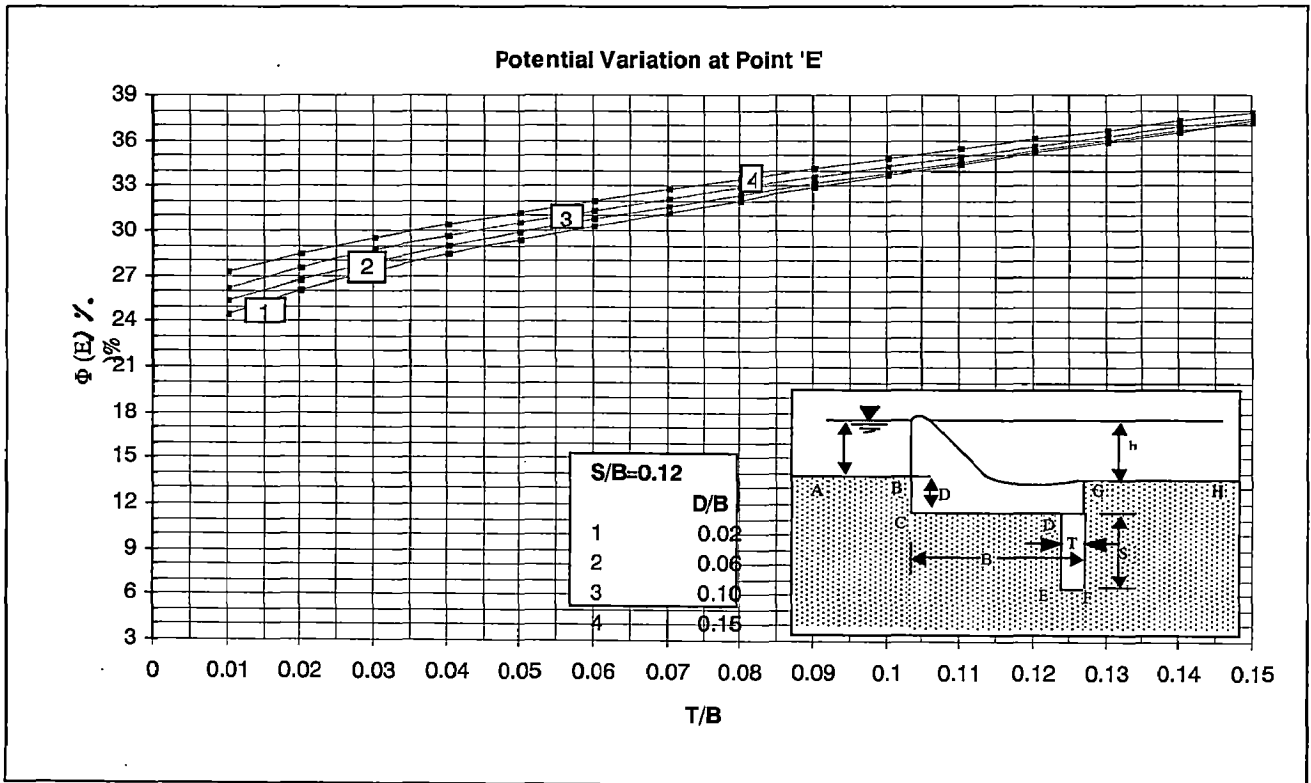


Figure 4.1.3 (b) Variation of ϕ_E with increasing cutoff thickness (d/s)

Table 4.1.4 Potential distribution with increasing cutoff depth of depressed weir with concrete cutoff (d/s)

D/B fixed, T/B varying									
D/B=0.05, T/B=0.05					D/B=0.05, T/B=0.10				
S.No.	S/B	$\phi_C\%$	$\phi_D\%$	$\phi_E\%$	$\phi_F\%$	$\phi_C\%$	$\phi_D\%$	$\phi_E\%$	$\phi_F\%$
1	0.01	83.668	21.045	20.418	11.25	83.81	25.488	24.985	11.186
2	0.03	83.859	24.485	22.802	13.203	84.022	28.606	27.21	13.031
3	0.05	84.048	27.301	24.707	14.9	84.229	31.207	29.008	14.641
4	0.07	84.237	29.763	26.347	16.413	84.432	33.502	30.562	16.08
5	0.09	84.425	31.978	27.804	17.783	84.634	35.58	31.943	17.386
6	0.11	84.613	34.004	29.12	19.039	84.834	37.49	33.192	18.584
7	0.13	84.801	35.88	30.323	20.199	85.033	39.264	34.333	19.691
8	0.15	84.988	37.63	31.432	21.277	85.229	40.923	35.384	20.72
D/B=0.05, T/B=0.15									
S.No.	S/B	$\phi_C\%$	$\phi_D\%$	$\phi_E\%$	$\phi_F\%$				
1	0.01	83.95	29.228	28.787	11.163				
2	0.03	84.18	32.144	30.896	12.951				
3	0.05	84.401	34.6	32.61	14.512				
4	0.07	84.618	36.78	34.094	15.906				
5	0.09	84.832	38.761	35.415	17.171				
6	0.11	85.043	40.588	36.609	18.331				
7	0.13	85.251	42.287	37.698	19.403				
8	0.15	85.457	43.879	38.701	20.398				

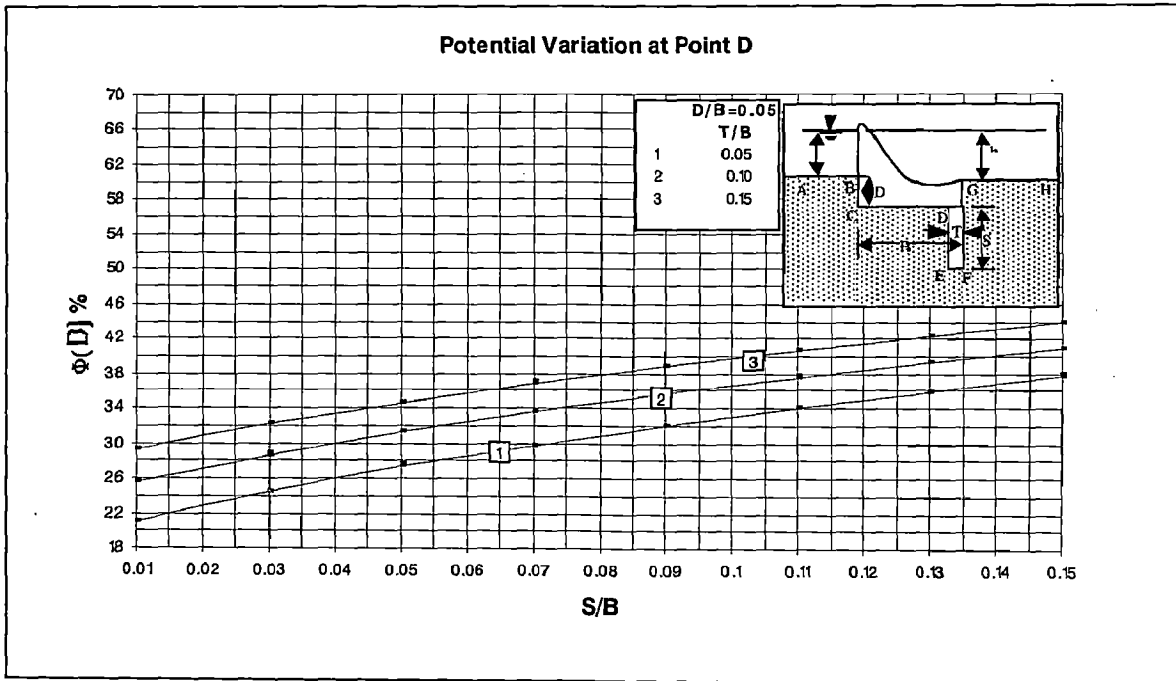


Figure 4.1.4 (a) Variation of ϕ_D with increasing cutoff depth (d/s)

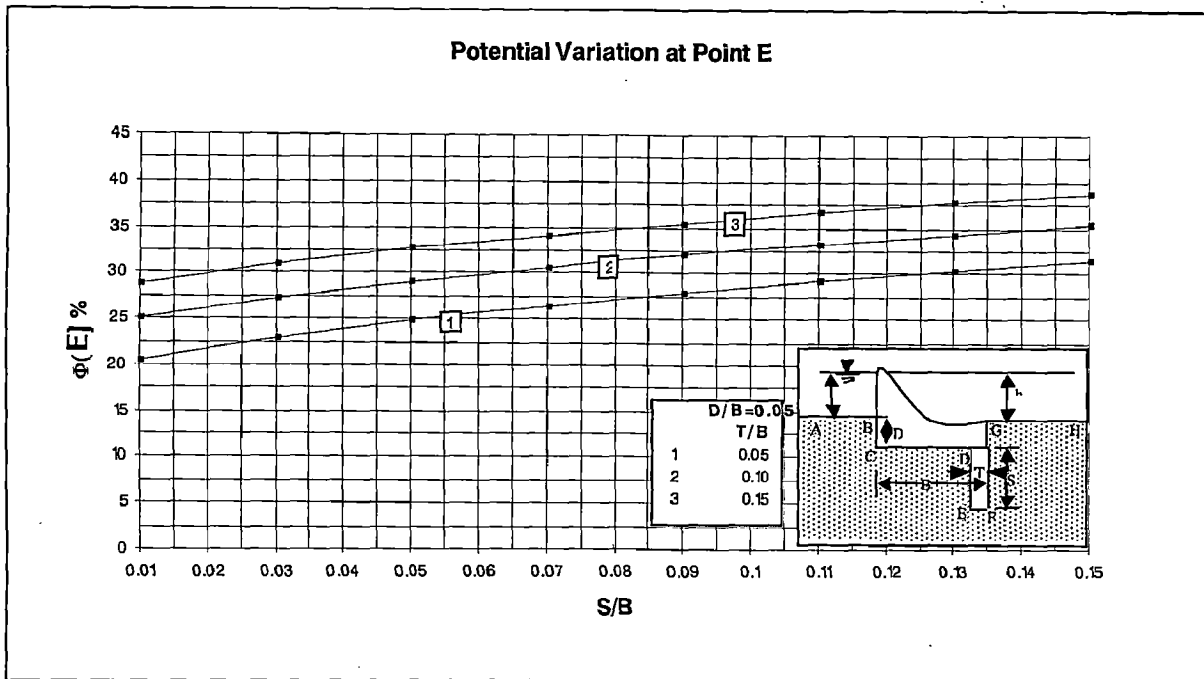


Figure 4.1.4 (b) Variation of ϕ_E with increasing cutoff depth (d/s)

Table 4.1.5 Potential distribution with increasing cutoff depth of depressed weir with concrete cutoff (d/s)

T/B fixed, D/B varying									
D/B=0.05, T/B=0.10					D/B=0.10, T/B=0.10				
S.No.	S/B	$\Phi_C\%$	$\Phi_D\%$	$\Phi_E\%$	$\Phi_F\%$	$\Phi_C\%$	$\Phi_D\%$	$\Phi_E\%$	$\Phi_F\%$
1	0.01	83.80964	25.48787	24.9852	11.186	80.38382	27.03429	26.57817	14.31846
2	0.03	84.02206	28.60641	27.21045	13.03081	80.60736	29.7637	28.48471	15.7088
3	0.05	84.22866	31.20659	29.00816	14.64094	80.82726	32.07051	30.04286	16.97133
4	0.07	84.4324	33.50164	30.56152	16.08012	81.04633	34.12948	31.40425	18.1326
5	0.09	84.63412	35.57962	31.94283	17.38615	81.26506	36.01075	32.62659	19.2095
6	0.11	84.83413	37.48982	33.19165	18.5839	81.48351	37.75327	33.74096	20.21412
7	0.13	85.03254	39.26378	34.33301	19.6909	81.70156	39.38196	34.7669	21.15561
8	0.15	85.22939	40.92342	35.38418	20.72013	81.91908	40.91418	35.71792	22.04113

D/B=0.15, T/B=0.10					
S.No.	S/B	$\Phi_C\%$	$\Phi_D\%$	$\Phi_E\%$	$\Phi_F\%$
1	0.01	78.21976	28.2376	27.81307	16.53296
2	0.03	78.44579	30.72707	29.53039	17.69657
3	0.05	78.66881	32.84299	30.93834	18.76794
4	0.07	78.89191	34.74197	32.174	19.76535
5	0.09	79.11562	36.48564	33.28849	20.69989
6	0.11	79.33991	38.10783	34.30894	21.57947
7	0.13	79.56463	39.63004	35.25224	22.41014
8	0.15	79.78954	41.06722	36.12996	23.19674

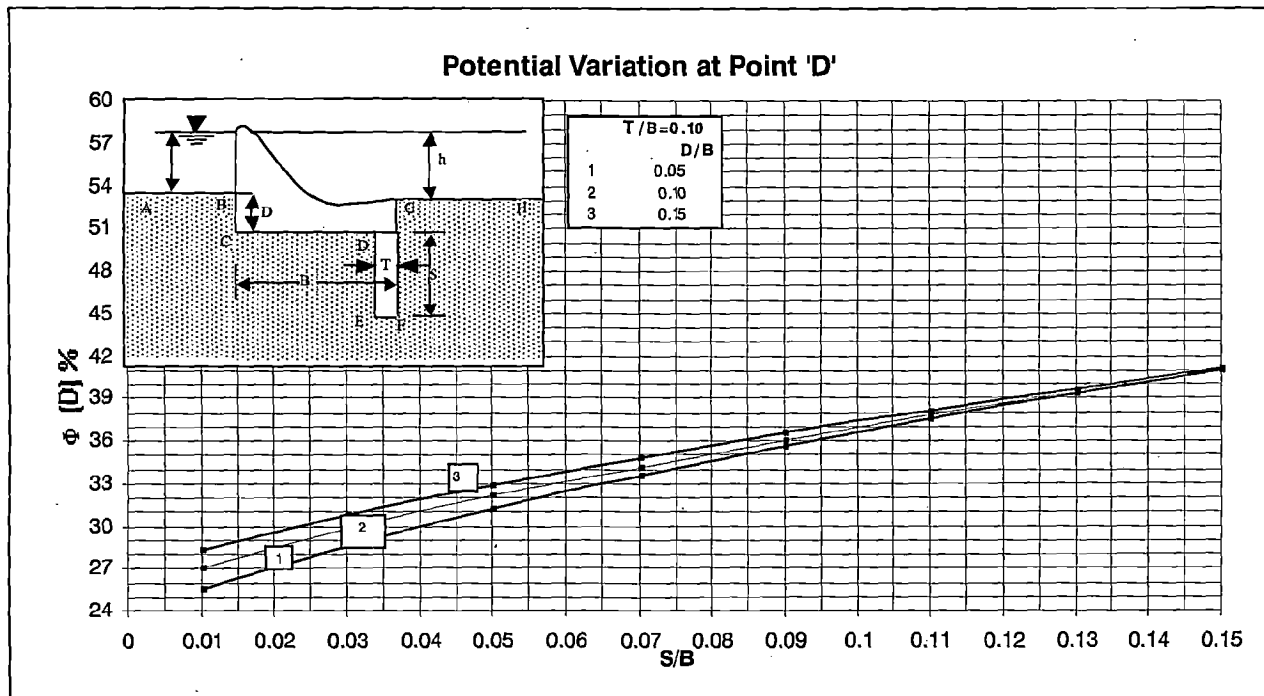


Figure 4.1.5 (a) Variation of Φ_D with increasing cutoff depth (d/s)

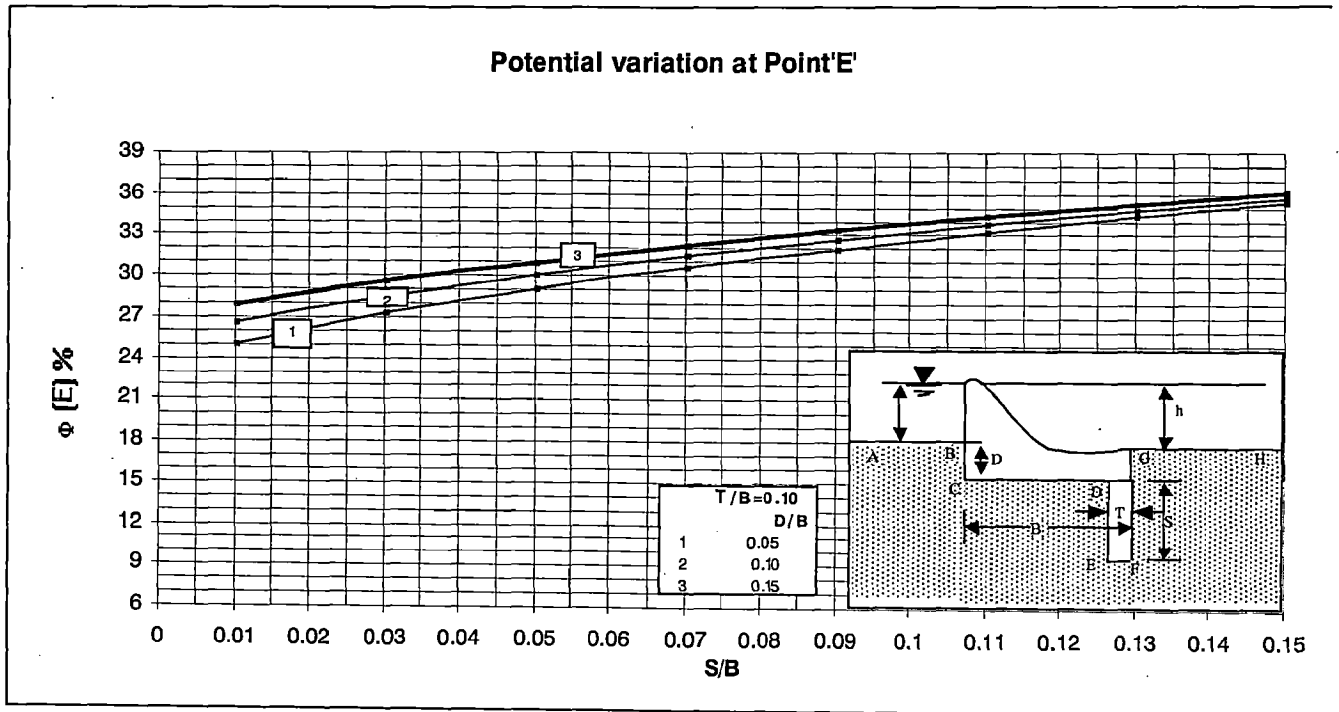


Figure 4.1.5 (b) Variation of ϕ_E with increasing cutoff depth (d/s)

Table 4.1.6 Potential distribution with increasing cutoff depth of depressed weir with concrete cutoff (d/s)

		T/B fixed, D/B varying							
		D/B=0.05, T/B=0.05				D/B=0.10, T/B=0.05			
S.No.	S/B	$\phi_C\%$	$\phi_D\%$	$\phi_E\%$	$\phi_F\%$	$\phi_C\%$	$\phi_D\%$	$\phi_E\%$	$\phi_F\%$
1	0.01	83.66751	21.04513	20.41763	11.24959	80.22076	23.01777	22.45477	14.37655
2	0.03	83.85861	24.48463	22.80184	13.20337	80.42271	25.99894	24.46953	15.87499
3	0.05	84.04784	27.30124	24.70729	14.90006	80.62423	28.47706	26.09936	17.22094
4	0.07	84.23669	29.76303	26.34742	16.41282	80.82708	30.66965	27.51924	18.4521
5	0.09	84.42526	31.97766	27.80365	17.78349	81.03121	32.66173	28.79324	19.58997
6	0.11	84.61348	34.00413	29.11965	19.03919	81.23634	34.4995	29.95508	20.64905
7	0.13	84.80118	35.87965	30.32273	20.19889	81.44215	36.21217	31.0257	21.63998
8	0.15	84.98823	37.62973	31.43161	21.27654	81.64833	37.81982	32.01939	22.57092
		D/B=0.15, T/B=0.05							
S.No.	S/B	$\phi_D\%$	$\phi_E\%$	$\phi_F\%$	$\phi_G\%$				
1	0.01	78.04	24.50	23.98	16.58				
2	0.03	78.2506	27.20941	25.78568	17.85414				
3	0.05	78.45527	29.4715	27.24727	19.00681				
4	0.07	78.66188	31.48466	28.5263	20.07189				
5	0.09	78.87053	33.32331	29.67934	21.06518				
6	0.11	79.08092	35.0275	30.73568	21.99713				
7	0.13	79.29274	36.62228	31.71324	22.87523				
8	0.15	79.50561	38.12491	32.6242	23.70535				

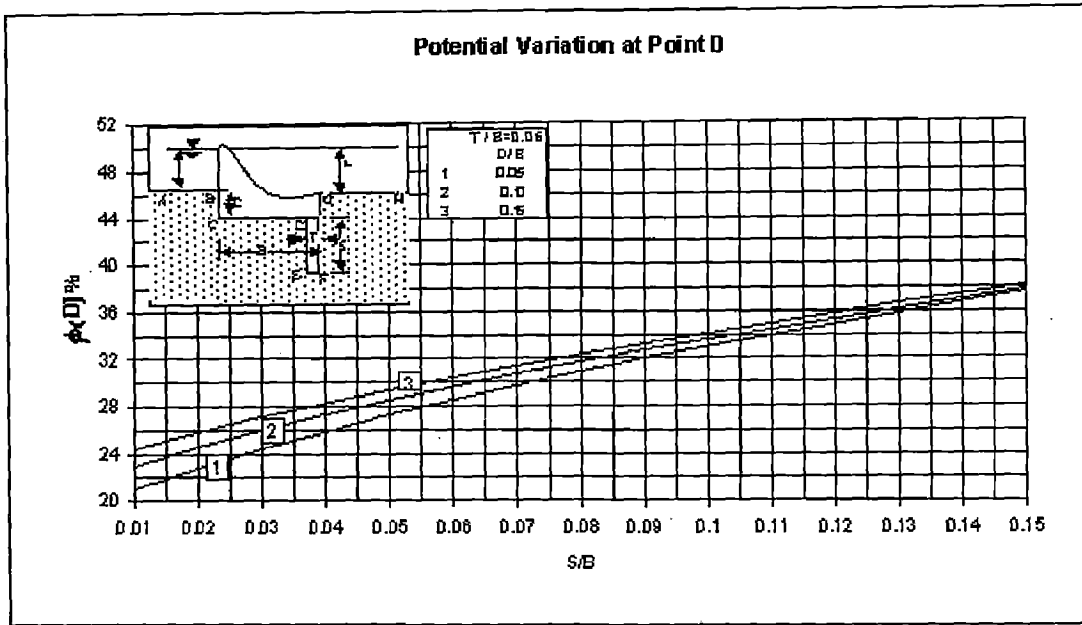


Figure 4.1.6 (a) Variation of ϕ_D with increasing cutoff depth (d/s)

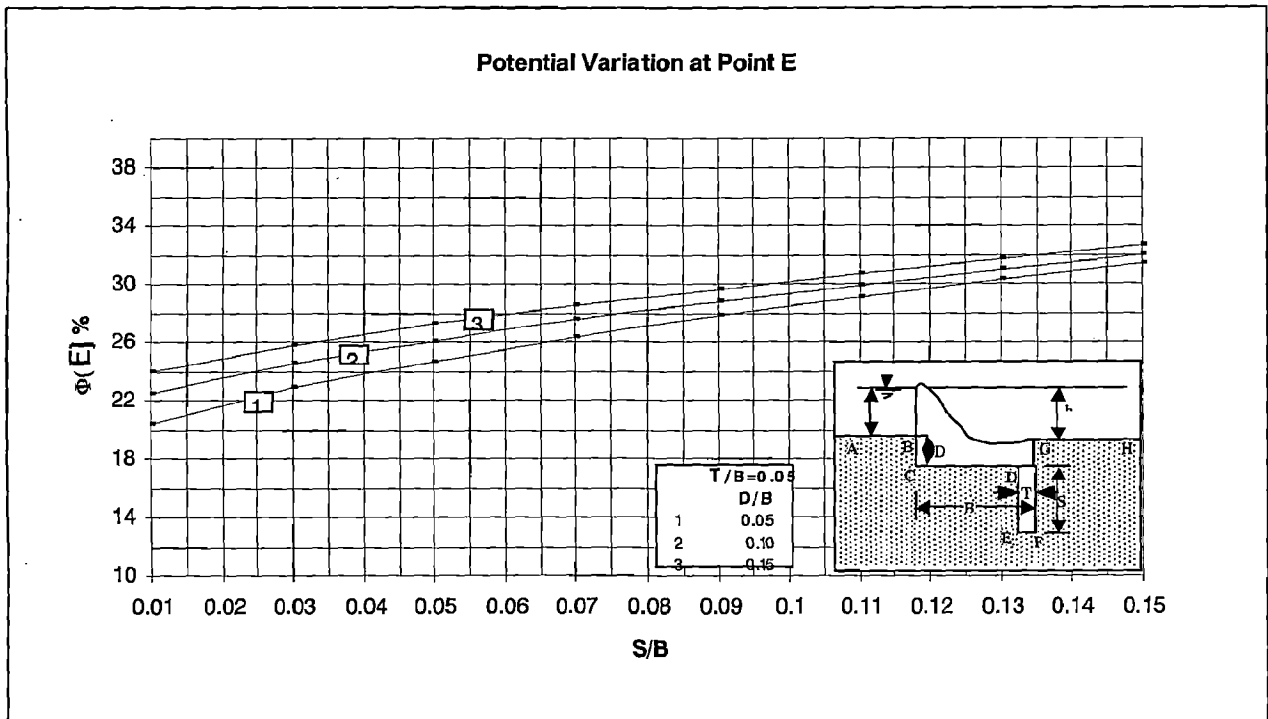


Figure 4.1.6 (b) Variation of ϕ_E with increasing cutoff depth (d/s)

Table 4.1.7 Variation of potential distribution with increasing depression for depressed weir with d/s concrete cutoff

S/B fixed T/B varying

S.No.	D/B	S/B=0.05, T/B=0.05				S/B=0.05, T/B=0.15			
		$\Phi_C\%$	$\Phi_D\%$	$\Phi_E\%$	$\Phi_F\%$	$\Phi_C\%$	$\Phi_D\%$	$\Phi_E\%$	$\Phi_F\%$
1	0.01	90.25843	26.34323	23.46338	12.38216	90.50086	34.37246	32.19062	11.98597
2	0.03	86.29103	26.78978	24.07529	13.73526	86.60913	34.39845	32.32751	13.34278
3	0.05	84.04784	27.30124	24.70729	14.90006	84.40134	34.60022	32.61013	14.51174
4	0.07	82.43665	27.79437	25.29776	15.91307	82.81213	34.84152	32.91732	15.53012
5	0.09	81.16993	28.25723	25.84277	16.80895	81.56062	35.09074	33.22272	16.43214
6	0.11	80.12373	28.68945	26.34616	17.61225	80.52559	35.33701	33.51814	17.24202
7	0.13	79.23208	29.09328	26.81281	18.34056	79.64241	35.57614	33.80103	17.97712
8	0.15	78.45527	29.4715	27.24727	19.00681	78.8722	35.80652	34.07089	18.65022

S/B=0.05, T/B=0.10					
S.No.	D/B	$\Phi_C\%$	$\Phi_D\%$	$\Phi_E\%$	$\Phi_F\%$
1	0.01	90.38236	30.65722	28.23575	12.11804
2	0.03	86.4537	30.86821	28.57564	13.47343
3	0.05	84.22866	31.20659	29.00816	14.64094
4	0.07	82.62875	31.5595	29.4376	15.65744
5	0.09	81.36987	31.90381	29.84691	16.55726
6	0.11	80.32944	32.23317	30.23295	17.36476
7	0.13	79.44218	32.54613	30.59624	18.09738
8	0.15	78.66881	32.84299	30.93834	18.76794

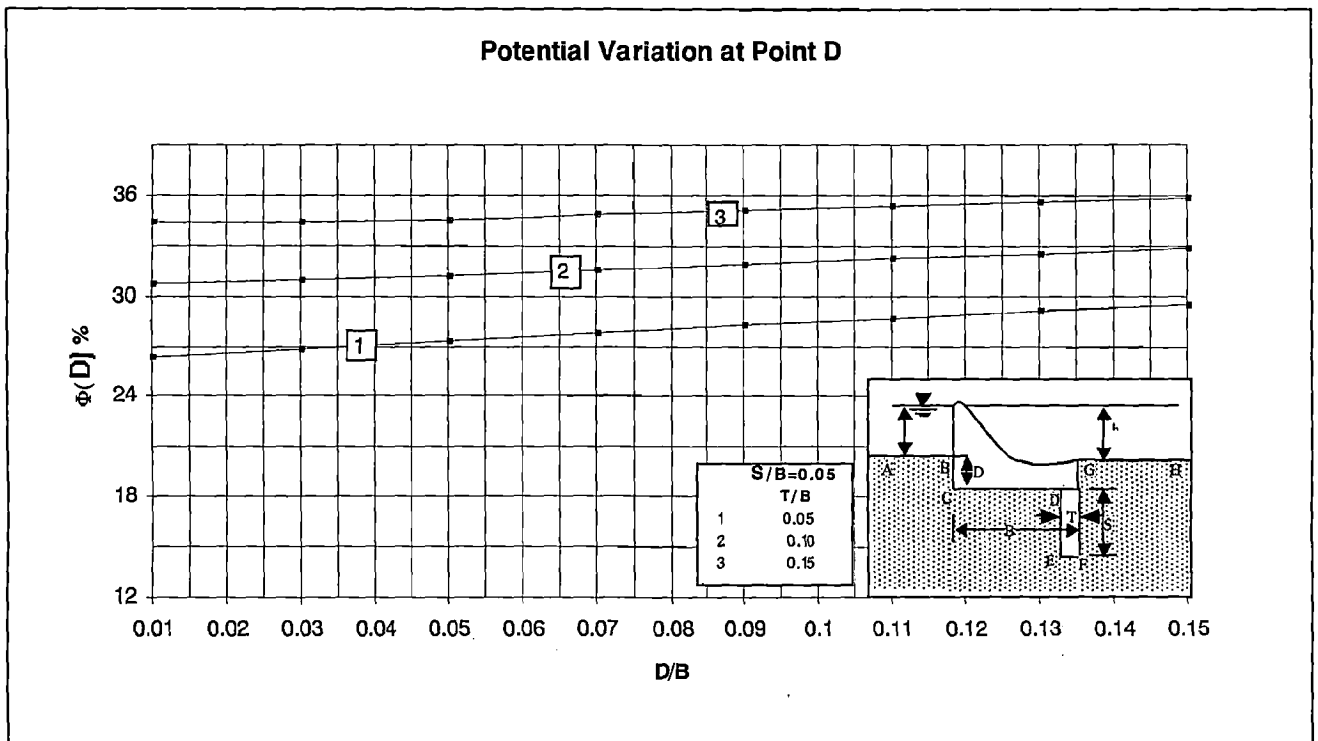


Figure 4.1.7 (a) Variation of Φ_D with increasing depression

Potential Variation at Point E

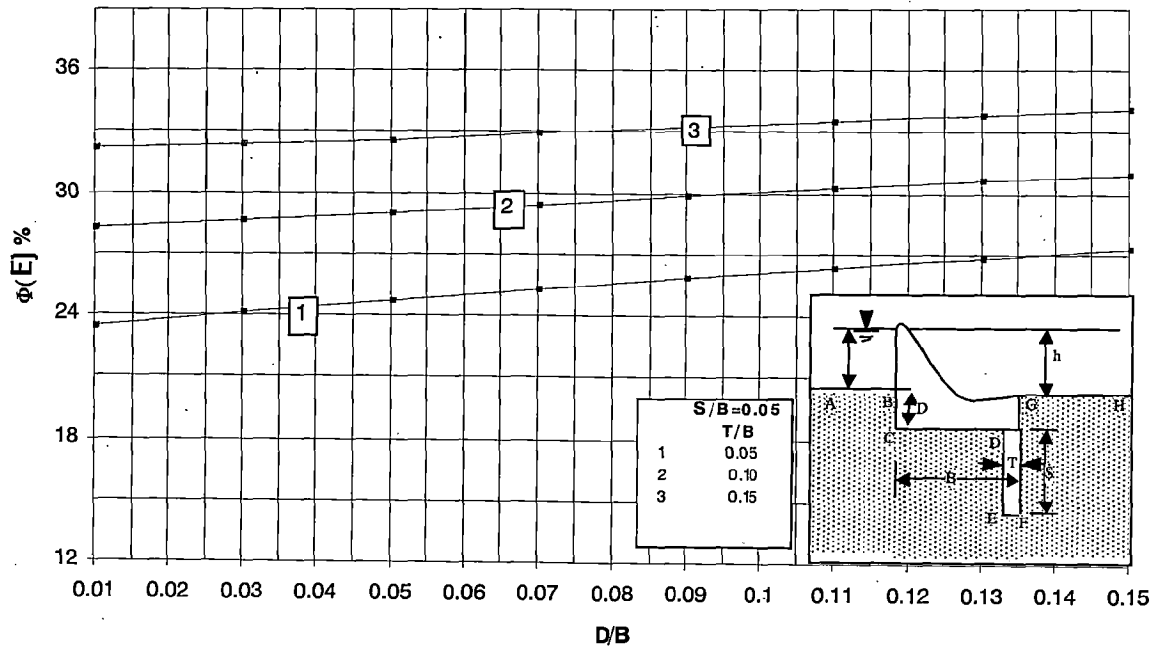


Figure 4.1.7 (b) Variation of ϕ_E with increasing depression

Table 4.1.8 Variation of potential distribution with increasing depression for depressed weir with concrete cutoff (D/S)

S.No.	D/B	T/B=0.05, S/B=0.05				T/B=0.05, S/B=0.10			
		$\phi_C\%$	$\phi_D\%$	$\phi_E\%$	$\phi_F\%$	$\phi_C\%$	$\phi_D\%$	$\phi_E\%$	$\phi_F\%$
1	0.01	90.25843	26.34323	23.46338	12.38216	90.59398	32.84916	27.90571	16.84591
2	0.03	86.29103	26.78978	24.07529	13.73526	86.72327	32.83703	28.12848	17.64487
3	0.05	84.04784	27.30124	24.70729	14.90006	84.51942	33.01174	28.47721	18.42438
4	0.07	82.43665	27.79437	25.29776	15.91307	82.92933	33.23643	28.84555	19.14723
5	0.09	81.16993	28.25723	25.84277	16.80895	81.67509	33.47647	29.20924	19.81427
6	0.11	80.12373	28.68945	26.34616	17.61225	80.63654	33.71879	29.56056	20.43124
7	0.13	79.23208	29.09328	26.81281	18.34056	79.74959	33.95764	29.89705	21.00413
8	0.15	78.45527	29.4715	27.24727	19.00681	78.97552	34.19041	30.2183	21.53831
T/B=0.05, S/B=0.15									
S.No.	D/B	$\phi_C\%$	$\phi_D\%$	$\phi_E\%$	$\phi_F\%$				
1	0.01	90.91869	37.95387	31.25848	20.23345				
2	0.03	87.14835	37.6671	31.25757	20.72851				
3	0.05	84.98823	37.62973	31.43161	21.27654				
4	0.07	83.42296	37.67809	31.65563	21.81278				
5	0.09	82.1842	37.7668	31.89679	22.32483				
6	0.11	81.15571	37.87663	32.14208	22.81038				
7	0.13	80.27536	37.9978	32.38552	23.27003				
8	0.15	79.50561	38.12491	32.6242	23.70535				

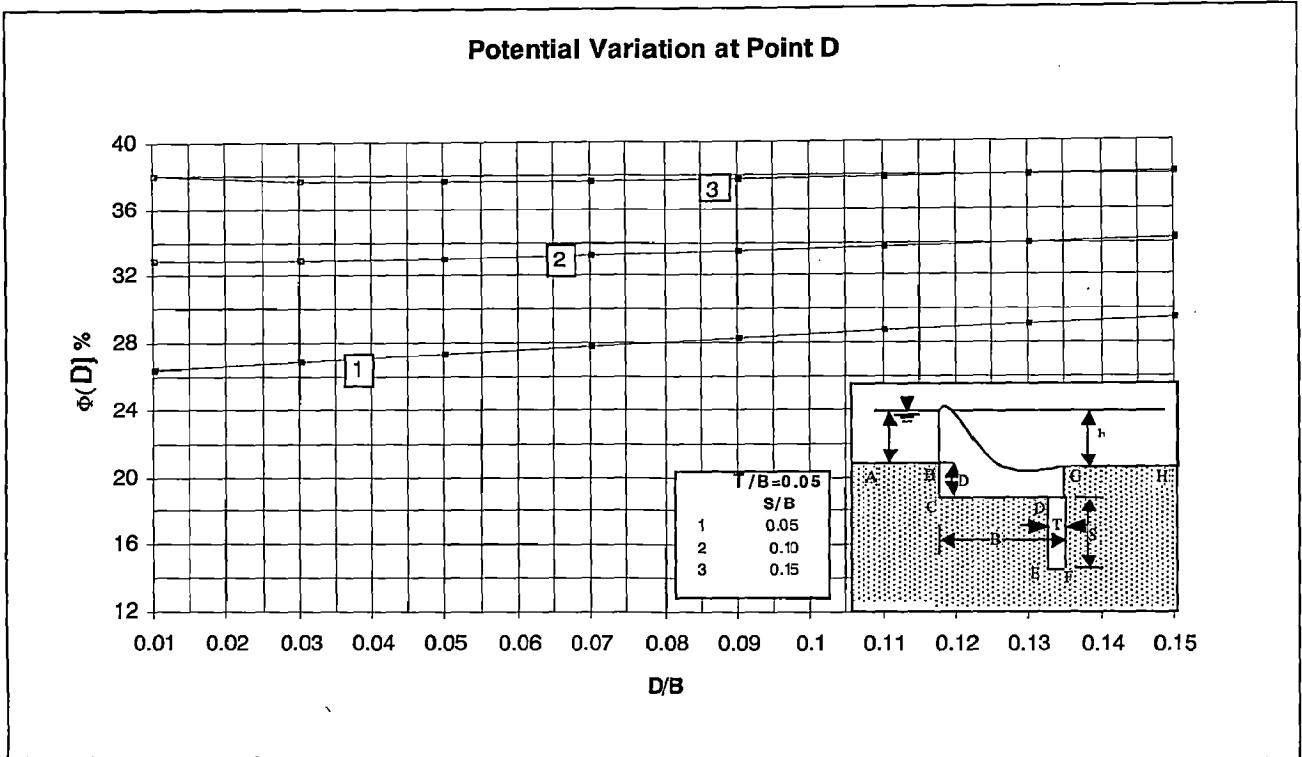


Figure 4.1.8 (a) Variation of ϕ_D with increasing depression

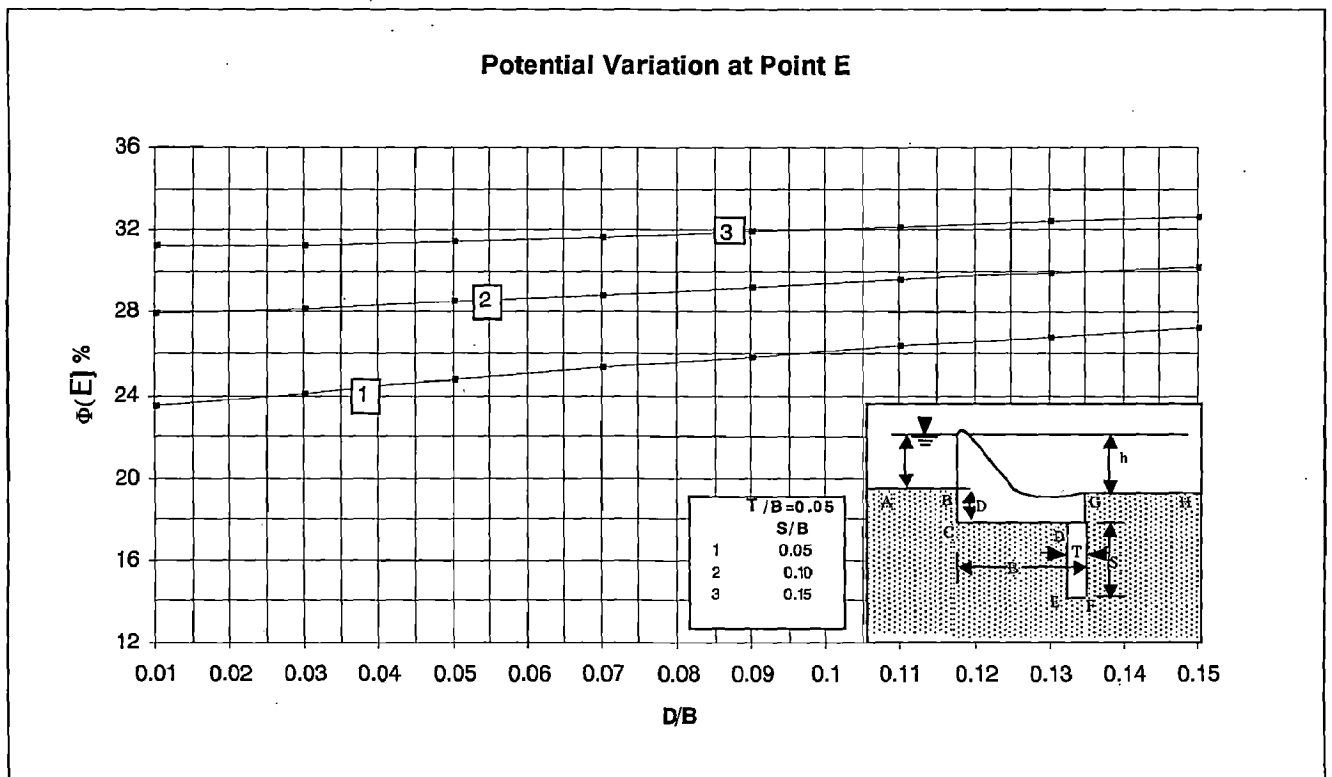


Figure 4.1.8 (b) Variation of ϕ_E with increasing depression

Table 4.1.9 Potential variation at the key points with increasing u/s and d/s depression respectively

S.No.	D1/B	D2/B	S/B	T/B	$\phi_D\%$	$\phi_E\%$	S.No.	D1/B	D2/B	S/B	T/B	$\phi_D\%$	$\phi_E\%$
1	0.02	0.02	0.05	0.01	22.19	13.78	1	0.02	0.02	0.05	0.03	24.56	13.3
2	0.05	0.02	0.05	0.01	21.57	13.4	2	0.05	0.02	0.05	0.03	23.88	12.93
3	0.07	0.02	0.05	0.01	21.27	13.22	3	0.07	0.02	0.05	0.03	23.55	12.76
4	0.09	0.02	0.05	0.01	21.02	13.06	4	0.09	0.02	0.05	0.03	23.27	12.61
5	0.11	0.02	0.05	0.01	20.8	12.93	5	0.11	0.02	0.05	0.03	23.03	12.48
6	0.13	0.02	0.05	0.01	20.6	12.81	6	0.13	0.02	0.05	0.03	22.81	12.37
7	0.15	0.02	0.05	0.01	20.42	12.7	7	0.15	0.02	0.05	0.03	22.61	12.26
S.No.	D1/B	D2/B	S/B	T/B	$\phi_D\%$	$\phi_E\%$	S.No.	D1/B	D2/B	S/B	T/B	$\phi_D\%$	$\phi_E\%$
1	0.02	0.02	0.05	0.01	22.19	13.78	1	0.02	0.02	0.05	0.03	24.56	13.3
2	0.02	0.05	0.05	0.01	23.94	16.01	2	0.02	0.05	0.05	0.03	26.19	15.53
3	0.02	0.07	0.05	0.01	24.95	17.26	3	0.02	0.07	0.05	0.03	27.13	16.78
4	0.02	0.09	0.05	0.01	25.86	18.38	4	0.02	0.09	0.05	0.03	27.98	17.91
5	0.02	0.11	0.05	0.01	26.7	19.39	5	0.02	0.11	0.05	0.03	28.77	18.92
6	0.02	0.13	0.05	0.01	27.47	20.32	6	0.02	0.13	0.05	0.03	29.49	19.86
7	0.02	0.15	0.05	0.01	28.19	21.18	7	0.02	0.15	0.05	0.03	30.18	20.72
S.No.	D1/B	D2/B	S/B	T/B	$\phi_D\%$	$\phi_E\%$	S.No.	D1/B	D2/B	S/B	T/B	$\phi_D\%$	$\phi_E\%$
1	0.02	0.02	0.05	0.05	26.54	13.08	1	0.02	0.02	0.05	0.1	30.73	12.82
2	0.05	0.02	0.05	0.05	25.8	12.73	2	0.05	0.02	0.05	0.1	29.87	12.48
3	0.07	0.02	0.05	0.05	25.45	12.56	3	0.07	0.02	0.05	0.1	29.46	12.31
4	0.09	0.02	0.05	0.05	25.15	12.41	4	0.09	0.02	0.05	0.1	29.11	12.17
5	0.11	0.02	0.05	0.05	24.88	12.28	5	0.11	0.02	0.05	0.1	28.81	12.05
6	0.13	0.02	0.05	0.05	24.65	12.17	6	0.13	0.02	0.05	0.1	28.54	11.94
7	0.15	0.02	0.05	0.05	24.44	12.07	7	0.15	0.02	0.05	0.1	28.29	11.84
S.No.	D1/B	D2/B	S/B	T/B	$\phi_D\%$	$\phi_E\%$	S.No.	D1/B	D2/B	S/B	T/B	$\phi_D\%$	$\phi_E\%$
1	0.02	0.02	0.05	0.05	26.54	13.08	1	0.02	0.02	0.05	0.1	30.73	12.82
2	0.02	0.05	0.05	0.05	28.07	15.31	2	0.02	0.05	0.05	0.1	32.09	15.04
3	0.02	0.07	0.05	0.05	28.96	16.56	3	0.02	0.07	0.05	0.1	32.88	16.29
4	0.02	0.09	0.05	0.05	29.77	17.68	4	0.02	0.09	0.05	0.1	33.61	17.41
5	0.02	0.11	0.05	0.05	30.52	18.7	5	0.02	0.11	0.05	0.1	34.29	18.42
6	0.02	0.13	0.05	0.05	31.22	19.64	6	0.02	0.13	0.05	0.1	34.92	19.36
7	0.02	0.15	0.05	0.05	31.87	20.51	7	0.02	0.15	0.05	0.1	35.51	20.23

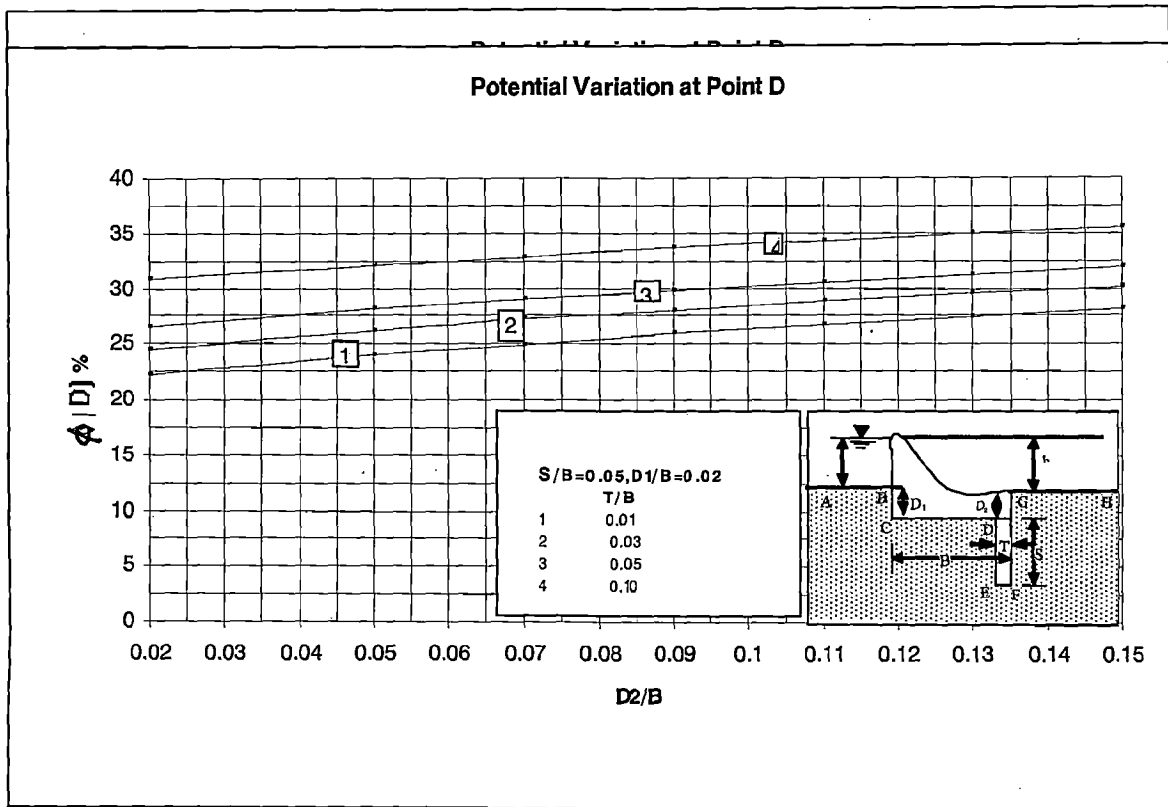
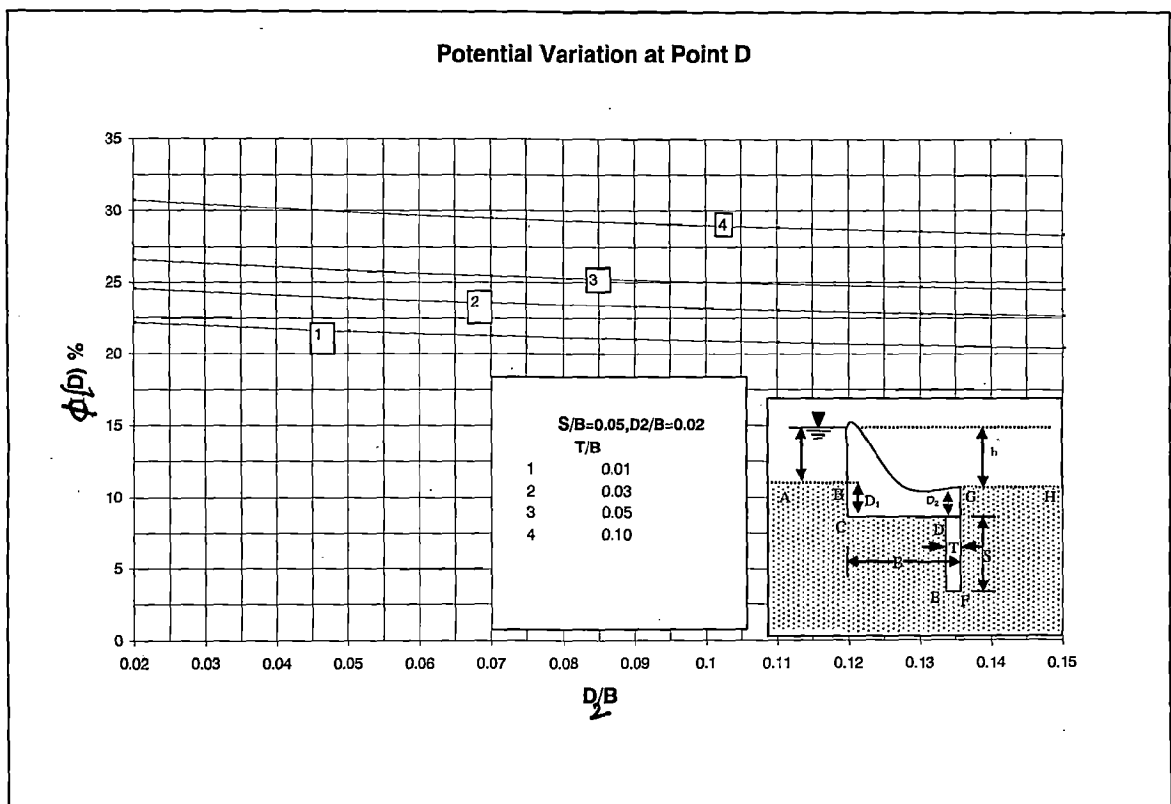


Figure 4.1.9 (a) Variation of ϕ_D with increasing u/s depression Figure 4.1.9 (b) Variation of



ϕ_D with increasing d/s depression

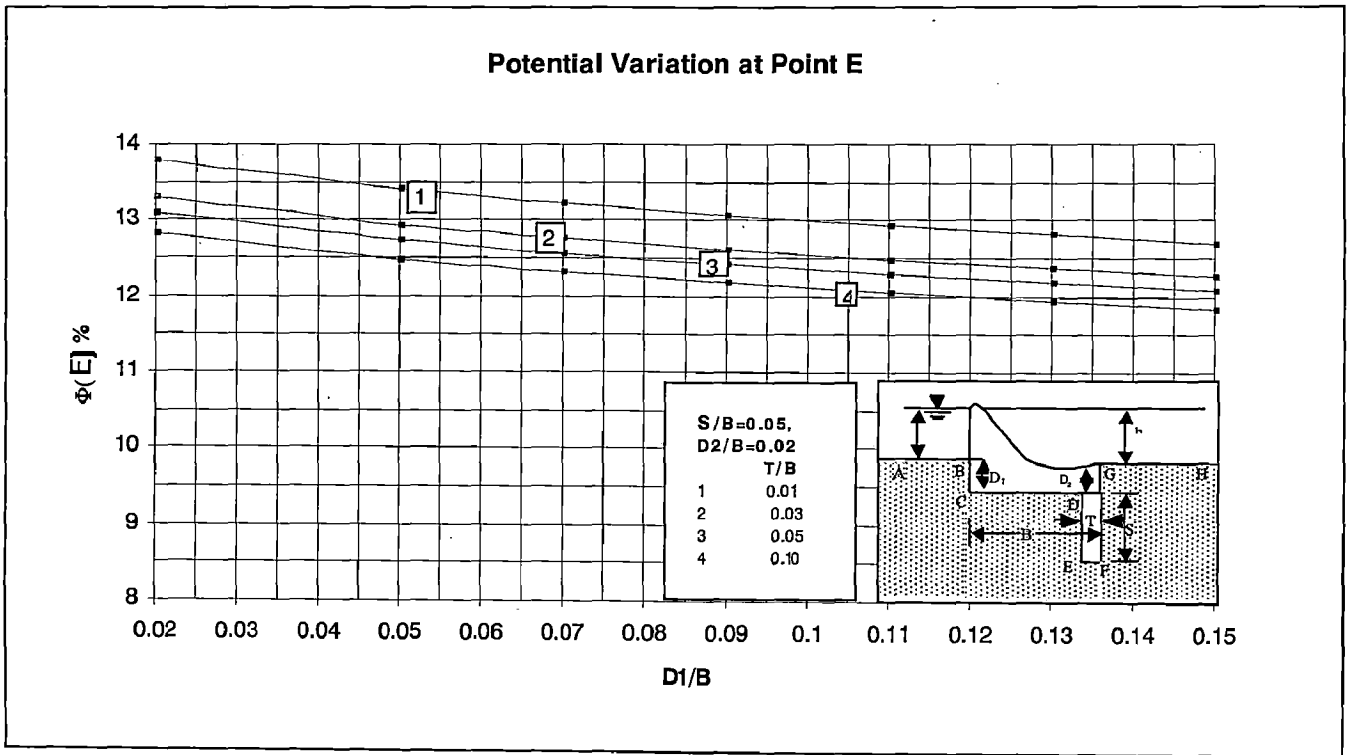


Figure 4.1.9 (c) Variation of ϕ_E with increasing u/s depression

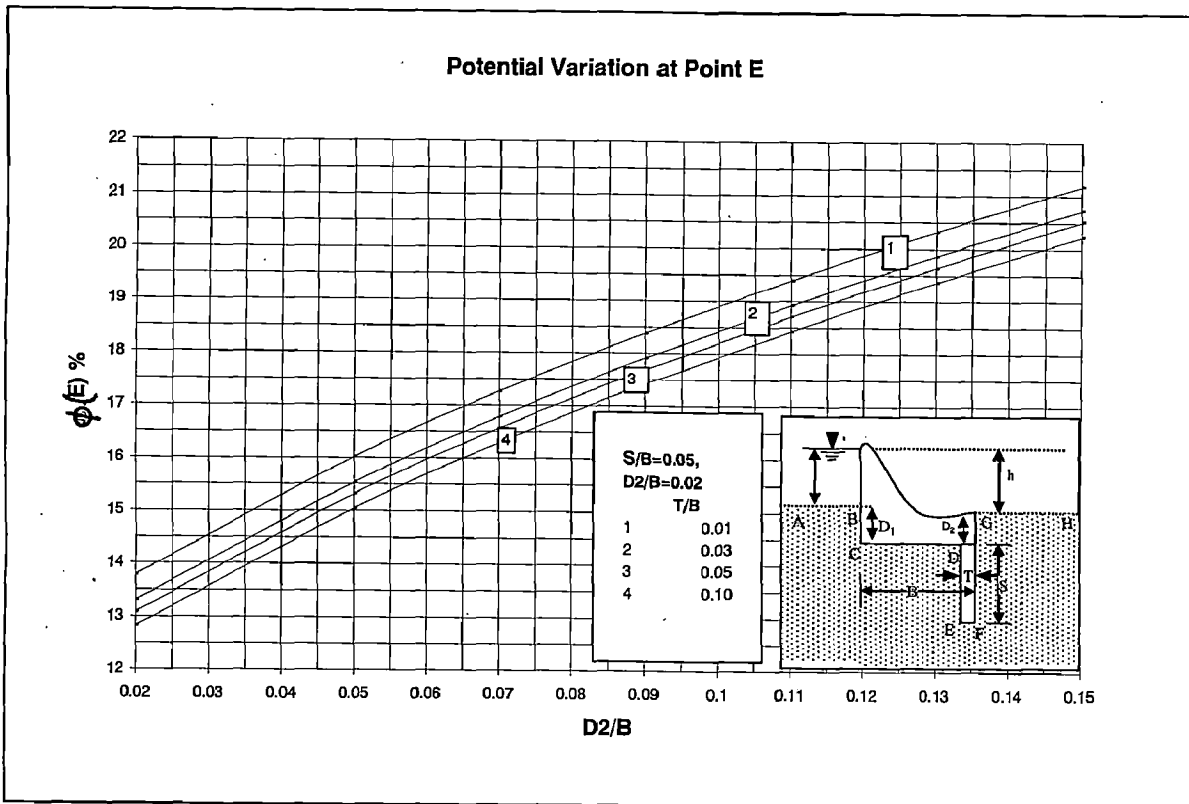


Figure 4.1.9 (d) Variation of ϕ_E with increasing d/s depression

4.2 Depressed Weir With Concrete Cutoff Upstream

Table 4.2.1 Variation of potential distribution with increasing thickness of cutoff for depressed weir with concrete cutoff (u/s)

S/B fixed D/B varying

S/B=0.05,D/B=0.02						S/B=0.05,D/B=0.06			
S.No.	T/B	$\Phi_C\%$	$\Phi_D\%$	$\Phi_E\%$	$\Phi_F\%$	$\Phi_C\%$	$\Phi_D\%$	$\Phi_E\%$	$\Phi_F\%$
1	0.01	85.22724	80.5547	76.6897	6.75088	83.12175	78.86159	75.30193	11.20359
2	0.02	85.17783	78.56258	75.14351	6.72538	83.06844	77.01862	73.85839	11.16114
3	0.03	85.08926	76.96685	73.82481	6.70564	82.97779	75.53385	72.62257	11.12806
4	0.04	84.99193	75.58438	72.64133	6.68903	82.87863	74.24271	71.51075	11.10007
5	0.05	84.89394	74.34137	71.55188	6.67447	82.77873	73.07872	70.48547	11.07547
6	0.06	84.79803	73.19891	70.53321	6.6614	82.68081	72.00676	69.52554	11.0533
7	0.07	84.70521	72.13342	69.5705	6.64948	82.58586	71.00546	68.61743	11.03302
8	0.08	84.61578	71.12926	68.65352	6.6384	82.49422	70.06062	67.75179	11.01422
9	0.09	84.52975	70.17544	67.77486	6.62808	82.40591	69.16222	66.92176	10.99665
10	0.1	84.44699	69.26379	66.92885	6.61835	82.32082	68.30285	66.12219	10.98008
11	0.11	84.36736	68.38817	66.11112	6.60915	82.23881	67.47682	65.34898	10.96439
12	0.12	84.29066	67.54368	65.31813	6.60038	82.15971	66.67974	64.59895	10.94945
13	0.13	84.21671	66.72644	64.54701	6.59201	82.08335	65.908	63.86938	10.93515
14	0.14	84.14532	65.93327	63.79539	6.58396	82.00954	65.15867	63.15808	10.92143
15	0.15	84.07633	65.16151	63.06122	6.57622	81.93813	64.42931	62.46319	10.9082
S/B=0.05,D/B=0.10						S/B=.05,D/B=0.15			
S.No.	T/B	$\Phi_C\%$	$\Phi_D\%$	$\Phi_E\%$	$\Phi_F\%$	$\Phi_C\%$	$\Phi_D\%$	$\Phi_E\%$	$\Phi_F\%$
1	0.01	81.55312	77.57738	74.23493	13.96867	80.02051	76.3095	73.17365	16.48389
2	0.02	81.49918	75.84245	72.86816	13.91604	79.96759	74.67882	71.88266	16.42259
3	0.03	81.4091	74.43931	71.69486	13.87482	79.87959	73.35535	70.77151	16.37433
4	0.04	81.31053	73.21599	70.63736	13.83985	79.78304	72.19874	69.76827	16.33325
5	0.05	81.21106	72.11108	69.66089	13.80901	79.68533	71.15221	68.84066	16.29695
6	0.06	81.11335	71.09206	68.74574	13.78117	79.58911	70.1857	67.97043	16.26411
7	0.07	81.01844	70.13911	67.87929	13.75566	79.49544	69.28085	67.14583	16.23396
8	0.08	80.92667	69.23907	67.05283	13.73197	79.40469	68.42545	66.35876	16.20593
9	0.09	80.83809	68.38258	66.25994	13.70982	79.31694	67.61086	65.60325	16.1797
10	0.1	80.75263	67.56281	65.49583	13.68893	79.23215	66.83064	64.8748	16.15493
11	0.11	80.67016	66.77441	64.75665	13.66912	79.15019	66.0799	64.16987	16.13142
12	0.12	80.5905	66.01328	64.03938	13.65023	79.07094	65.35478	63.4856	16.10901
13	0.13	80.51351	65.27606	63.34152	13.63218	78.99424	64.65215	62.81966	16.08757
14	0.14	80.43903	64.56002	62.661	13.61483	78.91994	63.96946	62.1701	16.06697
15	0.15	80.36689	63.86287	61.99606	13.59813	78.84792	63.30458	61.53529	16.04711

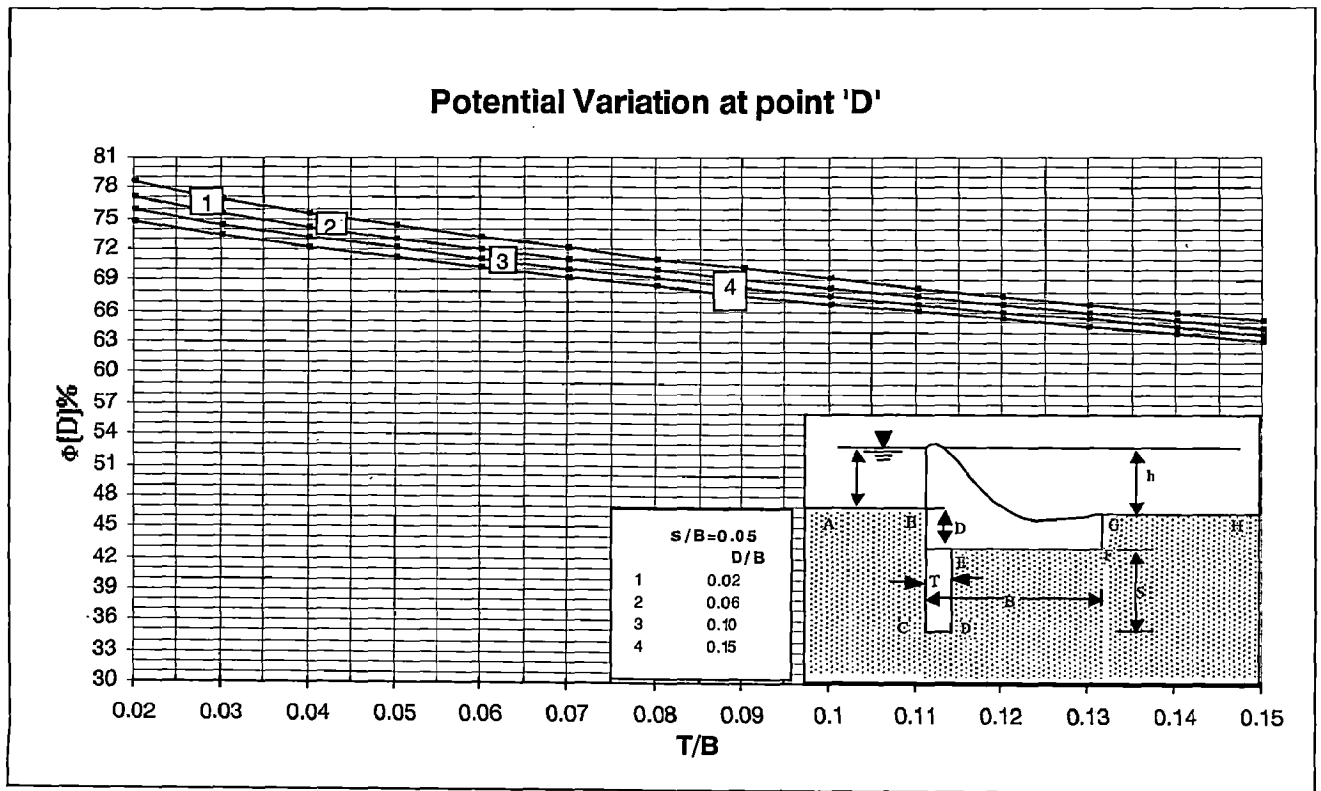


Figure 4.2.1(a) Variation of ϕ_D with increasing cutoff thickness (u/s)

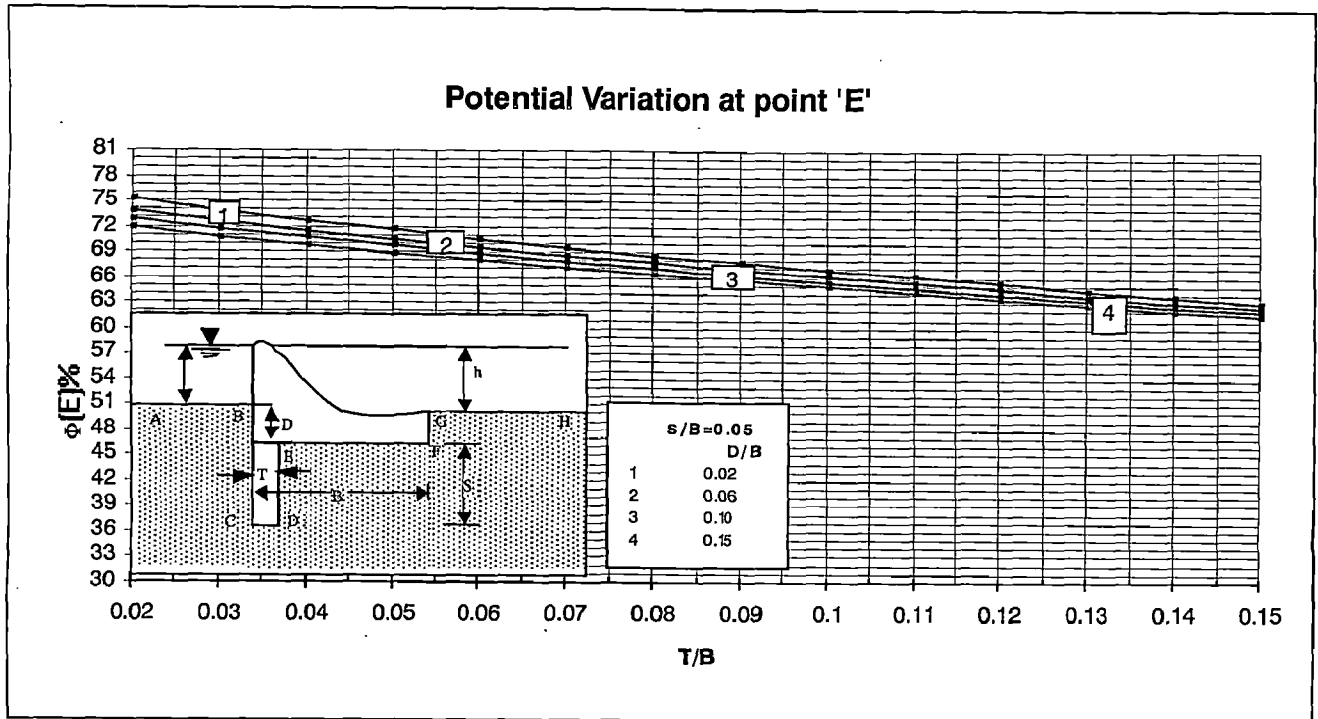


Figure 4.2.1(b) Variation of ϕ_E with increasing cutoff thickness (u/s)

**Table 4.2.2 Variation of potential distribution with increasing thickness of cutoff for depressed weir with concrete cutoff (u/s)
S/B fixed D/B varying**

		S/B=0.12,D/B=0.02				S/B=0.12,D/B=0.06			
S.No.	T/B	$\Phi_C\%$	$\Phi_D\%$	$\Phi_E\%$	$\Phi_F\%$	$\Phi_C\%$	$\Phi_D\%$	$\Phi_E\%$	$\Phi_F\%$
1	0.01	79.15711	74.37514	67.35476	6.51106	77.93521	73.45647	66.84656	10.85256
2	0.02	79.29071	72.54096	66.10265	6.47917	78.06179	71.73153	65.66107	10.80141
3	0.03	79.33522	71.07056	65.0125	6.4537	78.1033	70.34464	64.62706	10.76048
4	0.04	79.34319	69.79462	64.01926	6.43175	78.10972	69.1387	63.68382	10.72518
5	0.05	79.33235	68.64558	63.0941	6.41216	78.09795	68.05098	62.80437	10.6936
6	0.06	79.31066	67.58793	62.2206	6.39429	78.07566	67.04855	61.97348	10.66475
7	0.07	79.28238	66.60023	61.38832	6.37771	78.04694	66.11147	61.18134	10.63801
8	0.08	79.24994	65.6683	60.59002	6.36217	78.01414	65.22658	60.42118	10.61292
9	0.09	79.21485	64.78213	59.82032	6.34749	77.97874	64.38455	59.68801	10.58919
10	0.1	79.1781	63.93437	59.07519	6.33347	77.9417	63.57854	58.97802	10.56662
11	0.11	79.14034	63.1194	58.35143	6.32009	77.90364	62.80333	58.28822	10.54503
12	0.12	79.10206	62.33286	57.64647	6.30723	77.86503	62.05481	57.6162	10.52425
13	0.13	79.06353	61.57116	56.95818	6.29483	77.82617	61.32969	56.96	10.5042
14	0.14	79.02502	60.83146	56.28482	6.28278	77.78729	60.62527	56.31792	10.48478
15	0.15	78.98666	60.11132	55.62482	6.27108	77.74857	59.93932	55.68858	10.46593
		S/B=0.12,D/B=0.10				S/B=0.12,D/B=0.15			
S.No.	T/B	$\Phi_C\%$	$\Phi_D\%$	$\Phi_E\%$	$\Phi_F\%$	$\Phi_C\%$	$\Phi_D\%$	$\Phi_E\%$	$\Phi_F\%$
1	0.01	76.91286	72.66722	66.37638	13.56841	75.8429	71.82995	65.86134	16.05005
2	0.02	77.03427	71.02741	65.24364	13.50642	75.9593	70.27615	64.78268	15.97918
3	0.03	77.0738	69.70599	64.25417	13.45671	75.99704	69.02122	63.83901	15.92222
4	0.04	77.07935	68.55514	63.35064	13.4138	76.00197	67.92651	62.97636	15.87298
5	0.05	77.06721	67.5158	62.50755	13.3754	75.98973	66.93663	62.17076	15.82886
6	0.06	77.0448	66.55701	61.71051	13.34026	75.96747	66.02254	61.40866	15.78847
7	0.07	77.01608	65.66	60.95029	13.30766	75.93901	65.16662	60.68135	15.75097
8	0.08	76.98333	64.81234	60.22044	13.27708	75.90659	64.35723	59.98281	15.71578
9	0.09	76.94799	64.00529	59.51626	13.24818	75.8716	63.58614	59.30859	15.68247
10	0.1	76.91101	63.23237	58.83416	13.22064	75.83496	62.84729	58.6553	15.65076
11	0.11	76.87302	62.48868	58.17131	13.1943	75.79728	62.13604	58.02026	15.62041
12	0.12	76.83444	61.77032	57.52542	13.16895	75.759	61.44876	57.40135	15.59121
13	0.13	76.79561	61.0742	56.89461	13.14451	75.72043	60.78252	56.79677	15.56305
14	0.14	76.75672	60.39775	56.27732	13.12083	75.68178	60.13491	56.20504	15.53577
15	0.15	76.71796	59.73888	55.67219	13.09783	75.64322	59.50395	55.62489	15.50928

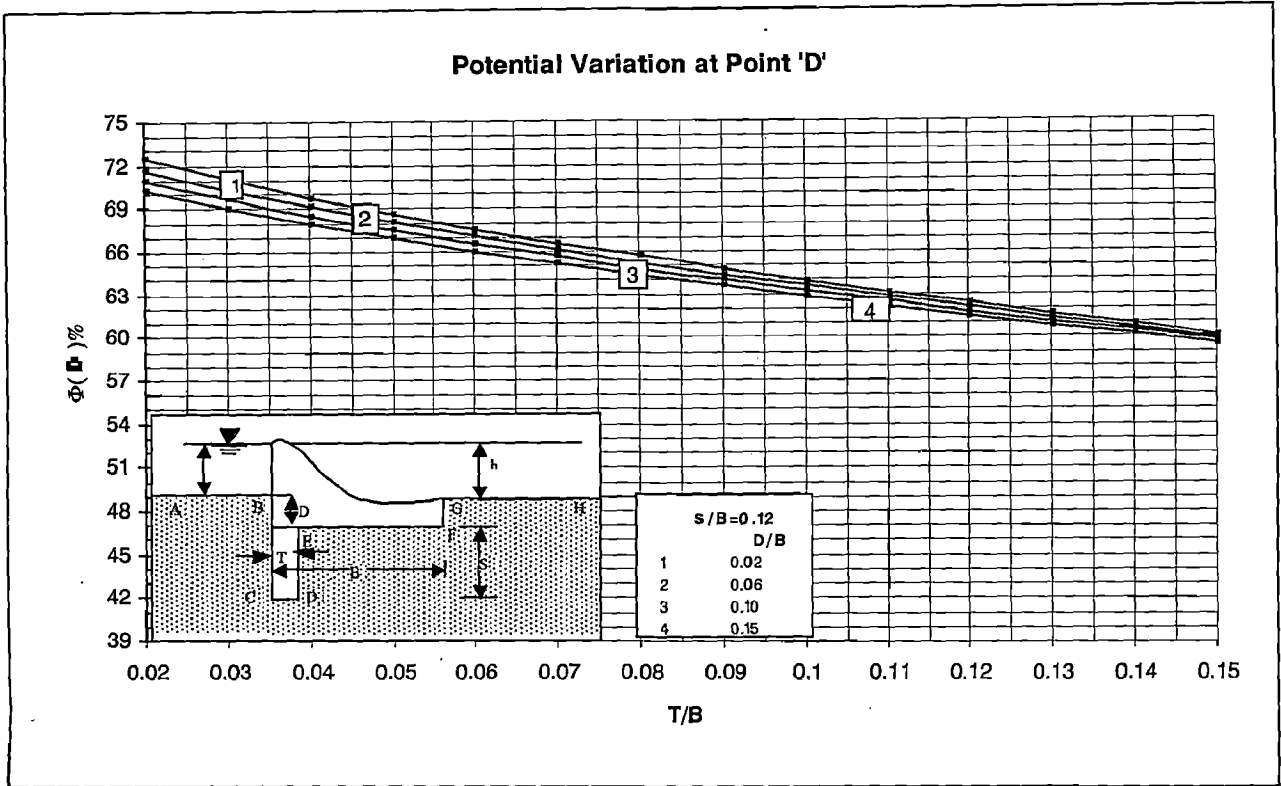


Fig 4.2.2 (a) Variation of ϕ_D with increasing cutoff thickness (u/s)

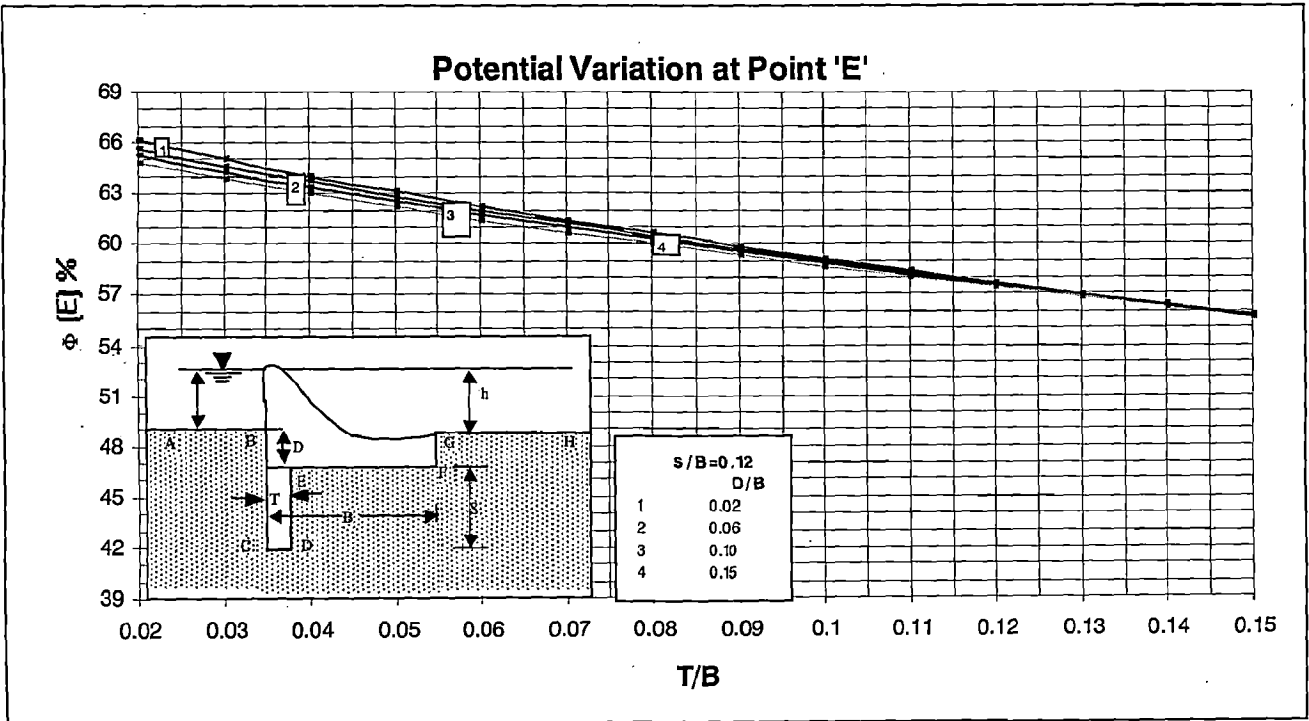
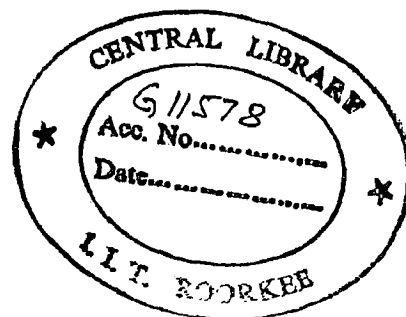


Figure 4.2.2 (b) Variation of ϕ_E with increasing cutoff thickness (u/s)

Table 4.2.3 Variation of potential distribution with increasing depth of cutoff for depressed weir with concrete cutoff (u/s)

T/B fixed D/B varying

		D/B=0.02,T/B=0.05				D/B=0.06,T/B=0.05			
S.No.	S/B	$\phi_C\%$	$\phi_D\%$	$\phi_E\%$	$\phi_F\%$	$\phi_C\%$	$\phi_D\%$	$\phi_E\%$	$\phi_F\%$
1	0.01	89.77888	79.58647	78.89573	6.83268	86.47588	77.45971	76.83531	11.28785
2	0.02	88.32421	77.97244	76.68649	6.79162	85.42955	76.1397	74.965	11.23494
3	0.03	87.05882	76.61444	74.79021	6.75189	84.47919	75.01008	73.33121	11.18205
4	0.04	85.92606	75.41912	73.0969	6.7129	83.60017	74.0006	71.85133	11.12892
5	0.05	84.89394	74.34137	71.55188	6.67447	82.77873	73.07872	70.48547	11.07547
6	0.06	83.94195	73.35461	70.1224	6.63641	82.00569	72.22555	69.20981	11.0217
7	0.07	83.05602	72.44147	68.78678	6.59865	81.27439	71.42875	68.00854	10.96764
8	0.08	82.22591	71.58976	67.52967	6.56112	80.57977	70.67965	66.87035	10.91331
9	0.09	81.44392	70.79047	66.33971	6.5237	79.9178	69.9718	65.78678	10.85872
10	0.10	80.70404	70.03677	65.20816	6.48645	79.28525	69.30025	64.75127	10.80388
11	0.11	80.00148	69.32325	64.12814	6.44927	78.67938	68.66104	63.75855	10.74884
12	0.12	79.33235	68.64558	63.0941	6.41216	78.09795	68.05098	62.80437	10.6936
13	0.13	78.6934	68.00018	62.10144	6.37517	77.53899	67.46741	61.88519	10.63817
14	0.14	78.08194	67.38408	61.14639	6.3382	77.00085	66.9081	60.99801	10.58261
15	0.15	77.49567	66.79481	60.22572	6.30128	76.48206	66.37112	60.14027	10.52688
		D/B=0.02,T/B=0.10				D/B=0.02,T/B=0.15			
S.No.	S/B	$\phi_C\%$	$\phi_D\%$	$\phi_E\%$	$\phi_F\%$	$\phi_C\%$	$\phi_D\%$	$\phi_E\%$	$\phi_F\%$
1	0.01	84.37857	76.05414	75.47178	14.04455	82.47019	74.74901	74.20476	16.5493
2	0.02	83.49023	74.86846	73.76812	13.98606	81.69002	73.66624	72.63483	16.48635
3	0.03	82.67863	73.85332	72.27534	13.92761	80.97752	72.74084	71.25803	16.42378
4	0.04	81.92259	72.94401	70.91816	13.86862	80.31267	71.91199	70.00431	16.36073
5	0.05	81.21106	72.11108	69.66089	13.80901	79.68533	71.15221	68.84066	16.29695
6	0.06	80.53696	71.33776	68.48253	13.74874	79.08925	70.44595	67.74788	16.23233
7	0.07	79.89536	70.61323	67.36925	13.68783	78.52014	69.78327	66.71336	16.16692
8	0.08	79.28249	69.92996	66.31124	13.62636	77.97485	69.15734	65.72826	16.1007
9	0.09	78.69543	69.28241	65.30117	13.56432	77.45096	68.56314	64.78603	16.03375
10	0.1	78.13178	68.66633	64.3334	13.5018	76.9465	67.99685	63.88157	15.96609
11	0.11	77.58961	68.07837	63.40343	13.43881	76.45987	67.45548	63.0109	15.89779
12	0.12	77.06721	67.5158	62.50755	13.3754	75.98973	66.93663	62.17076	15.82886
13	0.13	76.56316	66.97638	61.64274	13.31159	75.53493	66.43829	61.35843	15.75936
14	0.14	76.07622	66.45821	60.80642	13.24744	75.09448	65.95881	60.57163	15.68933
15	0.15	75.60529	65.95969	59.99641	13.18295	74.66751	65.49676	59.80845	15.61881



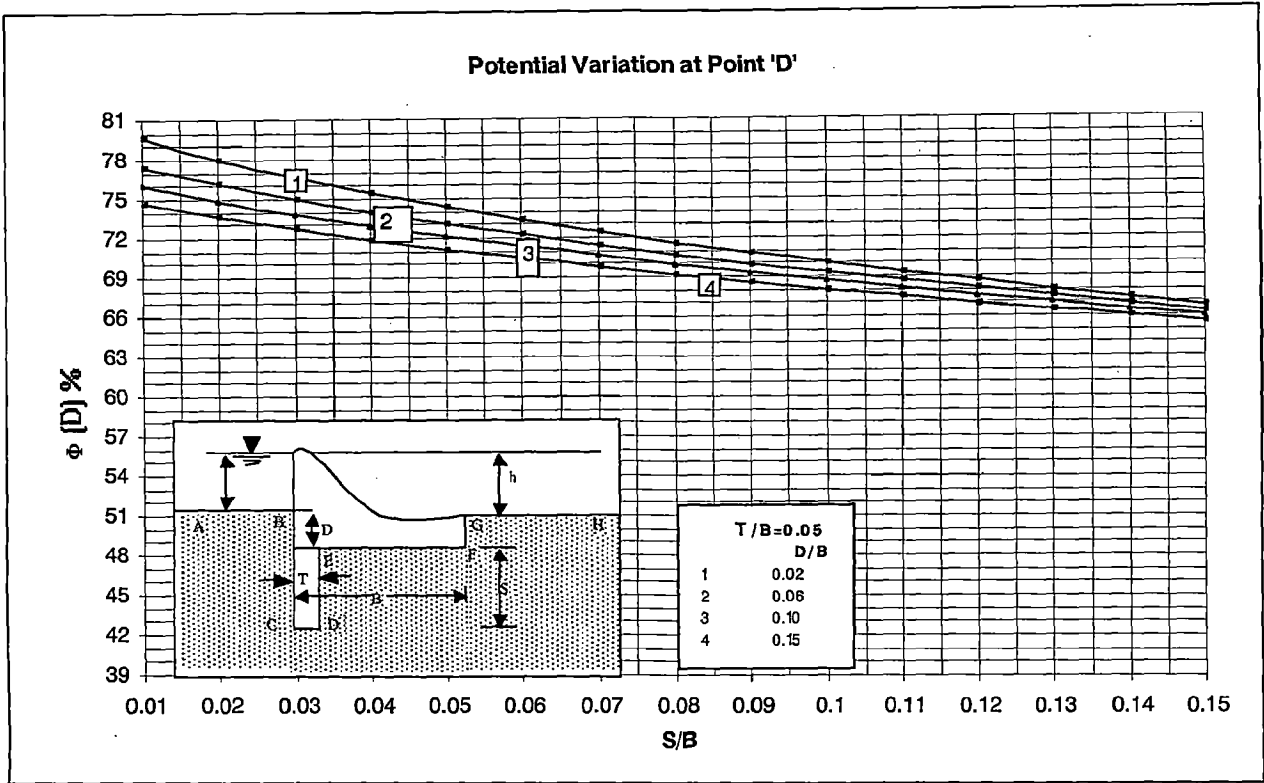


Figure 4.2.3 (a) Variation of ϕ_D with increasing cutoff depth (u/s)

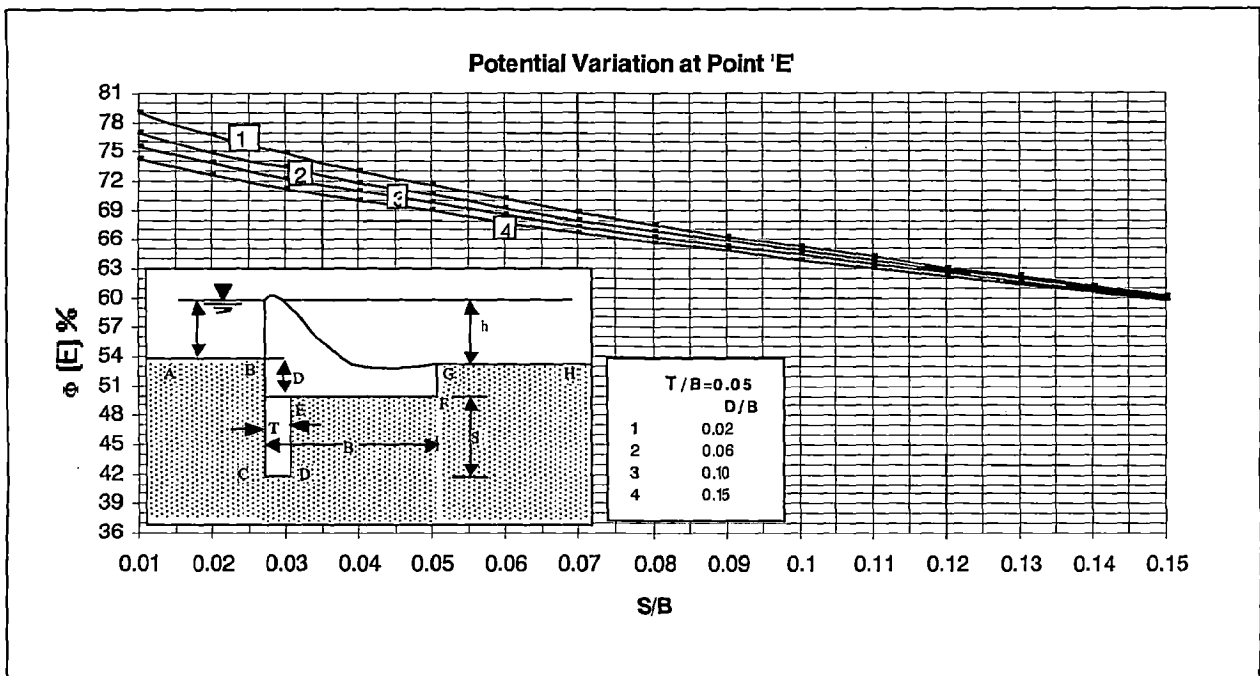


Figure 4.2.3 (b) Variation of ϕ_E with increasing cutoff depth (u/s)

Table 4.2.4 Variation of potential distribution with increasing depression for depressed weir with u/s concrete cutoff

		S/B=0.05,T/B=0.05				S/B=0.05,T/B=0.075			
S.No.	D/B	$\phi_C\%$	$\phi_D\%$	$\phi_E\%$	$\phi_F\%$	$\phi_C\%$	$\phi_D\%$	$\phi_E\%$	$\phi_F\%$
1	0.01	85.56288	74.72283	71.86897	4.78162	85.33207	71.95307	69.37963	4.75986
2	0.03	84.29173	73.98873	71.25583	8.07829	84.05569	71.31874	68.8502	8.04093
3	0.05	83.24239	73.36056	70.72475	10.20948	83.00386	70.77224	68.38821	10.16171
4	0.07	82.34779	72.81483	70.26099	11.85245	82.1084	70.29665	67.98421	11.79663
5	0.09	81.56718	72.33266	69.85004	13.20803	81.32794	69.87629	67.62622	13.14556
6	0.11	80.87434	71.90075	69.48119	14.3691	80.6359	69.49978	67.30508	14.301
7	0.13	80.25133	71.50961	69.14667	15.38783	80.01414	69.15891	67.01403	15.31486
8	0.15	79.68533	71.15221	68.84066	16.29695	79.44969	68.84758	66.74802	16.2197

		S/B=0.05,T/B=0.10				S/B=0.05,T/B=0.15			
S.No.	D/B	$\phi_C\%$	$\phi_D\%$	$\phi_E\%$	$\phi_F\%$	$\phi_C\%$	$\phi_D\%$	$\phi_E\%$	$\phi_F\%$
1	0.01	85.12202	69.54869	67.16344	4.7418	84.75714	65.3733	63.22934	4.71191
2	0.03	83.84042	68.99696	66.70632	8.00983	83.46537	64.95959	62.89779	7.95836
3	0.05	82.78584	68.51823	66.30396	10.12191	82.40498	64.59421	62.59881	10.05601
4	0.07	81.88911	68.10102	65.95158	11.75003	81.50509	64.27475	62.33587	11.67278
5	0.09	81.10833	67.73222	65.63938	13.09335	80.72286	63.99242	62.10299	13.00671
6	0.11	80.4166	67.40205	65.35954	14.24401	80.03082	63.74004	61.89468	14.14934
7	0.13	79.79557	67.1033	65.10616	15.25373	79.41029	63.51215	61.70657	15.15207
8	0.15	79.23215	66.83064	64.8748	16.15493	78.84792	63.30458	61.53529	16.04711

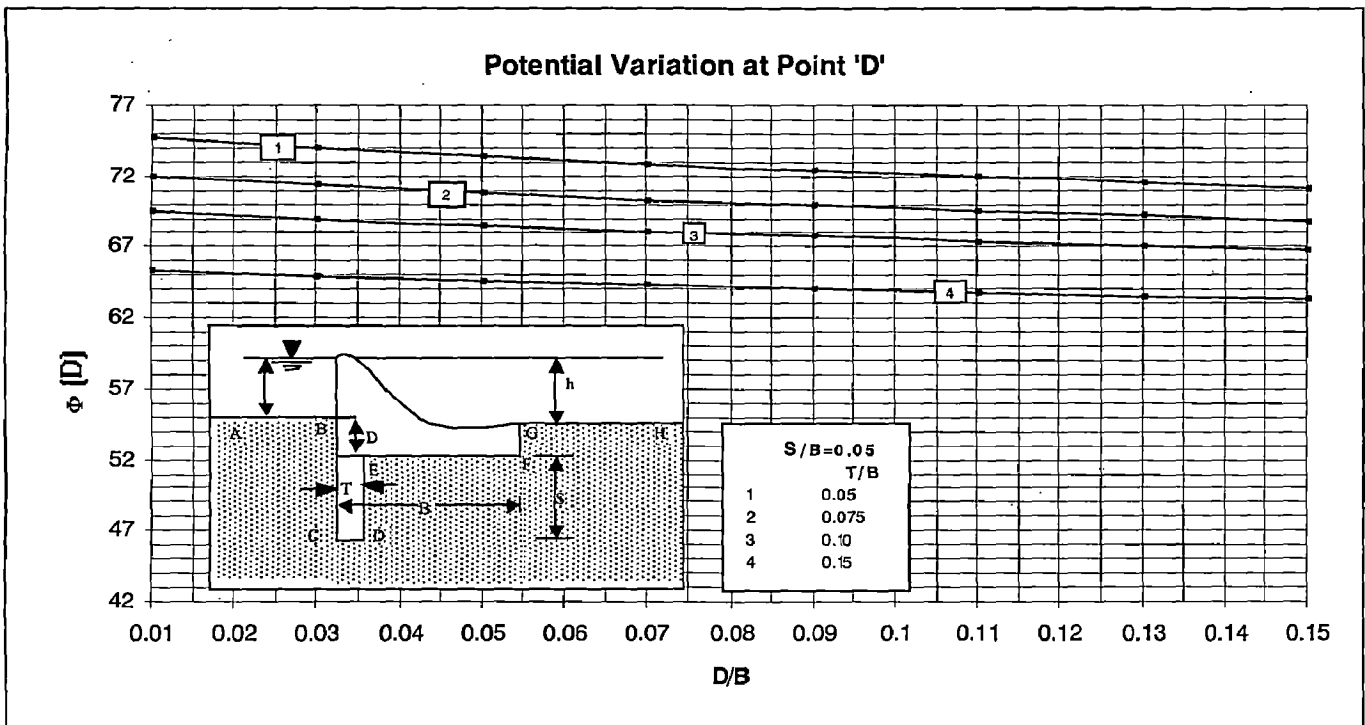


Figure 4.2.4(a) Variation of ϕ_D with increasing depression

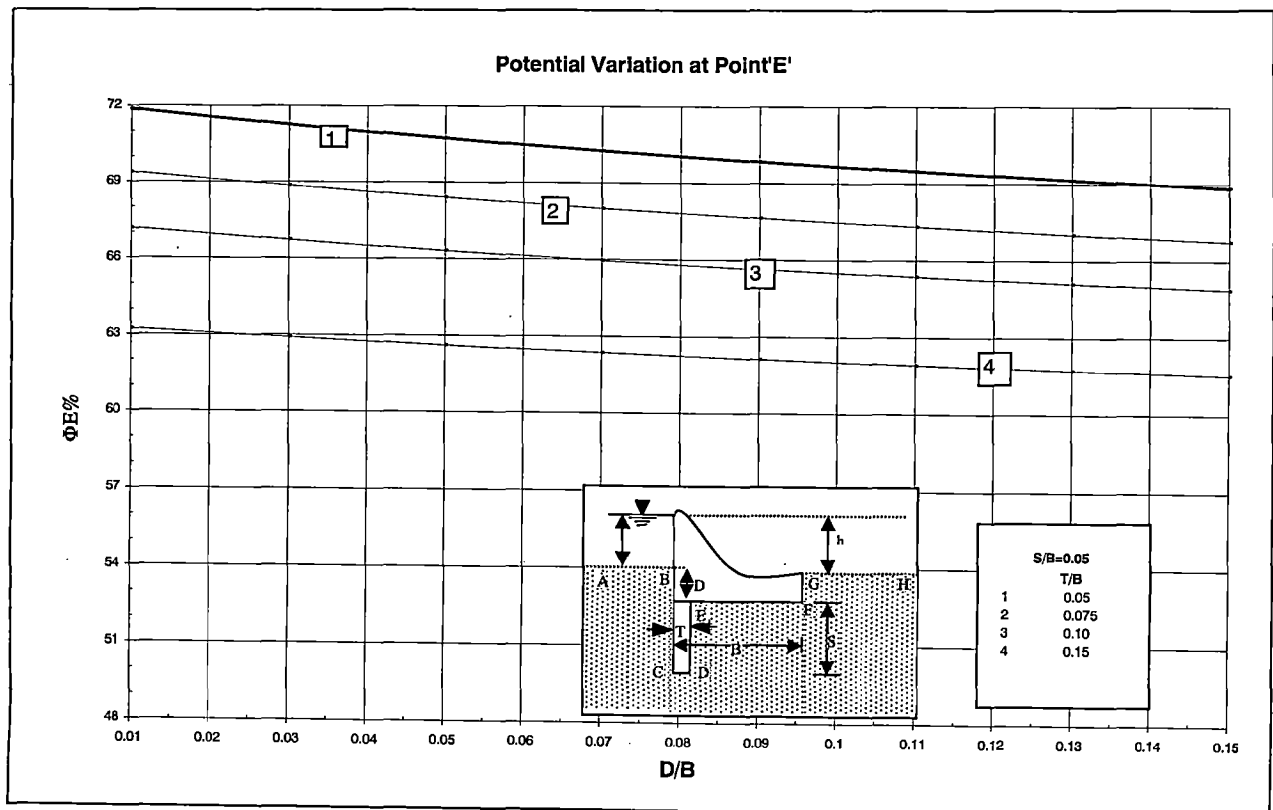


Figure 4.2.4 (b) Variation of ϕ_E with increasing depression

Table 4.2.5 Variation of potential distribution with increasing depression for depressed weir with u/s concrete cutoff

T/B fixed S/B varying

S.No.	D/B	T/B=0.05,S/B=0.05				T/B=0.05,S/B=0.075			
		$\phi_C\%$	$\phi_D\%$	$\phi_E\%$	$\phi_F\%$	$\phi_C\%$	$\phi_D\%$	$\phi_E\%$	$\phi_F\%$
1	0	85.56288	74.72283	71.86897	4.78162	83.14513	72.27713	68.34067	4.71022
2	0.02	84.29173	73.98873	71.25583	8.07829	82.16058	71.7496	67.95906	7.96882
3	0.05	83.24239	73.36056	70.72475	10.20948	81.3084	71.26997	67.59982	10.08106
4	0.07	82.34779	72.81483	70.26099	11.85245	80.56	70.83861	67.27217	11.71216
5	0.09	81.56718	72.33266	69.85004	13.20803	79.89334	70.4485	66.9735	13.05944
6	0.11	80.87434	71.90075	69.48119	14.3691	79.29255	70.09309	66.7	14.21442
7	0.13	80.25133	71.50961	69.14667	15.38783	78.74593	69.76704	66.44817	15.22848
8	0.15	79.68533	71.15221	68.84066	16.29695	78.24468	69.46606	66.21508	16.1339
S.No.	D/B	T/B=0.05,S/B=0.10				T/B=0.05,S/B=0.15			
		$\phi_C\%$	$\phi_D\%$	$\phi_E\%$	$\phi_F\%$	$\phi_C\%$	$\phi_D\%$	$\phi_E\%$	$\phi_F\%$
1	0	81.10962	70.22818	65.31223	4.64046	77.76633	66.88481	60.21153	4.50345
2	0.02	80.31922	69.84438	65.09427	7.85977	77.22955	66.69266	60.2177	7.64212
3	0.05	79.61132	69.47501	64.86366	9.9516	76.72223	66.47838	60.17133	9.6903
4	0.07	78.97563	69.13226	64.64187	11.56961	76.25067	66.26523	60.10638	11.27954
5	0.09	78.40012	68.81563	64.43291	12.90771	75.81271	66.0593	60.03388	12.59709
6	0.11	77.875	68.5226	64.23711	14.05589	75.40501	65.86244	59.95864	13.72988
7	0.13	77.39249	68.25049	64.05367	15.06474	75.02425	65.675	59.88308	14.72684
8	0.15	76.9465	67.99685	63.88157	15.96609	74.66751	65.49676	59.80845	15.61881

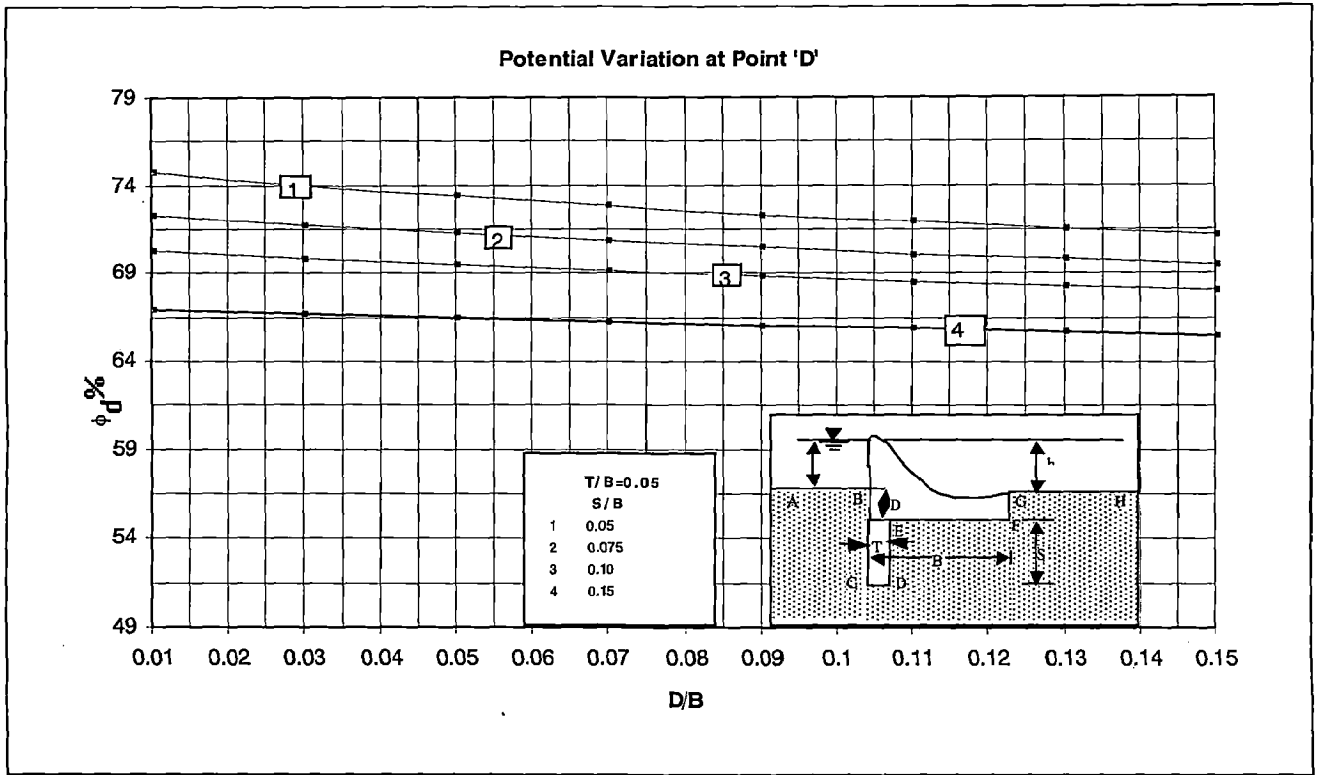


Figure 4.2.5 (a) Variation of ϕ_D with increasing depression

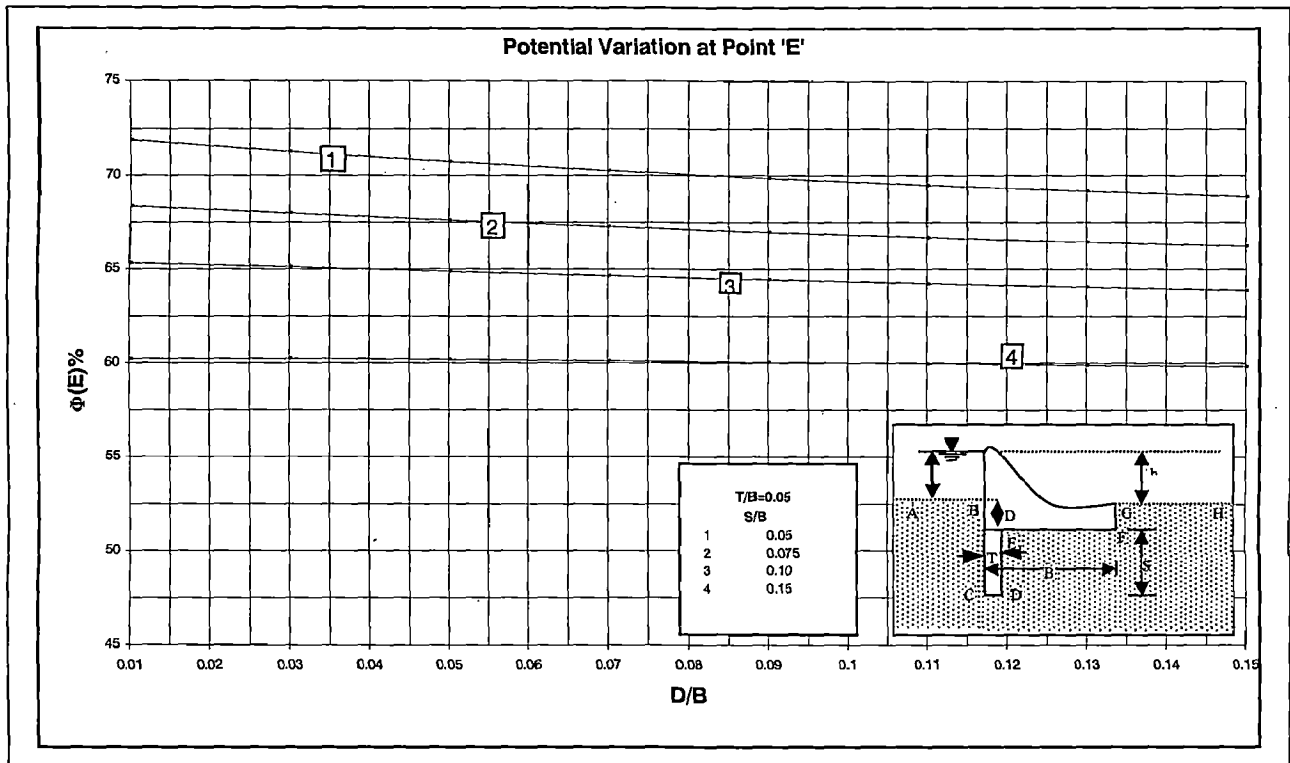


Figure 4.2.5 (b) Variation of ϕ_E with increasing depression

Table 4.2.6 Potential variation at the key point with increasing u/s and d/s depression respectively

D1=U/S Depression, D2=D/S Depression

S.No.	D1/B	D2/B	S/B	T/B	$\phi_D\%$	$\phi_E\%$	S.No.	D1/B	D2/B	S/B	T/B	$\phi_D\%$	$\phi_E\%$
1	0.02	0.02	0.05	0.01	80.55	76.69	1	0.02	0.02	0.05	0.01	80.55	76.69
2	0.05	0.02	0.05	0.01	78.85	75.16	2	0.02	0.05	0.05	0.01	80.91	77.12
3	0.07	0.02	0.05	0.01	77.89	74.28	3	0.02	0.07	0.05	0.01	81.12	77.37
4	0.09	0.02	0.05	0.01	77.02	73.49	4	0.02	0.09	0.05	0.01	81.3	77.59
5	0.11	0.02	0.05	0.01	76.23	72.77	5	0.02	0.11	0.05	0.01	81.47	77.79
6	0.13	0.02	0.05	0.01	75.51	72.1	6	0.02	0.13	0.05	0.01	81.62	77.98
7	0.15	0.02	0.05	0.01	74.83	71.48	7	0.02	0.15	0.05	0.01	81.77	78.16
S.No.	D1/B	D2/B	S/B	T/B	$\phi_D\%$	$\phi_E\%$	S.No.	D1/B	D2/B	S/B	T/B	$\phi_D\%$	$\phi_E\%$
1	0.02	0.02	0.05	0.05	74.34	71.55	1	0.02	0.02	0.05	0.05	74.34	71.55
2	0.05	0.02	0.05	0.05	72.87	70.18	2	0.02	0.05	0.05	0.05	74.81	72.08
3	0.07	0.02	0.05	0.05	72.03	69.4	3	0.02	0.07	0.05	0.05	75.08	72.38
4	0.09	0.02	0.05	0.05	71.28	68.69	4	0.02	0.09	0.05	0.05	75.32	72.65
5	0.11	0.02	0.05	0.05	70.59	68.04	5	0.02	0.11	0.05	0.05	75.54	72.89
6	0.13	0.02	0.05	0.05	69.95	67.44	6	0.02	0.13	0.05	0.05	75.75	73.12
7	0.15	0.02	0.05	0.05	69.36	66.88	7	0.02	0.15	0.05	0.05	75.94	73.34
S.No.	D1/B	D2/B	S/B	T/B	$\phi_D\%$	$\phi_E\%$	S.No.	D1/B	D2/B	S/B	T/B	$\phi_D\%$	$\phi_E\%$
1	0.02	0.02	0.05	0.1	69.26	66.93	1	0.02	0.02	0.05	0.1	69.26	66.93
2	0.05	0.02	0.05	0.1	67.94	65.68	2	0.02	0.05	0.05	0.1	69.83	67.55
3	0.07	0.02	0.05	0.1	67.18	64.96	3	0.02	0.07	0.05	0.1	70.15	67.89
4	0.09	0.02	0.05	0.1	66.5	64.31	4	0.02	0.09	0.05	0.1	70.44	68.21
5	0.11	0.02	0.05	0.1	65.87	63.72	5	0.02	0.11	0.05	0.1	70.71	68.49
6	0.13	0.02	0.05	0.1	65.3	63.17	6	0.02	0.13	0.05	0.1	70.95	68.76
7	0.15	0.02	0.05	0.1	64.76	62.66	7	0.02	0.15	0.05	0.1	71.18	69.01

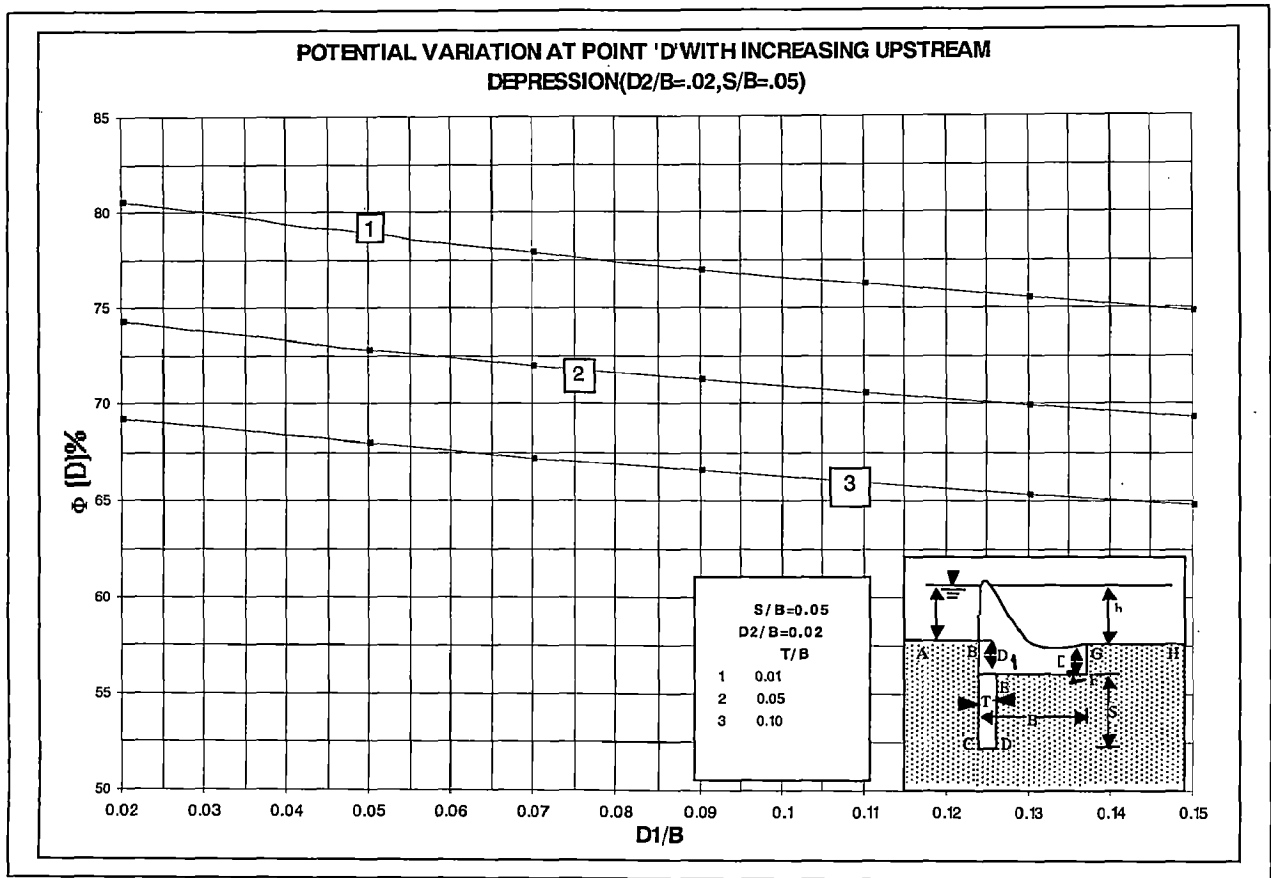


Figure 4.2.6 (a) Variation of ϕ_D with increasing u/s depression

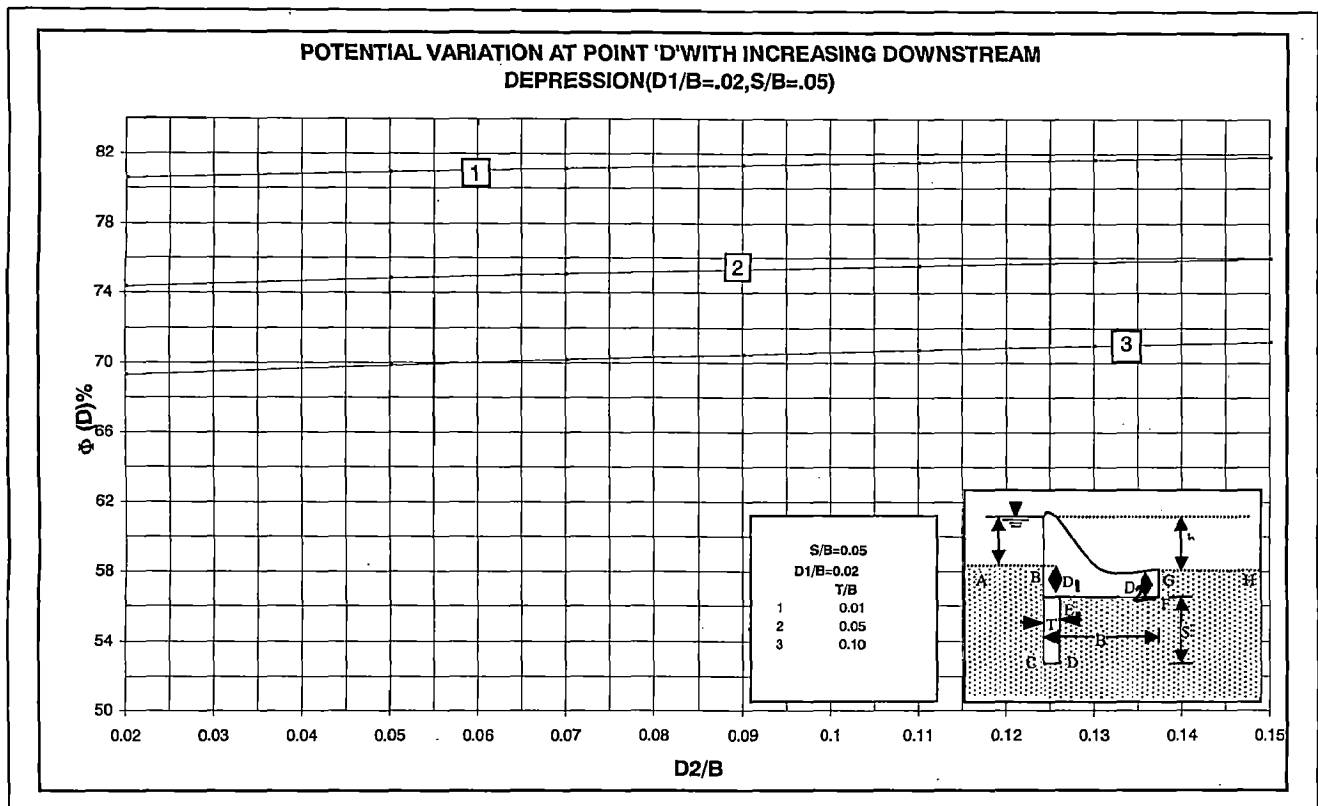


Figure 4.2.6 (b) Variation of ϕ_D with increasing d/s depression

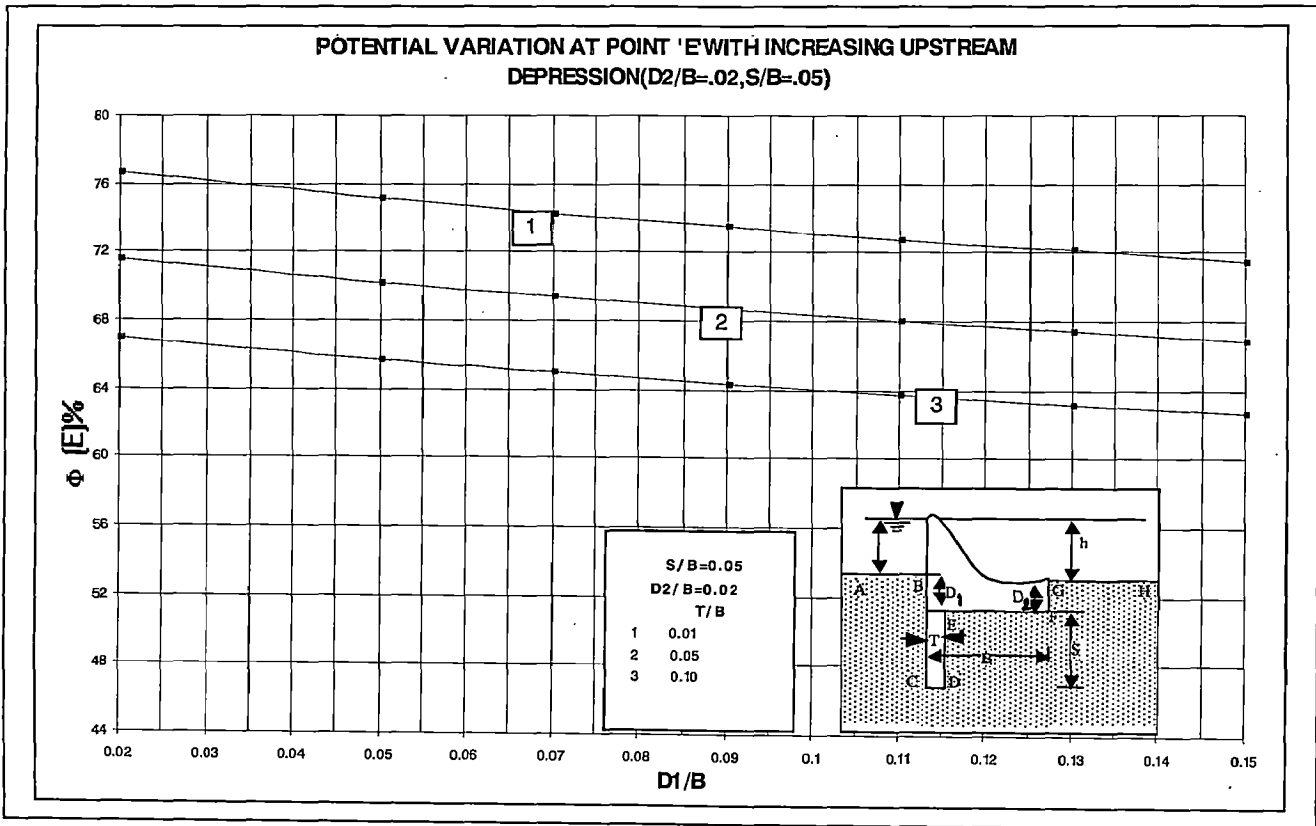


Figure 4.2.6 (c) Variation of ϕ_E with increasing u/s depression

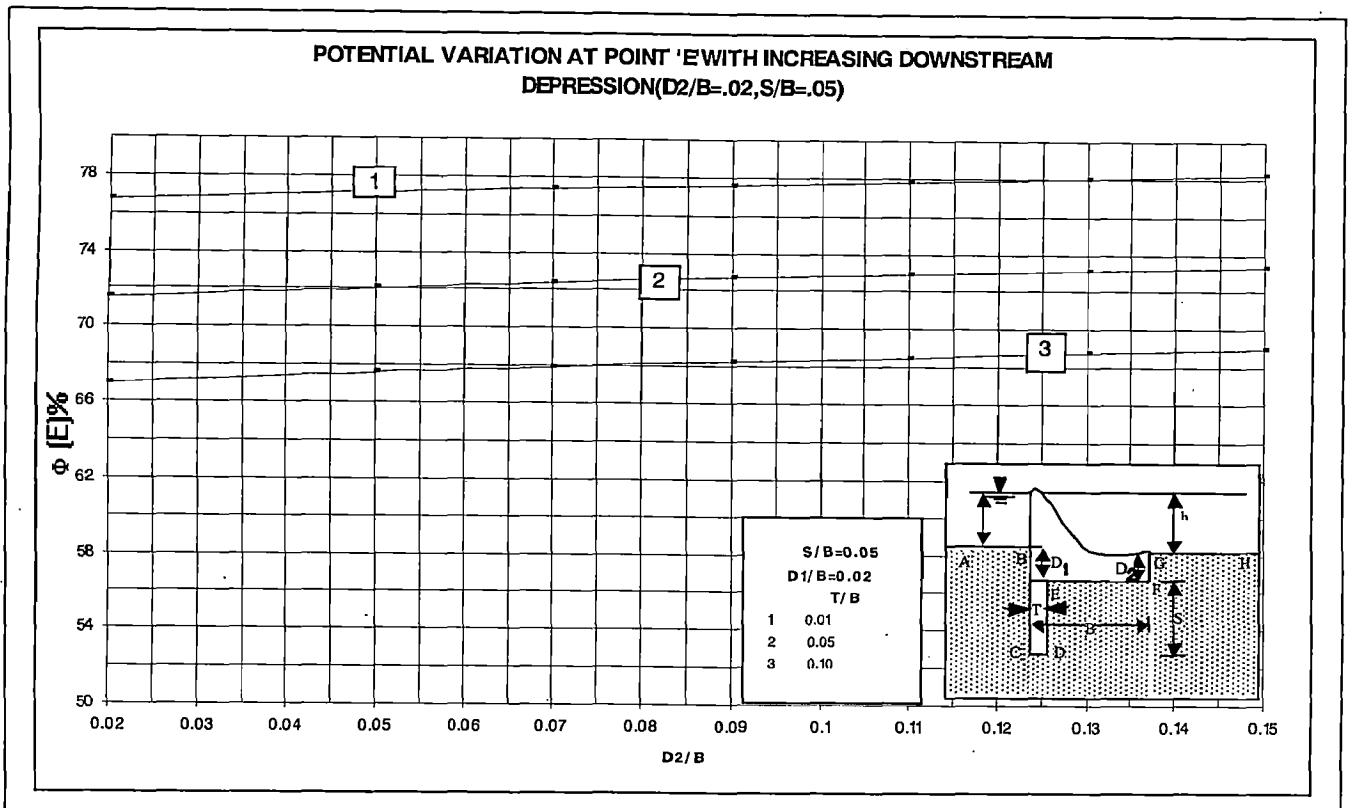


Figure 4.2.6 (d) Variation of ϕ_E with increasing d/s depression

4.3 Comparison in the Variation of Potential Values of Concrete Cutoff at Different Points of the Horizontal Floor with the Sheet Pile.

Table 4.3.1 Potential variation at point 'D' for different case.

S.No.	B1/B	Sheet pile	B/S=5, B/T=10			B/S=30, B/T=10			
			B/D1=25 B/D2=25	B/D1=10 B/D2=80	B/D1=80 B/D2=10	Sheet pile	B/D1=25 B/D2=25	B/D1=10 B/D2=80	B/D1=80 B/D2=10
1	0	100	100	100	100	100	100	100	100
2	0.1	90.73	92.03	88.25	94.44	82.68	85.39	80.91	88.69
3	0.2	82.37	84.04	80.42	86.56	73.05	75.34	71.59	78.24
4	0.3	74.94	77.11	73.75	79.61	65.37	67.94	64.57	70.69
5	0.4	68.24	70.96	67.83	73.42	58.56	61.54	58.43	64.26
6	0.5	62.1	65.38	62.45	67.82	52.12	55.63	52.69	58.38
7	0.6	56.38	60.23	57.47	62.65	45.77	49.83	47.11	52.75
8	0.7	50.99	55.45	52.87	57.86	39.25	44.24	41.5	47.17
9	0.8	45.92	51.13	48.36	53.48	32.23	38.4	35.6	41.49
10	0.9	41.83	47.55	45.42	49.74	24.22	32.38	29.73	35.64
11	1	38.93	44.7845	42.58804	47.2573	15.79	28.8265	26.2838	32.2745

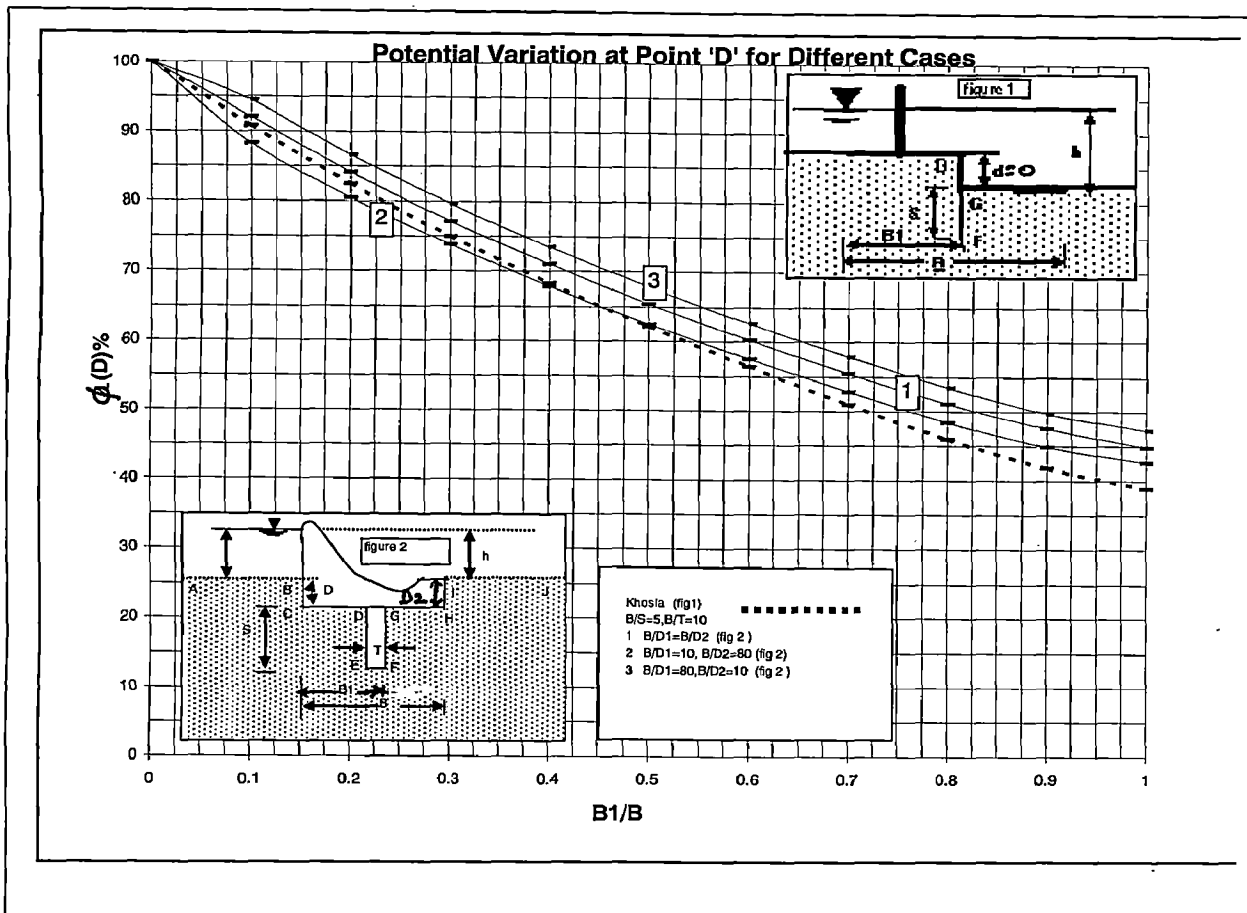


Figure 4.3.1 (a) Variation of ϕ_D at B/S=5 and B/T=10 for different cases

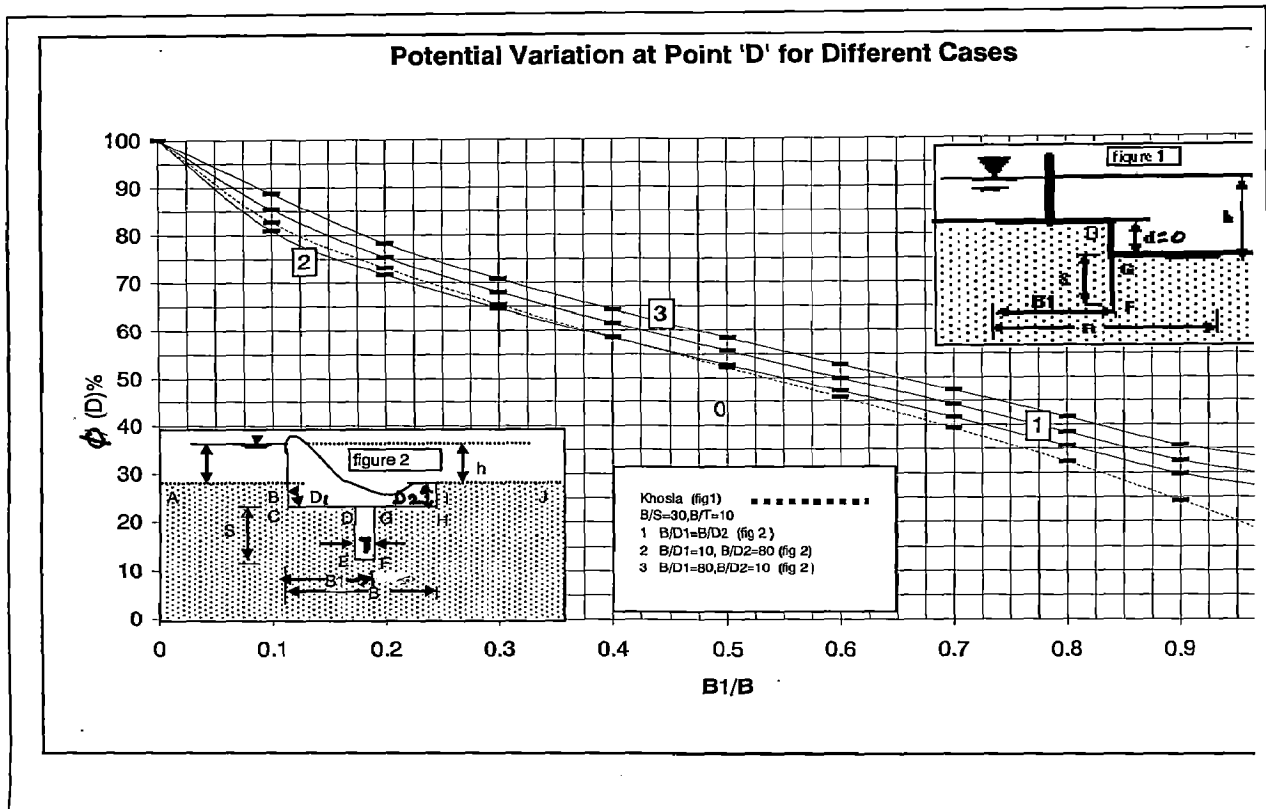


Figure 4.3.1 (b) Variation of ϕ_D at $B/S=30$ and $B/T=10$ for different cases

Table 4.3.2 Potential variation at point 'F' for different case.									
S.No.	B1/B	B/S=5, B/T=10				B/S=30, B/T=10			
		Sheet pile	B/D1=25 B/D2=25	B/D1=10 B/D2=80	B/D1=80 B/D2=10	Sheet pile	B/D1=25 B/D2=25	B/D1=10 B/D2=80	B/D1=80 B/D2=10
1	0	73.27	62.79	59.88	64.52	88.2	73.33	69.39	75.69
2	0.1	70.7	59.94	57.65	61.94	79	69.18	65.85	71.84
3	0.2	66.5	56.52	54.06	58.77	70.8	63	59.86	65.7
4	0.3	62	52.33	49.84	54.76	63.75	57.08	54.11	59.81
5	0.4	55.5	47.79	45.31	50.34	56.8	51.37	48.52	54.17
6	0.5	50	43.05	40.61	45.72	50	45.68	42.92	48.59
7	0.6	44.5	38.18	35.78	40.96	43.2	39.74	37.11	42.9
8	0.7	38	33.25	30.91	36.12	36.25	33.59	30.85	36.89
9	0.8	34	28.49	25.85	31.38	29.2	26.53	23.56	30.16
10	0.9	29.3	24.62	22.7	27.33	21	17.71	14.63	21.89
11	1	26.73	22.8055	21.0229	25.4622	11.8	12.66205	9.81143	16.9956

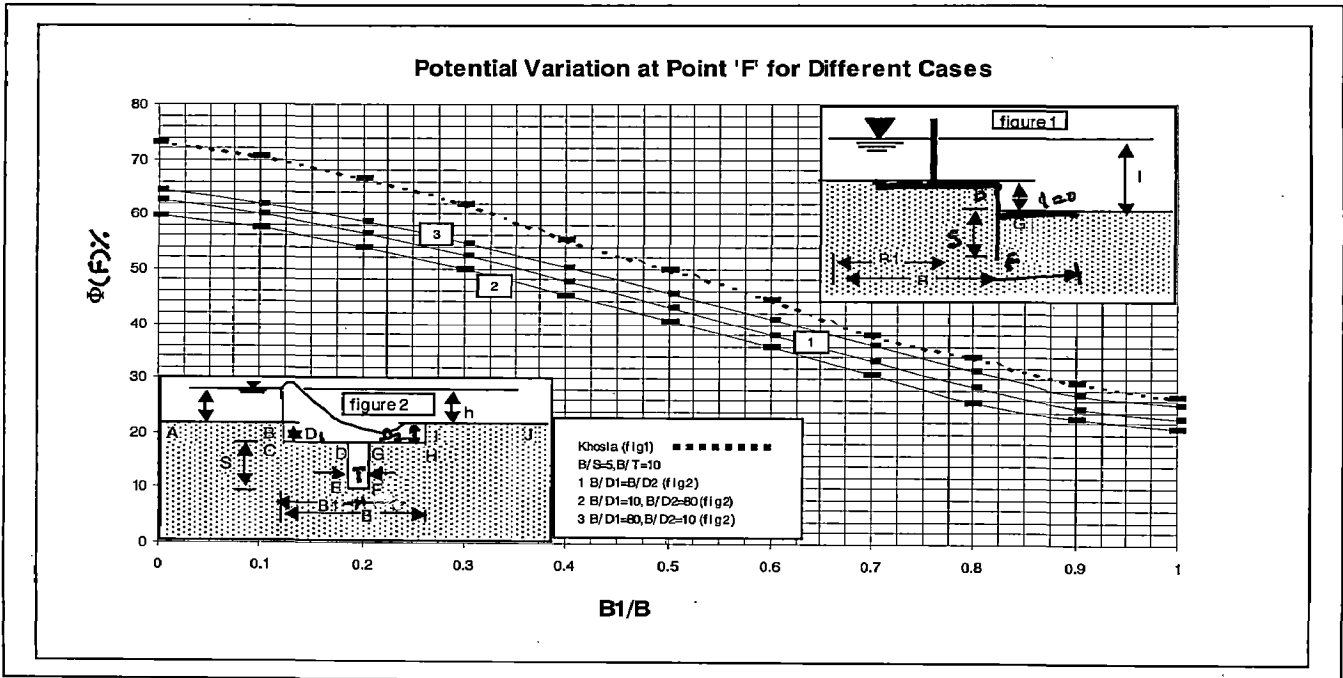


Figure 4.3.2 (a) Variation of ϕ_F at $B/S=5$ and $B/T=10$ for different cases

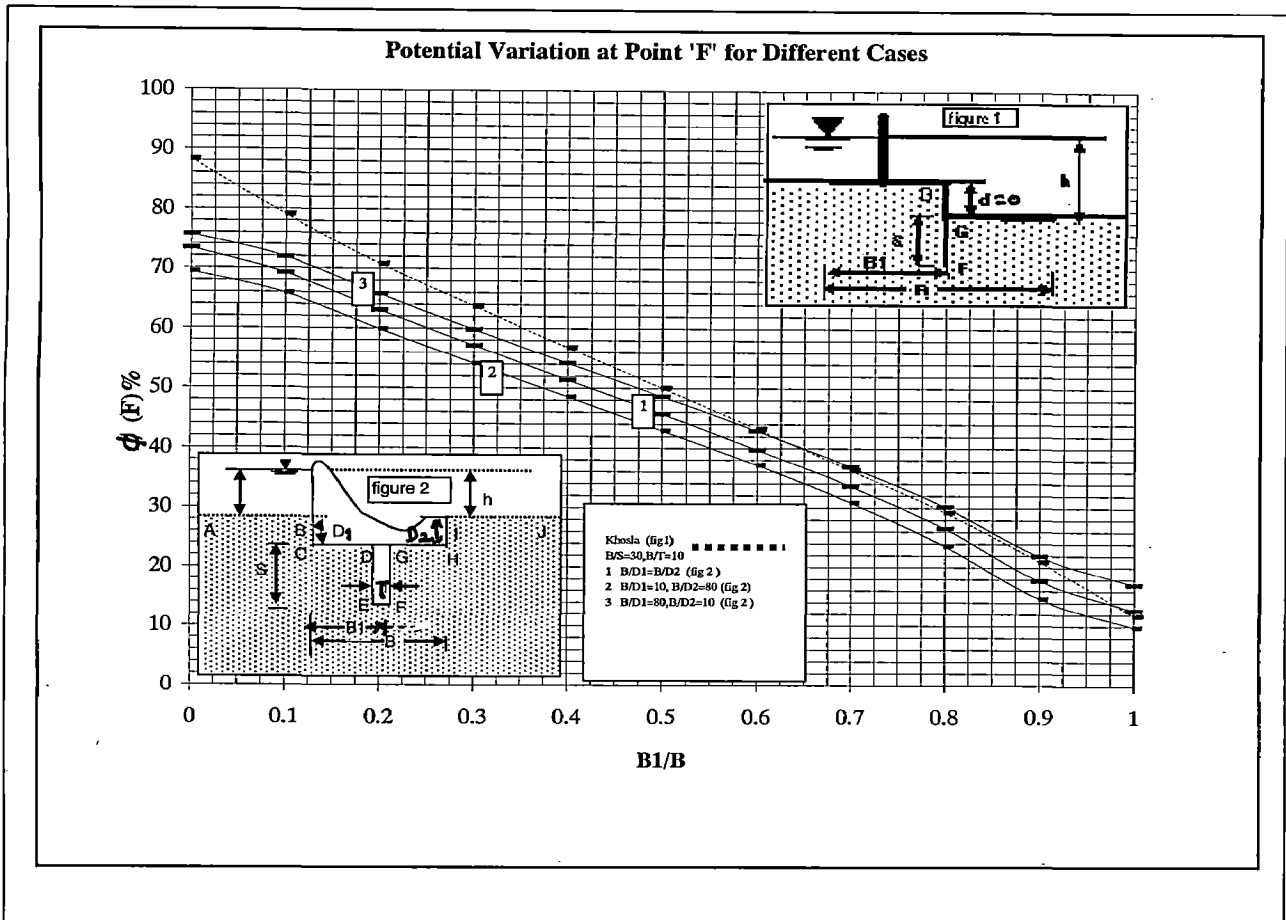


Figure 4.3.2 (b) Variation of ϕ_F at $B/S=30$ and $B/T=10$ for different cases

Table 4.3.3 Potential variation at point 'G' for different case.

S.No.	B1/B	B/S=5, B/T=10				B/S=30, B/T=10			
		Sheet pile	B/D1=25 B/D2=25	B/D1=10 B/D2=80	B/D1=80 B/D2=10	Sheet pile	B/D1=25 B/D2=25	B/D1=10 B/D2=80	B/D1=80 B/D2=10
1	0	61.07	54.66	52.80	56.54	84.21	70.76	67.88	75.11
2	0.1	58.17	52.45	50.26	54.38	75.78	67.62	64.36	70.27
3	0.2	54.08	48.87	46.52	51.26	67.77	61.6	58.51	64.3
4	0.3	49.01	44.55	42.14	47.13	60.75	55.76	52.83	58.5
5	0.4	43.62	39.77	37.35	42.53	54.23	50.08	47.25	52.89
6	0.5	37.9	34.62	32.18	37.55	47.88	44.37	41.62	47.31
7	0.6	31.76	29.04	26.58	32.17	41.44	38.36	35.74	41.57
8	0.7	25.06	22.89	20.39	26.25	34.63	32.06	29.31	35.43
9	0.8	17.63	15.96	12.69	19.58	26.95	24.66	21.62	28.41
10	0.9	9.27	7.97	5.56	11.75	17.32	14.61	11.31	19.09
11	1	0	0	0	0	0	0	0	0

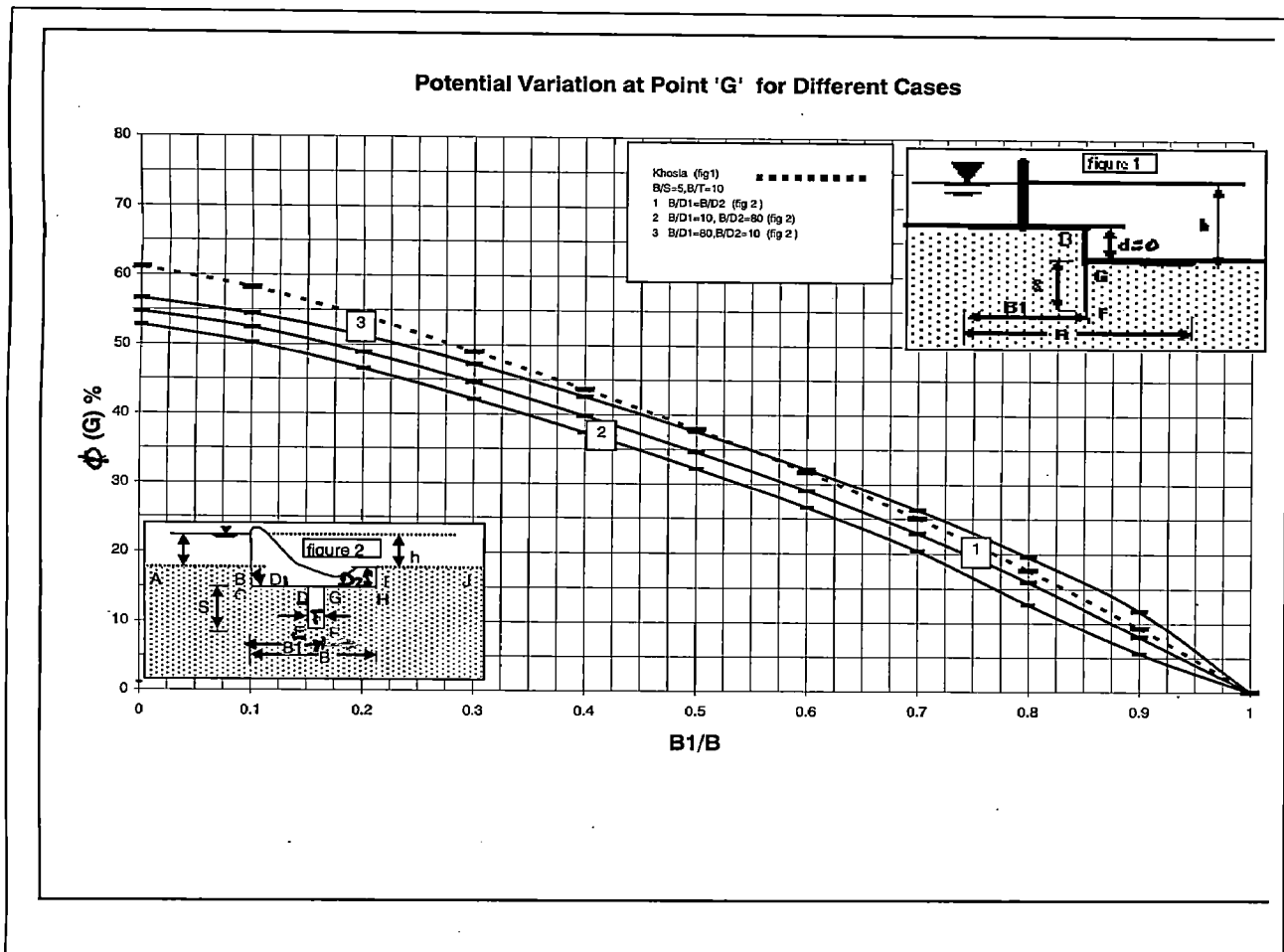


Figure 4.3.3 (a) Variation of ϕ_G at $B/S=5$ and $B/T=10$ for different cases

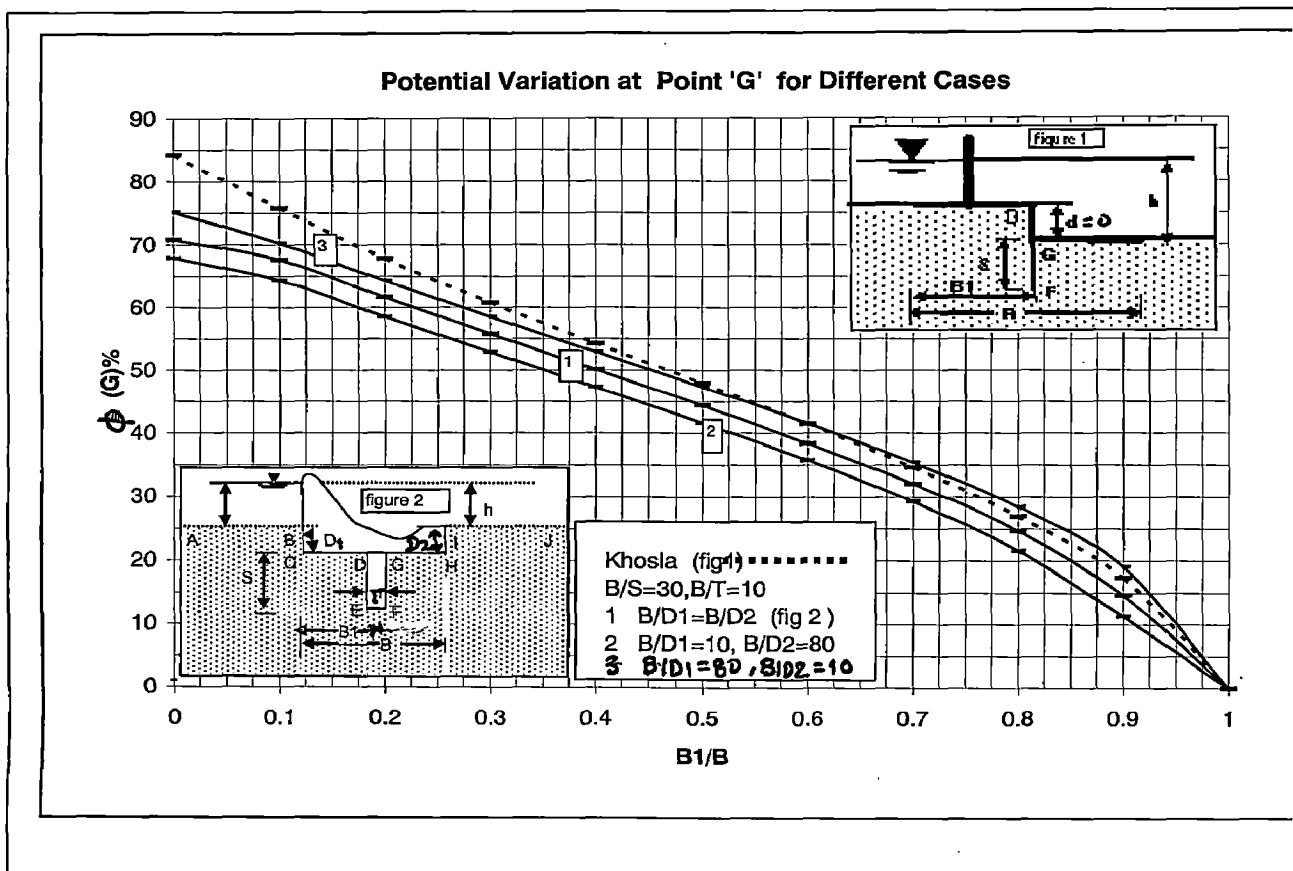


Figure 4.3.3 (b) Variation of ϕ_G at $B/S=30$ and $B/T=10$ for different cases

Table 4.3.4 Potential variation at point 'D' for different case.

S.No.	B1/B	B/S=5, B/T=20				B/S=30, B/T=20			
		Sheet pile	B/D1=25 B/D2=25	B/D1=10 B/D2=80	B/D1=80 B/D2=10	Sheet pile	B/D1=25 B/D2=25	B/D1=10 B/D2=80	B/D1=80 B/D2=10
1	0	100	100	100	100	100	100	100	100
2	0.1	90.7	89.71	88.15	91.22	82.68	82.22	79.97	84.5
3	0.2	82.4	81.88	79.6	83.9	73.05	73.13	69.49	75.5
4	0.3	74.9	75.07	71.74	77.59	65.37	66.05	62.76	68.8
5	0.4	68.2	69	65.9	71.49	58.56	59.8	56.74	62.53
6	0.5	62.1	63.44	60.53	65.91	52.12	54.04	51.04	56.72
7	0.6	56.4	58.26	55.51	60.73	45.77	48.22	45.44	50.81
8	0.7	51	53.4	50.81	55.87	39.25	42.47	39.76	45.75
9	0.8	45.9	48.92	46.91	51.37	32.23	36.46	33.85	39.94
10	0.9	41.8	45.1	42.92	47.42	24.22	30.23	27.21	33.64
11	1	38.9	41.6	39.48743	44.16	15.79	25.83	22.08	28.28

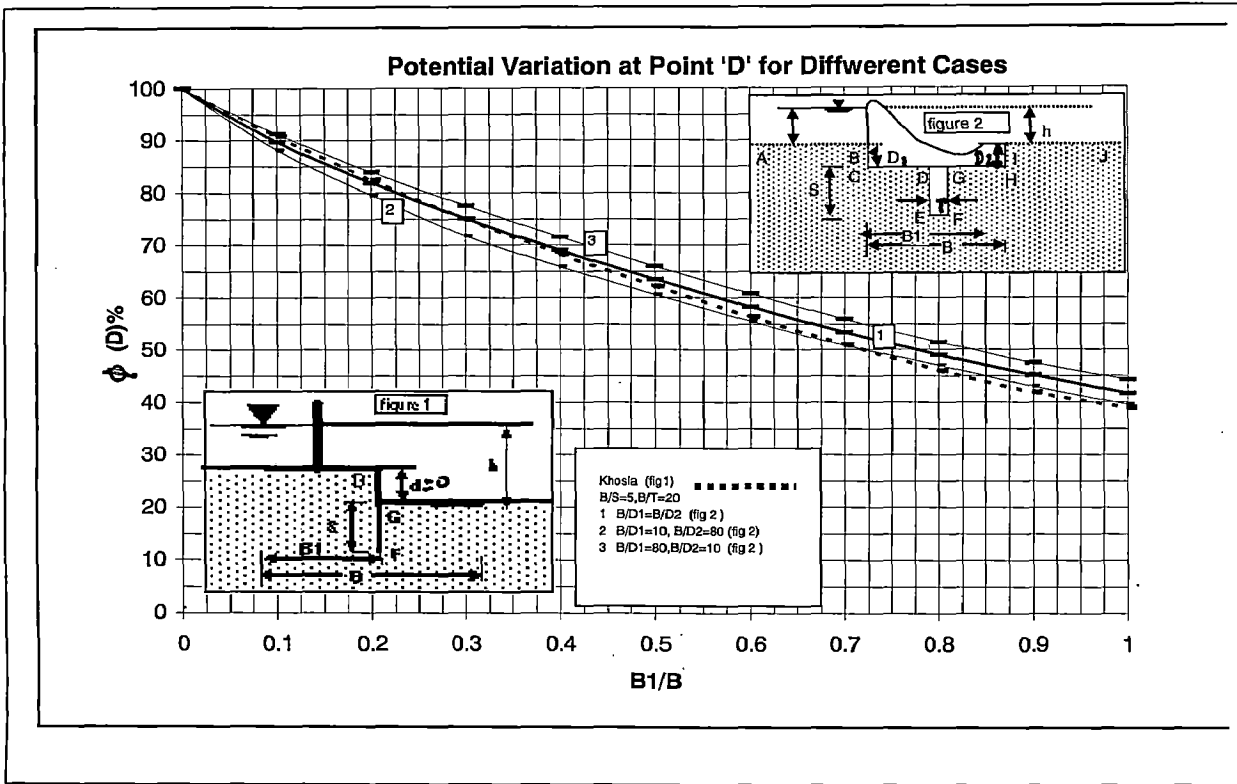


Figure 4.3.4 (a) Variation of ϕ_D at $B/S=5$ and $B/T=20$ for different cases

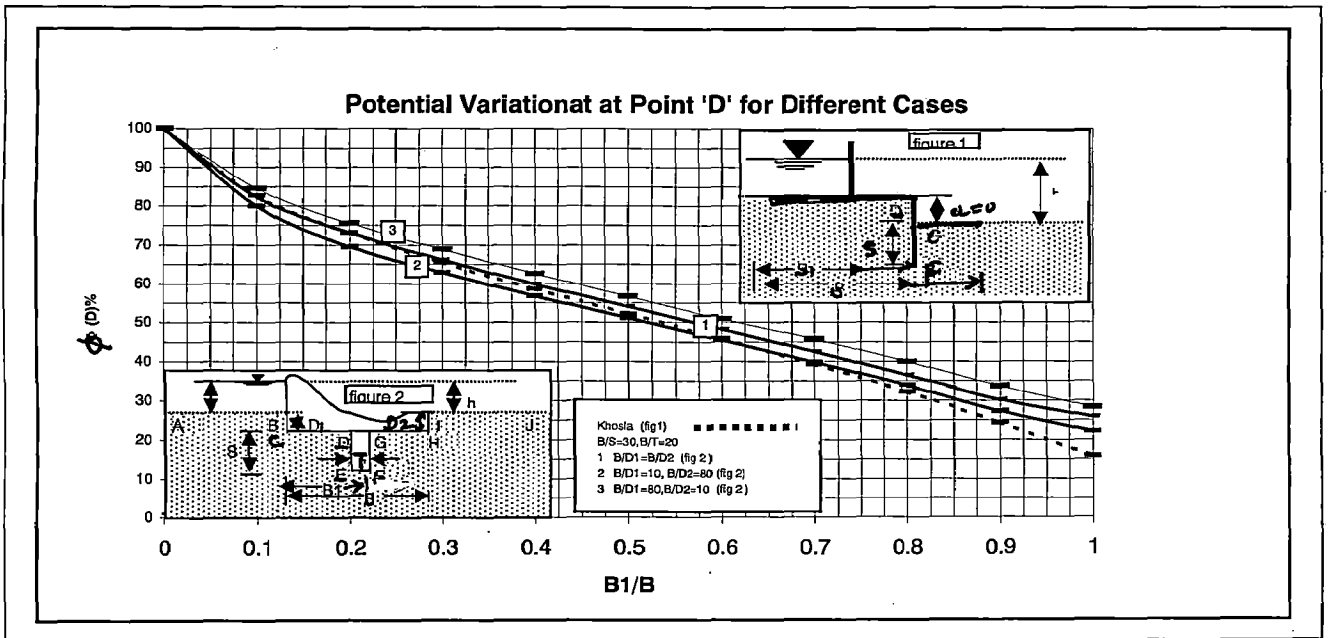


Figure 4.3.4 (b) Variation of ϕ_D at $B/S=30$ and $B/T=20$ for different cases

Table 4.3.5 Potential variation at point 'F' for different case.

S.No.	B1/B	Sheet pile	B/S=5, B/T=20			B/S=30, B/T=20			
			B/D1=25 B/D2=25	B/D1=10 B/D2=80	B/D1=80 B/D2=10	Sheet pile	B/D1=25 B/D2=25	B/D1=10 B/D2=80	B/D1=80 B/D2=10
1	0	73.27	64.57	62.11184	67.77	88.2	76.33	72.25983	79.8
2	0.1	70.7	63.16	60.68	65.22	79	71.72	68.21	74.48
3	0.2	66.5	59.36	56.77	61.66	70.8	65.04	61.8	67.76
4	0.3	62	54.91	52.31	57.35	63.75	58.92	55.88	61.65
5	0.4	55.5	50.19	47.63	52.75	56.8	53.11	50.22	55.89
6	0.5	50	45.34	42.83	48	50	47.5	44.61	50.28
7	0.6	44.5	40.4	37.94	43.16	43.2	41.58	38.87	44.34
8	0.7	38	35.39	32.99	38.25	36.25	35.48	32.77	39.02
9	0.8	34	30.47	28.64	33.38	29.2	28.68	25.99	32.56
10	0.9	29.3	26.2	24.15	29.01	21	20.73	17.29	24.36
11	1	26.73	23.75	21.6535	26.16775	11.8	13.75	9.97692	17.20517

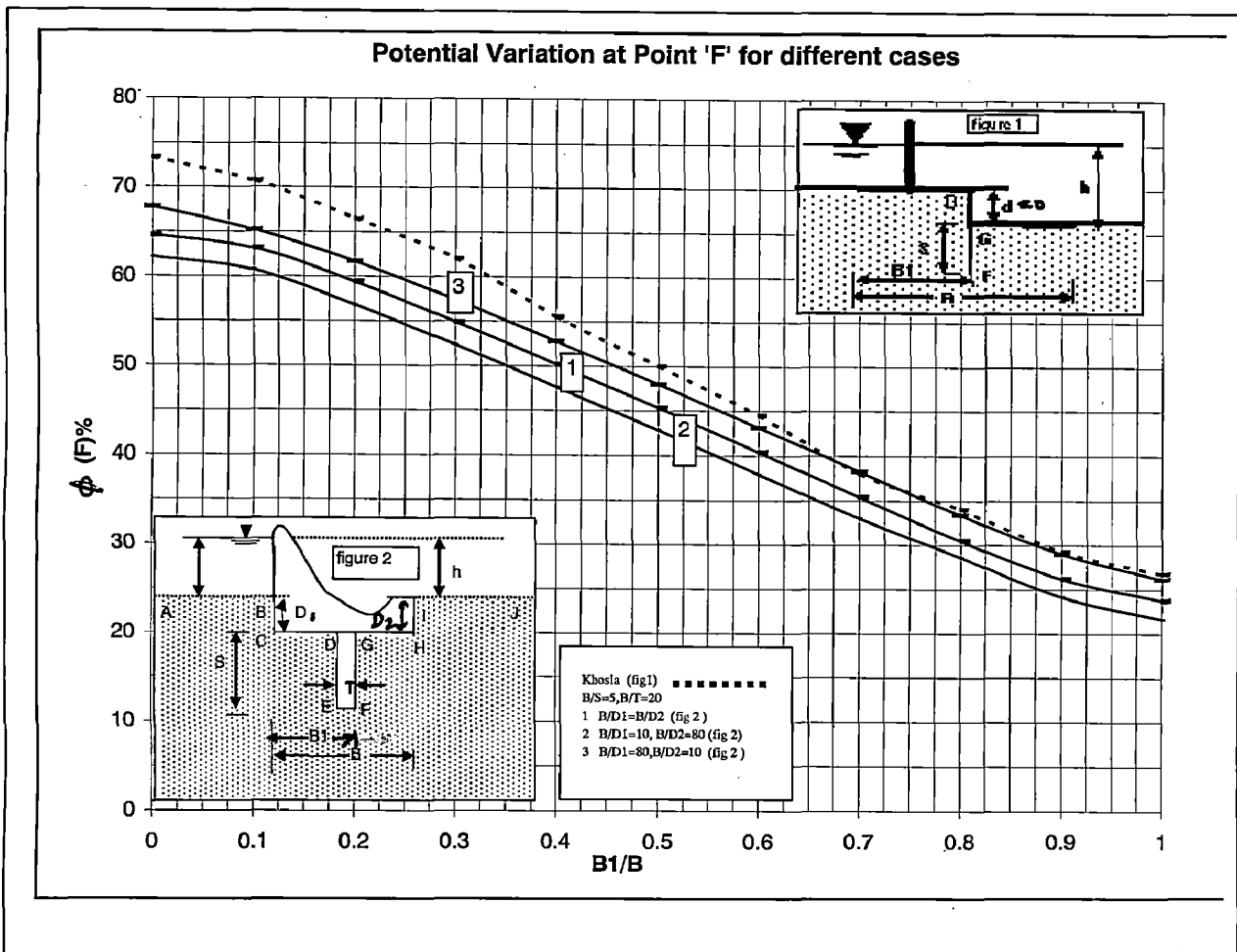


Figure 4.3.5 (a) Variation of ϕ_F at $B/S=5$ and $B/T=20$ for different cases

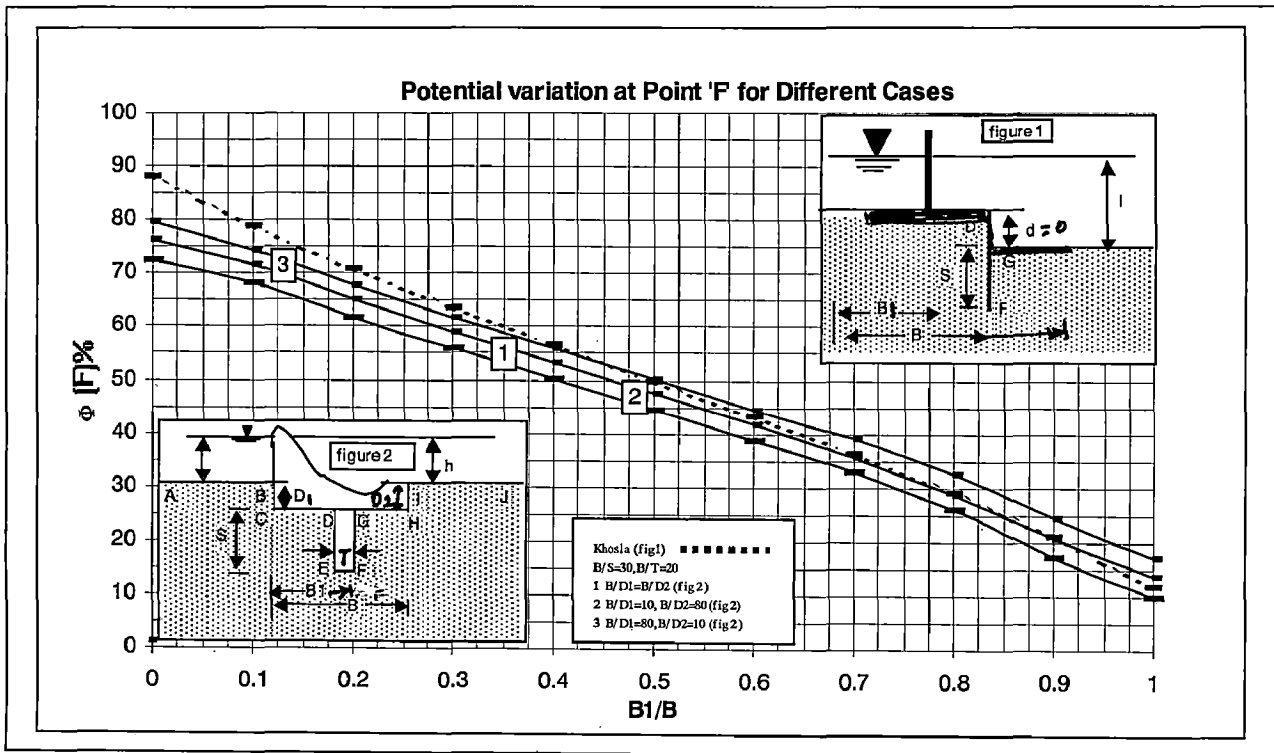


Figure 4.3.5 (b) Variation of ϕ_F at $B/S=30$ and $B/T=20$ for different cases

Table 4.3.6 Potential variation at point 'G' for different case.

S.No.	B1/B	B/S=5				B/S=30			
		Sheet pile	B/D1=25 B/D2=25	B/D1=10 B/D2=80	B/D1=80 B/D2=10	Sheet pile	B/D1=25 B/D2=25	B/D1=10 B/D2=80	B/D1=80 B/D2=10
1	0	61.07	56.16	54.26	58.00	84.21	73.45	70.44	75.78
2	0.1	58.17	54.9	52.58	57.08	75.78	69.99	66.57	72.72
3	0.2	54.08	51.08	48.63	53.49	67.77	63.54	60.36	66.26
4	0.3	49.01	46.6	44.13	49.19	60.75	57.53	54.53	60.26
5	0.4	43.62	41.74	39.27	44.49	54.23	51.76	48.91	54.56
6	0.5	37.9	36.56	34.09	39.47	47.88	46.15	43.28	48.96
7	0.6	31.76	31	28.51	34.1	41.44	40.18	37.47	42.97
8	0.7	25.06	24.93	22.41	28.26	34.63	33.95	31.23	37.56
9	0.8	17.63	18.12	16.28	21.71	26.95	26.87	24.15	30.87
10	0.9	9.27	10.29	7.77	14.1	17.32	18.15	14.5	21.84
11	1	0	0	0	0	0	0	0	0

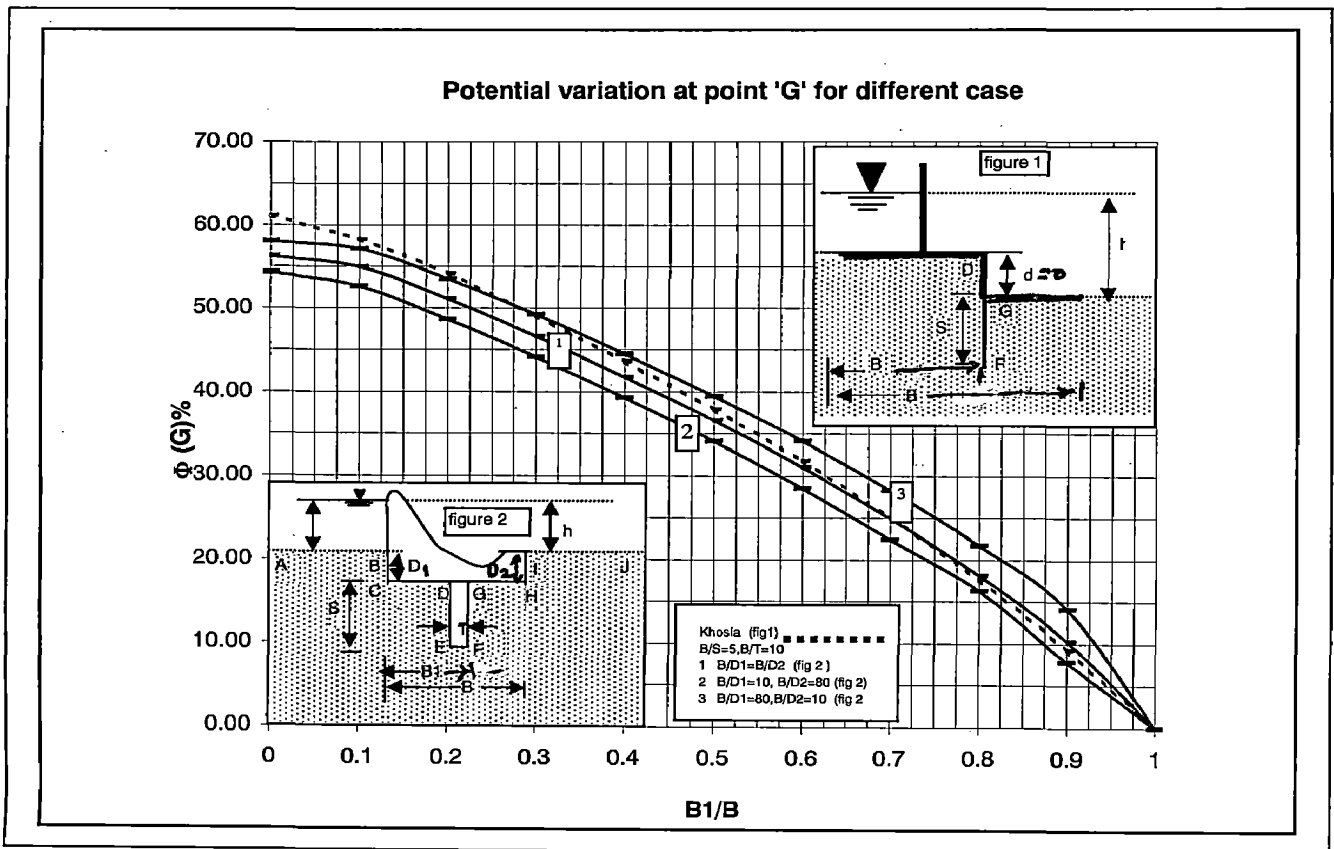


Figure 4.3.6 (a) Variation of ϕ_G at $B/S=5$ and $B/T=20$ for different cases

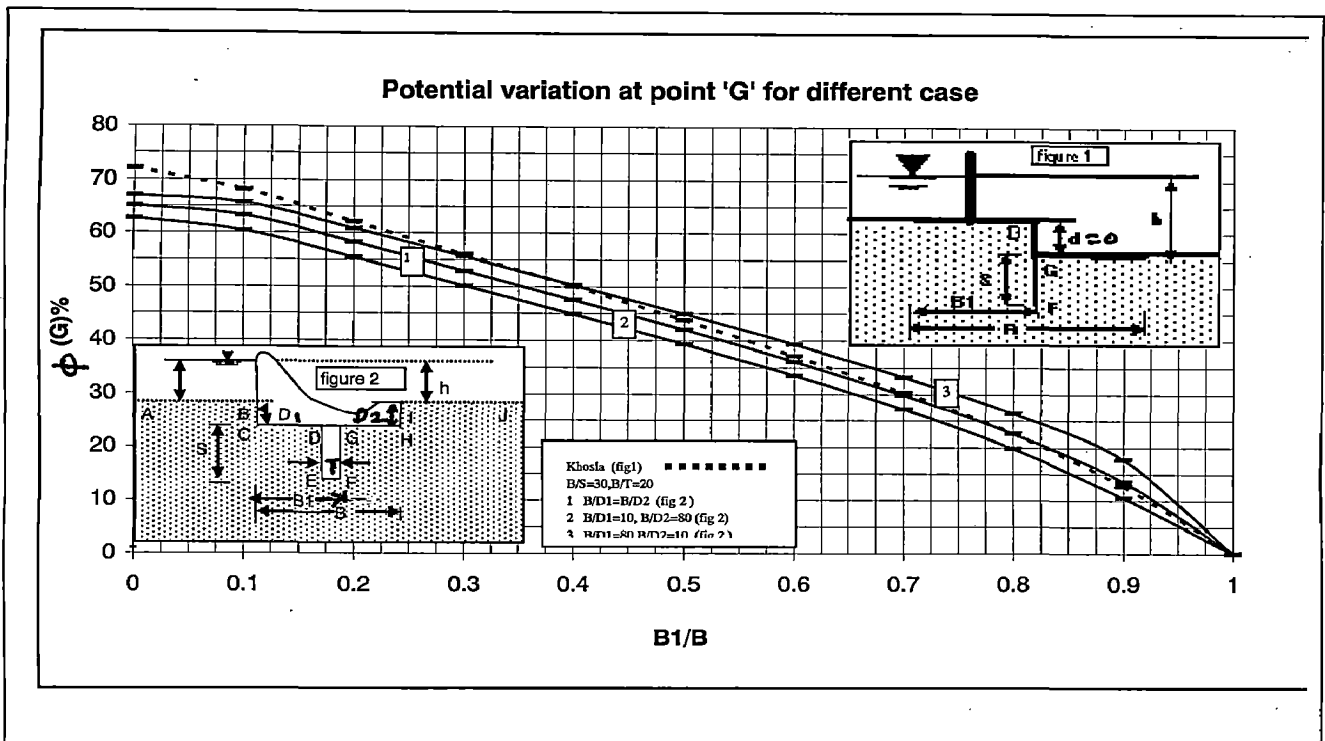


Figure 4.3.6 (b) Variation of ϕ_G at $B/S=30$ and $B/T=20$ for different cases

4.4 Exit Gradient Curves for Different Cases

Table 4.4.1 Exit Gradient Calculation Equal Depression u/s and d/s

D/S=0.20								
T/S=0.20			T/S=0.40		T/S=0.60		T/S=0.80	
S.No.	B/S	(IE/h)*S	B/S	(IE/h)*S	B/S	(IE/h)*S	B/S	(IE/h)*S
1	0.45	0.23612	0.65	0.2212	0.821	0.2103	1.1	0.2
2	0.6	0.23267	0.801	0.2183	0.91	0.2089	4	0.1528
3	0.8	0.22747	1	0.214	1	0.2074	10	0.1084
4	1	0.22192	4	0.1564	4	0.1544	20	0.0803
5	5	0.14712	10	0.1103	10	0.1092	40	0.0584
6	10	0.11194	20	0.0816	20	0.0809	50	0.0525
7	20	0.08269	40	0.0593	40	0.0587		
8	40	0.06002	50	0.0533	50	0.0529		
9	50	0.054						
D/S=0.40								
T/S=0.20			T/S=0.40		T/S=0.60			
S.No.	B/S	(IE/h)*S	B/S	(IE/h)*S	B/S	(IE/h)*S		
1	0.436	0.20565	0.56	0.195	0.811	0.185		
2	0.51	0.20411	0.8	0.1908	1	0.182		
3	0.8	0.19752	1	0.1869	4	0.1365		
4	1	0.1927	4	0.138	10	0.0978		
5	4	0.14015	10	0.0987	20	0.073		
6	10	0.09998	20	0.0736	40	0.0534		
7	20	0.07452	40	0.0538	50	0.0482		
8	40	0.05445	50	0.0485				
9	50	0.04907						
D/S=0.60				D/S=0.80				
T/S=0.20		T/S=0.40		T/S=0.80				
B/S	(IE/h)*S	B/S	(IE/h)*S	B/S	(IE/h)*S			
1	0.46	0.1818	0.65	0.1723	1.2	0.1419		
2	0.6	0.1791	0.8	0.1698	4	0.1112		
3	0.8	0.17501	1	0.1663	10	0.0815		
4	1	0.17082	4	0.1241	20	0.0617		
5	4	0.1258	10	0.0898	40	0.0456		
6	10	0.09079	20	0.0675	50	0.0412		
7	20	0.06817	40	0.0496				
8	40	0.05008	50	0.0448				
9	50	0.0452						

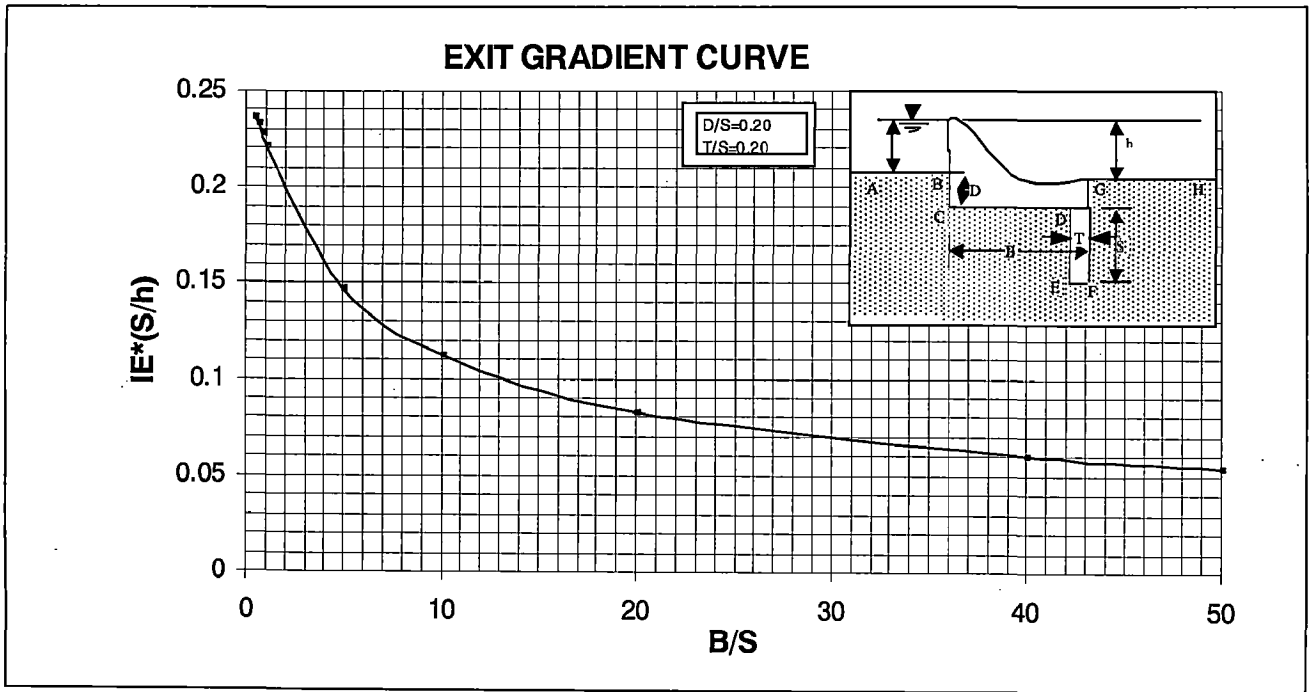


Figure 4.4.1(a) Exit Gradient Curve for $D/S=0.20$ and $T/S=0.20$

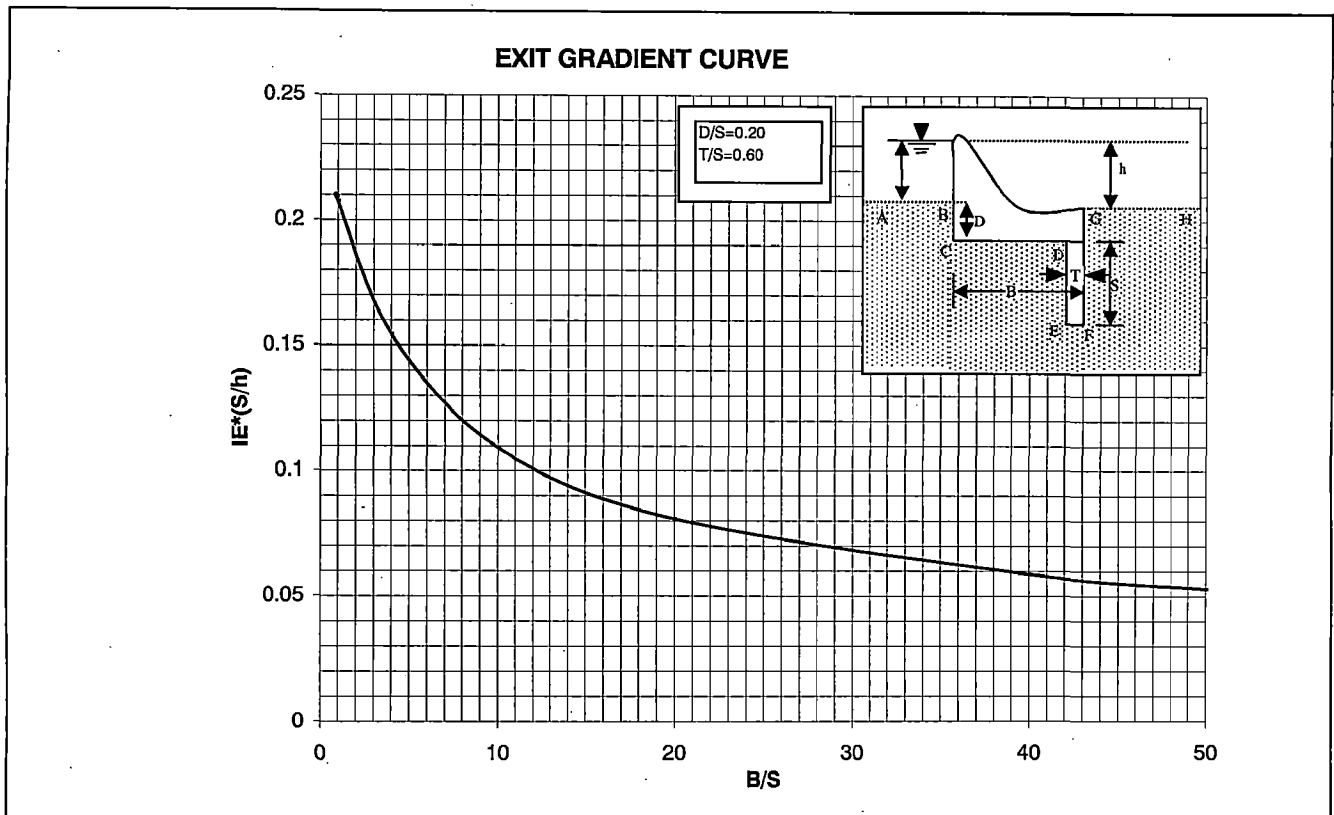


Figure 4.4.1(b) Exit Gradient Curve for $D/S=0.20$ and $T/S=0.60$

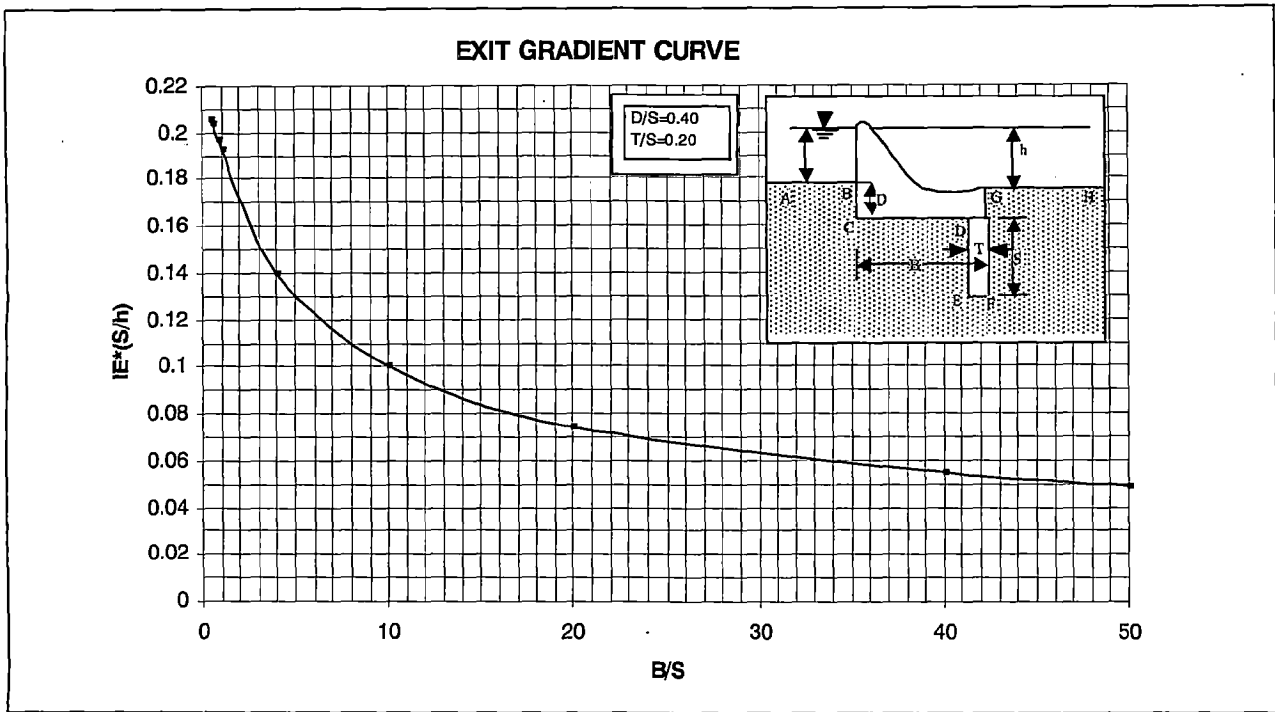


Figure 4.4.1(c) Exit Gradient Curve for $D/S=0.40$ and $T/S=0.20$

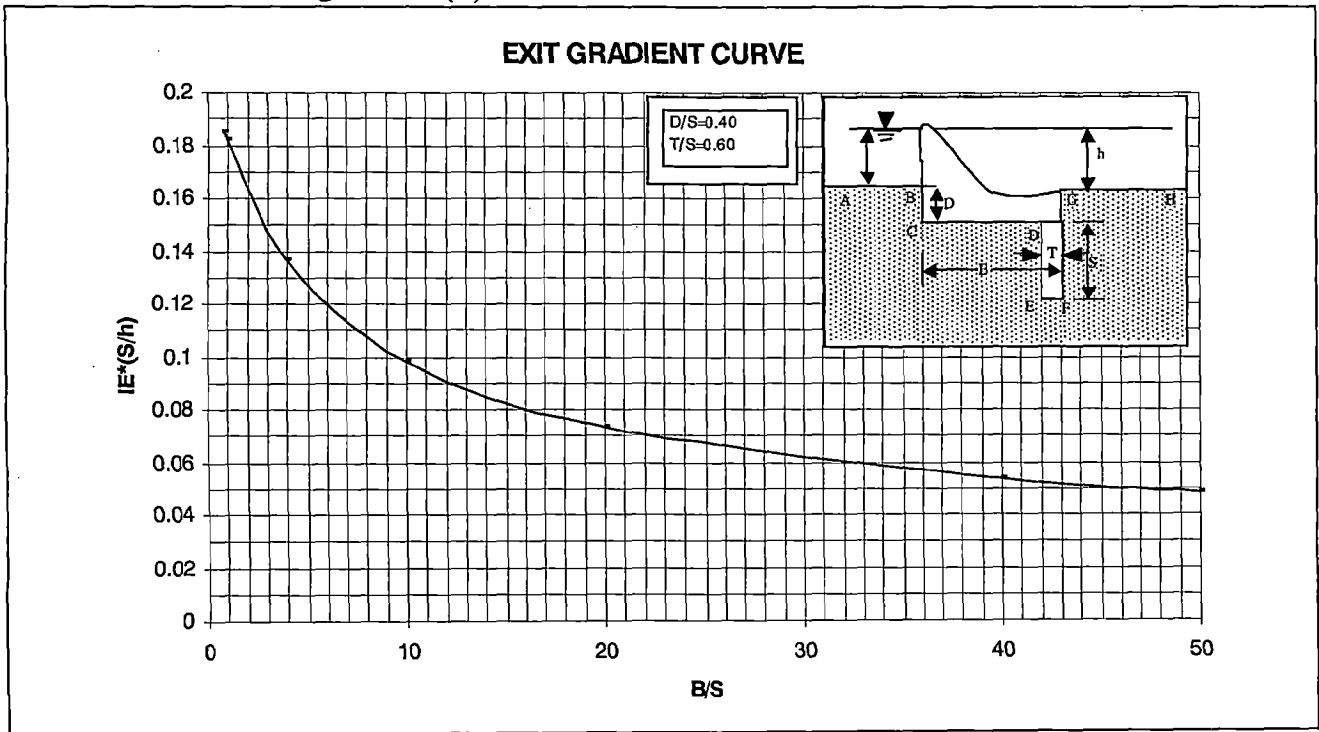


Figure 4.4.1(d) Exit Gradient Curve for $D/S=0.40$ and $T/S=0.60$

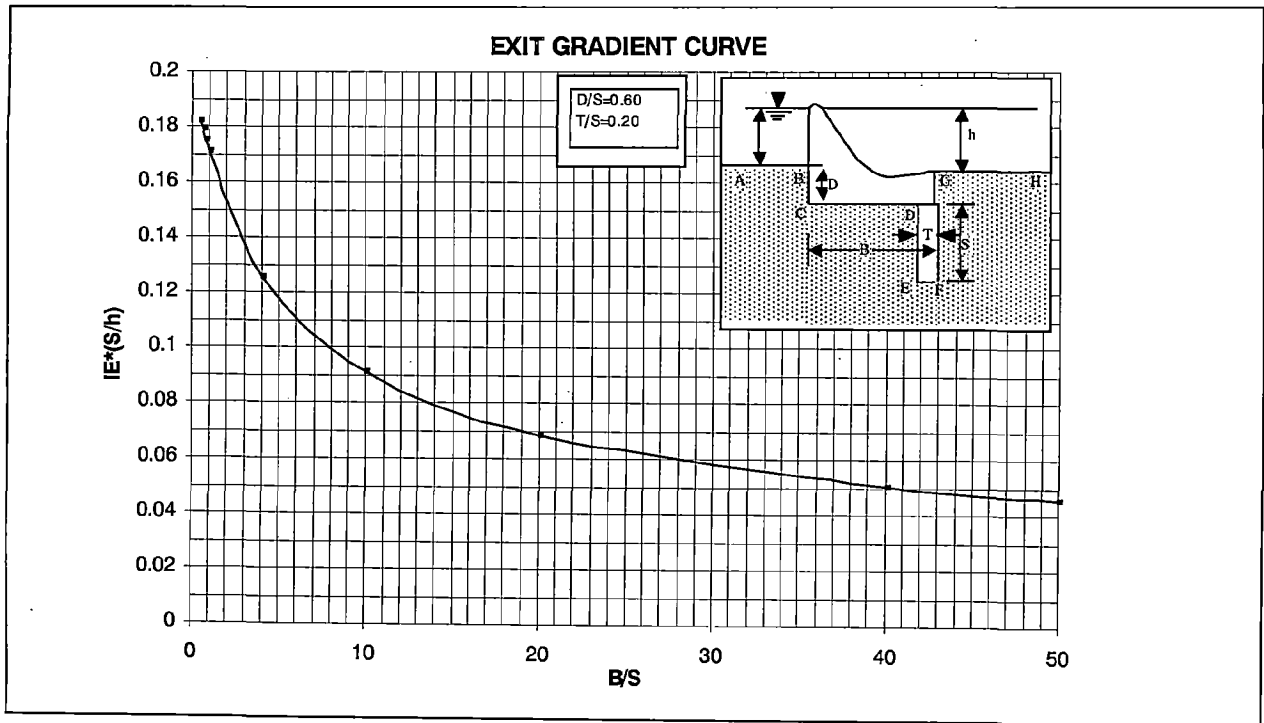


Figure 4.4.1(e) Exit Gradient Curve for $D/S=0.60$ and $T/S=0.20$

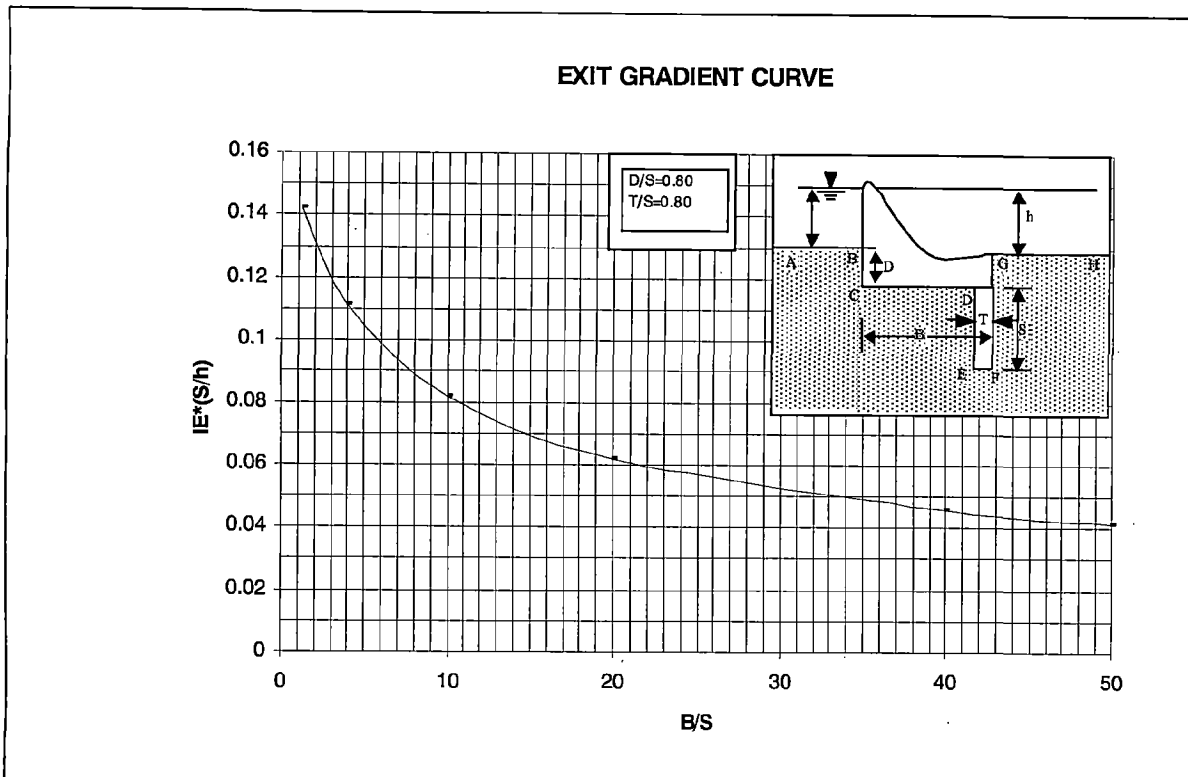


Figure 4.4.1(f) Exit Gradient Curve for $D/S=0.80$ and $T/S=0.80$

Table 4.4.2 Exit Gradient Calculation for Unequal Depression u/s and d/s

S.No.	D1/S	D2/S	T/S	B/S	I _E	D1/S	D2/S	T/S	B/S	I _E
1	0.4	0.1	0.2	1	0.23	0.1	0.6	0.4	1	0.176
2	0.4	0.1	0.2	5	0.152	0.1	0.6	0.4	5	0.122
3	0.4	0.1	0.2	10	0.116	0.1	0.6	0.4	10	0.094
4	0.4	0.1	0.2	20	0.086	0.1	0.6	0.4	20	0.07
5	0.4	0.1	0.2	40	0.062	0.1	0.6	0.4	40	0.051
6	0.4	0.1	0.2	50	0.056	0.1	0.6	0.4	50	0.046
7	0.4	0.1	0.4	1	0.222	0.1	0.6	0.6	1.02	0.17
8	0.4	0.1	0.4	5	0.149	0.1	0.6	0.6	5	0.121
9	0.4	0.1	0.4	10	0.114	0.1	0.6	0.6	10	0.093
10	0.4	0.1	0.4	20	0.085	0.1	0.6	0.6	20	0.069
11	0.4	0.1	0.4	40	0.062	0.1	0.6	0.6	40	0.05
12	0.4	0.1	0.4	50	0.055	0.1	0.6	0.6	50	0.045
13	0.6	0.1	0.4	1	0.218	0.6	0.1	0.6	1	0.212
14	0.6	0.1	0.4	5	0.147	0.6	0.1	0.6	5	0.145
15	0.6	0.1	0.4	10	0.112	0.6	0.1	0.6	10	0.111
16	0.6	0.1	0.4	20	0.084	0.6	0.1	0.6	20	0.083
17	0.6	0.1	0.4	40	0.061	0.6	0.1	0.6	40	0.061
18	0.6	0.1	0.4	50	0.055	0.6	0.1	0.6	50	0.055

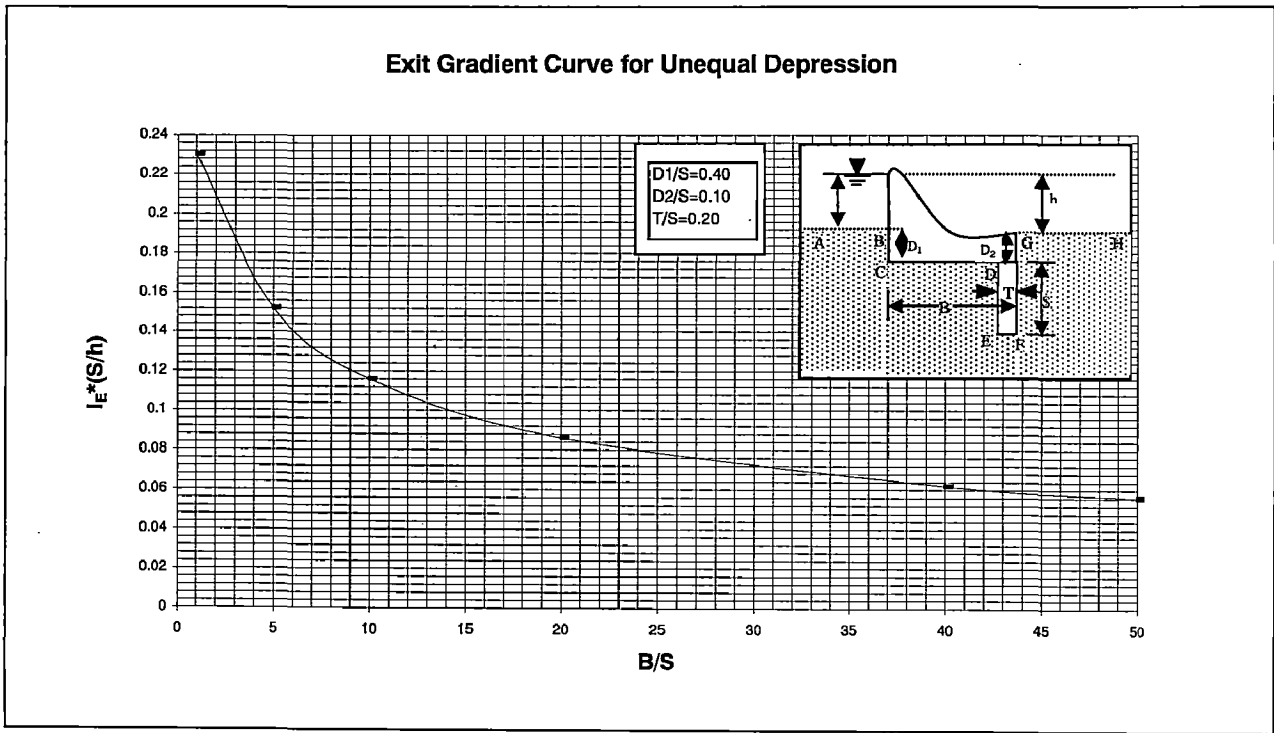


Figure 4.4.2 (a) Exit Gradient Curve for $D_1/S=0.40$, $D_2/S=0.10$ and $T/S=0.20$

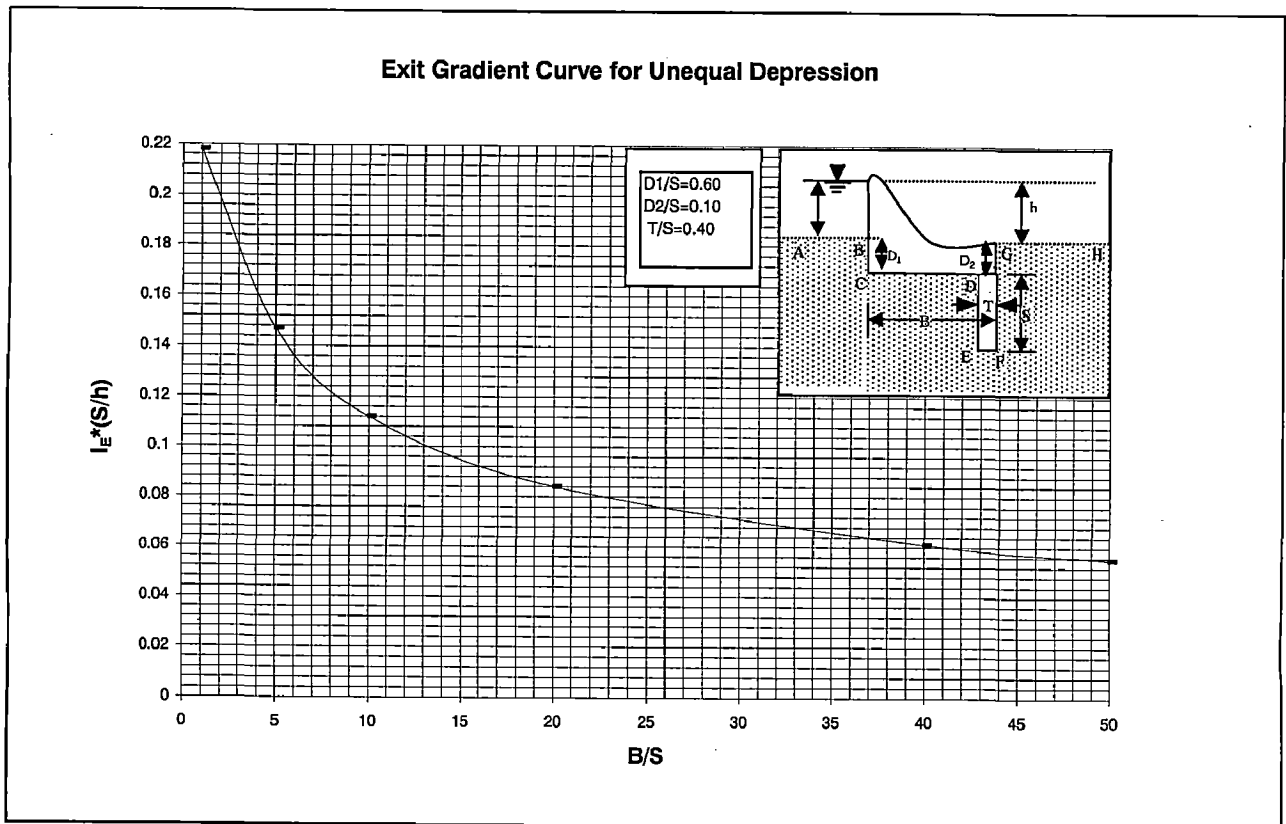


Figure 4.4.2 (b) Exit Gradient Curve for $D_1/S=0.60$, $D_2/S=0.10$ and $T/S=0.40$

Exit Gradient Curve for Unequa Depression

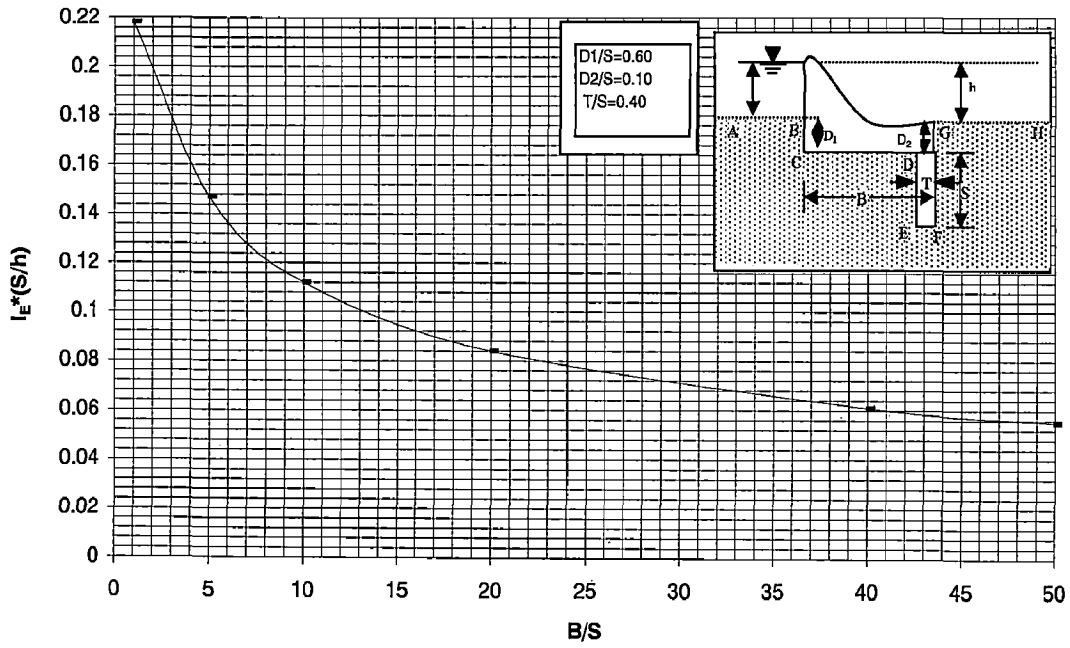


Figure 4.4.2 (c) Exit Gradient Curve for $D_1/S=0.60$, $D_2/S=0.10$ and $T/S=0.40$

Exit Gradient Curve for Unequa Depression

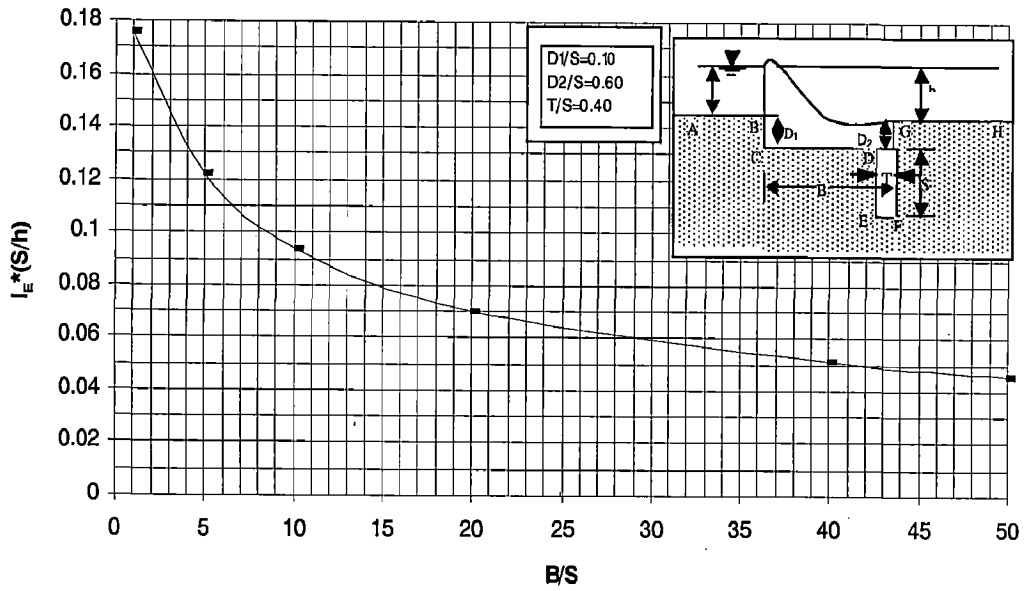


Figure 4.4.2 (d) Exit Gradient Curve for $D_1/S=0.10$, $D_2/S=0.60$ and $T/S=0.40$

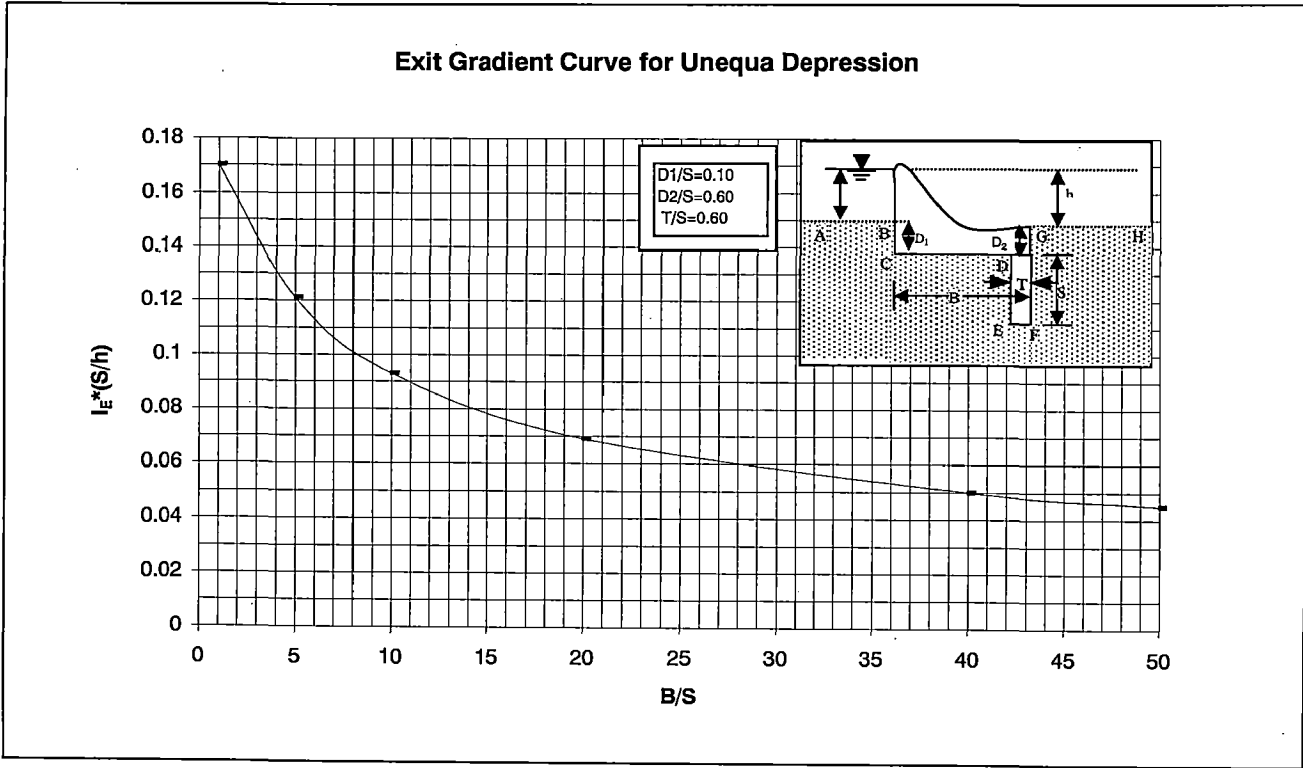


Figure 4.4.2 (e) Exit Gradient Curve for $D_1/S=0.10$, $D_2/S=0$

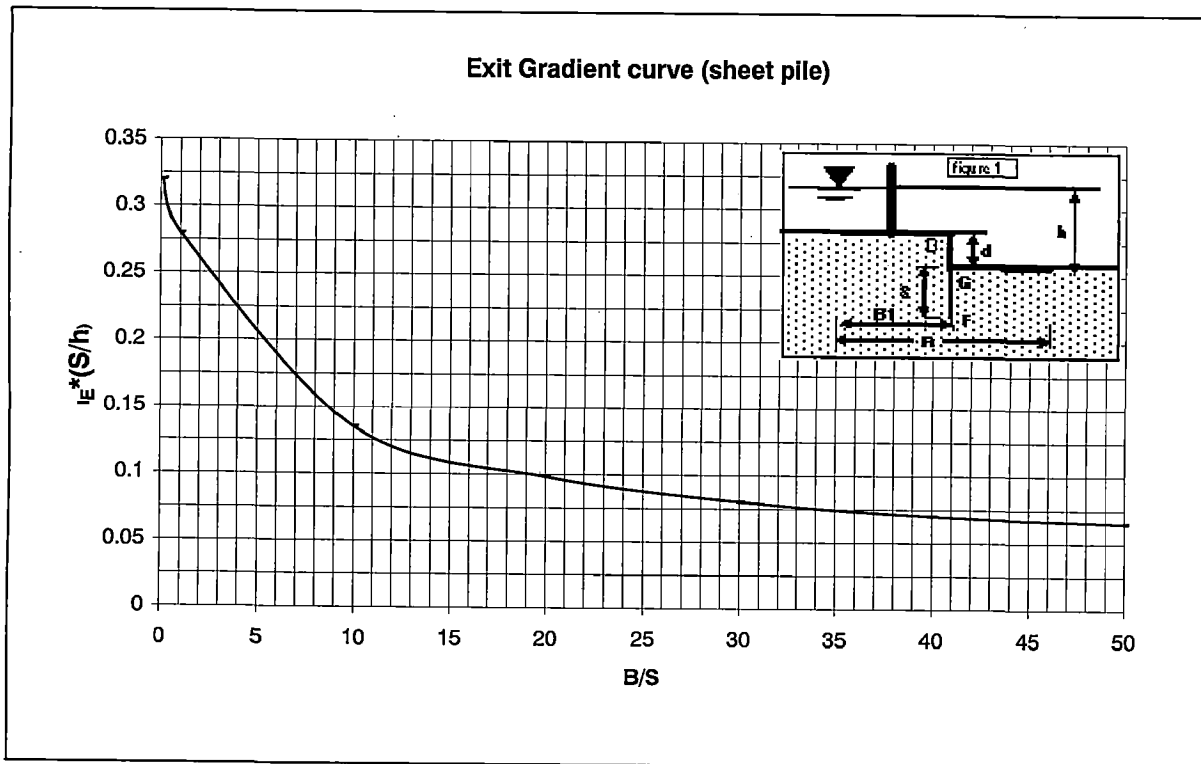


Figure 4.5 Exit Gradient curve (sheet pile)

CHAPTER 5

RESULTS, DISCUSSION AND CONCLUSION

The constant c in the definition of ϕ is assumed to be zero, and $\phi = -k\left(\frac{P}{\gamma_w} + y\right)$

While presenting the result, ϕ has been non-dimensionlized dividing ϕ by $-kh$ where h is the head difference causing seepage to occur.

5.1 Variation of Potential Distribution under a weir with Concrete Cutoff toe

Potential Variation At key points 'D' and 'E'

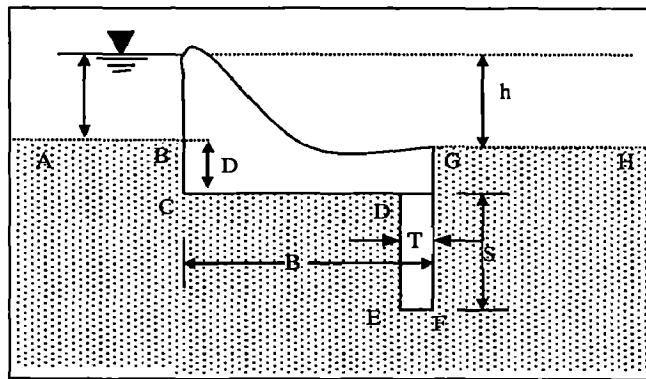


Figure 5.1.1 Depressed weir with concrete cutoff downstream
 B =Total horizontal floor length, T =Thickness of concrete cutoff

S = Depth of concrete cutoff, D =Depth of depression in upstream and downstream side

Table 5.1.1 Variation in ϕ_D and ϕ_E with variation of T/B ; T varying

		D/B=0.05								
		S/B=0.05			S/B=0.10			S/B=0.15		
S.No.	T/B	0.01	0.15	Difference in %	0.01	0.15	Difference in %	0.01	0.15	Difference in %
1	ϕ_D %	23.28	34.6	11.32	29.49	39.69	10.2	34.42	43.88	9.46
2	ϕ_E %	19.78	32.61	12.83	23.76	36.03	12.27	26.88	38.7	11.82
		S/B=0.05								
		D/B=0.02			D/B=0.06			D/B=0.10		
		Difference in %			Difference in %			Difference in %		
	T/B	0.01	0.15	%	0.01	0.15	%	0.01	0.15	%
3	ϕ_D %	22.19	34.34	12.15	23.62	34.72	11.1	24.82	35.215	10.3946
4	ϕ_E %	18.39	32.22	13.83	20.19	32.76	12.57	21.642	33.372	11.72996
		S/B=0.12								
		D/B=0.02			D/B=0.06			D/B=0.10		
		Difference in %			Difference in %			Difference in %		
	T/B	0.01	0.15	%	0.01	0.15	%	0.01	0.15	%
5	ϕ_D %	31.31	41.73	10.42	31.7	41.43	9.73	32.23	41.45	9.22
6	ϕ_E %	24.42	37.21	12.79	25.32	37.2	11.88	26.21	37.44	11.23

From the variation of T/B from 0.01 to 0.15 for the same depression and cutoff depth it is found that:

- I. The velocity potential (at D and E) increases as the thickness of cutoff increases.
- II. The rate of increment of the velocity potential ϕ_D and ϕ_E decreases with increase in cutoff thickness. For S/B=0.05 the rate of increment of ϕ_D and ϕ_E is 11.32% and 12.83% while for S/B=0.15 the values are 9.46% and 11.82% respectively.
- III. The velocity potential increases more for smaller cutoff depth than for greater depth also the rate of increment in potential values is more in smaller cutoff depth.
- IV. The rate of increment of the velocity potential ϕ_D and ϕ_E decreases with increase in cutoff depth.
- V. The rate of increment of velocity potential decreases marginally as the depression increases.

Table 5.1.2 Variation ϕ_D and ϕ_E with variation of S/B; S varying

		D/B=0.05								
		T/B=0.05			T/B=0.10			T/B=0.15		
		S/B		Difference in %	S/B		Difference in %	S/B		Difference in %
		0.01	0.15		0.01	0.15		0.01	0.15	
7	ϕ_D %	21.05	37.63	16.58	25.49	40.92	15.43	29.22	43.88	14.66
8	ϕ_E %	20.41	31.43	11.02	24.99	35.38	10.39	28.78	38.7	9.92
		T/B=0.05								
		D/B=0.05			D/B=0.10			D/B=0.15		
		S/B		Difference in %	S/B		Difference in %	S/B		Difference in %
		0.01	0.15		0.01	0.15		0.01	0.15	
9	ϕ_D %	21.04	37.63	16.59	23.02	37.82	14.8	25.5	38.12	12.62
10	ϕ_E %	20.41	31.43	11.02	22.45	32.02	9.57	23.98	32.62	8.64
		T/B=0.10								
		D/B=0.05			D/B=0.10			D/B=0.15		
		S/B		Difference in %	S/B		Difference in %	S/B		Difference in %
		0.01	0.15		0.01	0.15		0.01	0.15	
11	ϕ_D %	25.48	40.92	15.44	27.03	40.91	13.88	28.23	41.06	12.83
12	ϕ_E %	24.98	35.38	10.4	26.57	35.71	9.14	27.81	36.13	8.32

From the variation of S/B from 0.01 to 0.15 for the same depression and cutoff depth it is seen that

- I. The rate of decrease in ϕ_D values are found to be 1.15% and 0.77% and that of ϕ_E values are 0.63% and 0.47% corresponding to the change in cutoff thickness T/B from 0.05 to 0.10 and 0.10 to 0.15 respectively.

- II. The increment in velocity potential ϕ_D and ϕ_E is more in smaller cutoff thickness than in greater thickness.
- III. Depression D/B has lesser impact for the velocity potential than the thickness of cutoff T/B. As mentioned in the Table 5.2 that the velocity potentials ϕ_D and ϕ_E for D/B=0.05 and T/B=0.15 are 14.66% and 9.92% while these values for T/B=0.05 and D/B=0.15 are 12.62% and 8.64% respectively.
- IV. The potential values increase as the thickness of cutoff increases.

Table 5.1.3 Variation in ϕ_D and ϕ_E with variation of D/B; D varying

		S/B=0.05								
		T/B=0.05			T/B=0.10			T/B=0.15		
	D/B	0.01	0.15	Difference in %	0.01	0.15	Difference in %	0.01	0.15	Difference in %
13	ϕ_D %	26.34	29.47	3.13	30.65	32.84	2.19	34.37	35.8	1.43
14	ϕ_E %	23.46	27.24	3.78	28.23	30.93	2.702	32.19	34.07	1.88
		T/B=0.05								
		S/B=0.05			S/B=0.10			S/B=0.15		
	D/B	0.01	0.15	Difference in %	0.01	0.15	Difference in %	0.01	0.15	Difference in %
15	ϕ_D %	26.34	29.47	3.13	32.85	34.19	1.34	37.95	38.12	0.17
16	ϕ_E %	23.46	27.24	3.78	27.91	30.22	2.31	31.25	32.62	1.37

From the variation of D/B from 0.01 to 0.15 for the same thickness and cutoff depth it is observed from table 5.1.3 that::

- I. The values of ϕ_D and ϕ_E increase marginally as the depression D/B increases.
- II. The effect of depression in the velocity potential is more in smaller cutoff thickness and cutoff depth than in smaller cutoff thickness and greater depth. As listed in the Table 5.3 the increment values of ϕ_D and ϕ_E for T/B=0.05 and S/B=0.05 are 3.13% and 3.78% while these values for T/B=0.05 and S/B=0.15 are 0.17% and 1.37% respectively.
- III. Depression has more impact in the ϕ_E values than in ϕ_D values.

Table 5.1.4 Variation in ϕ_D and ϕ_E with variation of D_1/B and D_2/B : D_1 and D_2 varying

Varying with 'D ₁ '												
S/B=0.05, D ₂ /B=0.02												
		T/B=0.03		Difference in %		T/B=0.05		Difference in %		T/B=0.10		
	D ₁ /B	0.02	0.15			0.02	0.15			0.01	0.15	
17	ϕ_D %	22.19	20.42	-1.77		26.54	24.44	-2.1		30.73	28.29	-2.44
18	ϕ_E %	13.78	12.7	-1.08		13.08	12.07	-1.01		12.82	11.94	-0.88
Varying with 'D ₂ '												
S/B=0.05												
		T/B=0.03		Difference in %		T/B=0.05		Difference in %		T/B=0.10		
	D ₂ /B	0.02	0.15			0.02	0.15			0.01	0.15	
19	ϕ_D %	24.56	30.18	5.62		26.54	31.87	5.33		30.73	35.51	4.78
20	ϕ_E %	13.3	20.72	7.42		13.08	20.51	7.43		12.82	20.23	7.41

From the variation of D_1/B from 0.02 to 0.15 for the same thickness, d/s depression and cutoff depth it is seen that:

- I. The decrement in velocity potential ϕ_D increases and ϕ_E decreases with increase in thickness of cutoff.

From the variation of D_2/B from 0.02 to 0.15 for the same thickness, u/s depression and cutoff depth it is observed that:

- I. The velocity potential ϕ_D increase with increase in the thickness of cutoff while the velocity potential ϕ_E remains constant. The increment rate of ϕ_D value decrease as the thickness of cutoff increases.

5.2 Variation of Potentials Distribution for a weir with a Concrete Cutoff

Upstream

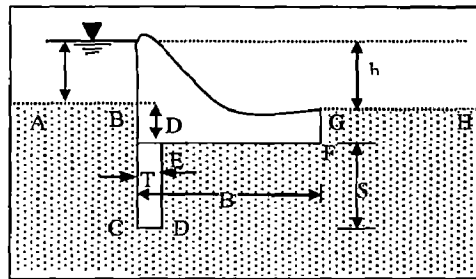


Figure 5.2.1 Depressed weir with concrete cutoff upstream

B=Total horizontal floor length, T=Thickness of concrete cutoff

S= Depth of concrete cutoff, D=Depression in upstream and downstream side whereas

Table 5.2.1 Variation in ϕ_D and ϕ_E with variation of T/B; T varying

		S/B=0.05								
		D/B=0.02			D/B=0.06			D/B=0.10		
S.No.	T/B	0.01	0.15	Difference in %	0.01	0.15	Difference in %	0.01	0.15	Difference in %
1	ϕ_D %	80.55	65.16	-15.39	78.86	64.43	-14.43	77.58	63.86	-13.72
2	ϕ_E %	76.69	63.06	-13.63	75.3	62.46	-12.84	74.23	62	-12.23
		S/B=0.12								
		D/B=0.02			D/B=0.06			D/B=0.10		
S.No.	T/B	0.01	0.15	Difference in %	0.01	0.15	Difference in %	0.01	0.15	Difference in %
3	ϕ_D %	74.38	60.11	-14.27	73.46	59.94	-13.52	72.67	59.74	-12.93
4	ϕ_E %	67.35	55.62	-11.73	66.85	55.69	-11.16	66.38	55.67	-10.71

From the variation of T/B from 0.01 to 0.15 for the same depression and cutoff depth it is observed from table 5.2.1 that:

- I. The velocity potential decreases as the thickness of cutoff increases.
- II. With the increase in the depression D/B from 0.02 to 0.06 the velocity potential ϕ_D and ϕ_E decrease by 2% and 1.39% respectively.
- III. The decrement rate of potential values is lesser for greater depression than for smaller one.
- IV. ϕ_D and ϕ_E decrease by 6.19% and 9.34% respectively as the depth of cutoff S/B increases from 0.05 to 0.12 for the same depression D/B=0.02.

Table 5.2.2 Variation in ϕ_D and ϕ_E with variation of S/B; S varying

		T/B=0.05								
		D/B=0.02			D/B=0.06			D/B=0.10		
S.No.	S/B	0.01	0.15	Difference in %	0.01	0.15	Difference in %	0.01	0.15	Difference in %
5	ϕ_D %	79.59	66.79	-12.8	77.46	66.37	-11.09	76.05	65.96	-10.09
6	ϕ_E %	78.9	60.23	-18.67	76.84	60.14	-16.7	75.47	60	-15.47

From the variation of S/B from 0.01 to 0.15 for the same depression and cutoff thickness we observe from Table 5.2.2 that:

- I. The rate of decrement of ϕ_D is 12.8% for D/B=0.02 and 10.09% for D/B=0.15 while these values of ϕ_E is 18.67% and 15.47% respectively for the same cutoff thickness T/B=0.05.

II. As the depth of cutoff increases the velocity potentials decrease.

Table 5.2.3 Variation in ϕ_D and ϕ_E with variation of D/B ; D varying

		S/B=0.05								
		T/B=0.05			T/B=0.10			T/B=0.15		
S.No.	D/B	0.01	0.15	Difference in %	0.01	0.15	Difference in %	0.01	0.15	Difference in %
7	ϕ_D %	74.72	71.15	-3.57	69.54	66.83	-2.71	65.37	63.3	-2.07
8	ϕ_E %	71.86	68.74	-3.12	67.16	64.87	-2.29	63.22	61.54	-1.68
		T/B=0.05								
		S/B=0.05			S/B=0.10			S/B=0.15		
S.No.	D/B	0.01	0.15	Difference in %	0.01	0.15	Difference in %	0.01	0.15	Difference in %
9	ϕ_D %	74.72	71.15	-3.57	70.23	68	-2.23	66.88	65.5	-1.38
10	ϕ_E %	71.86	68.74	-3.12	65.31	63.88	-1.43	60.21	59.8	-0.41

We observe from Table 5.2.3 that:

- I. The rate of decrement for ϕ_D is more in smaller depth and greater thickness while for ϕ_E it is more in smaller thickness and greater depth. As mentioned in Table 5.2.3 the ϕ_D value for, S/B=0.05 and T/B=0.15 is 65.37%, and, for S/B=0.15 and T/B=0.05 is 66.8% while these values for ϕ_E is 63.22% and 60.21% respectively.

Table 5.2.4 Variation in ϕ_D and ϕ_E with variation of D_1/B and D_2/B

		Varying with 'D ₁ '								
		S/B=0.05, D ₂ /B=0.02								
		T/B=0.01			T/B=0.05			T/B=0.10		
	D ₁ /B	0.02	0.15	Difference in %	0.02	0.15	Difference in %	0.01	0.15	Difference in %
11	ϕ_D %	80.55	74.83	-5.72	74.34	69.36	-4.98	69.26	64.76	-4.5
12	ϕ_E %	76.69	71.48	-5.21	71.55	66.88	-4.67	66.93	62.66	-4.27
		Varying with 'D ₂ '								
		S/B=0.05								
		T/B=0.01			T/B=0.05			T/B=0.10		
	D ₂ /B	0.02	0.15	Difference in %	0.02	0.15	Difference in %	0.02	0.15	Difference in %
13	ϕ_D %	80.55	81.77	1.22	74.34	75.94	1.6	69.26	71.18	1.92
14	ϕ_E %	76.69	78.16	1.47	71.55	73.34	1.79	66.93	69.01	2.08

From the variation of D_1/B from 0.02 to 0.15 for the same thickness, d/s depression and cutoff depth we see from table 5.2.4 that:

- I. Potential values decrease with increase in the upstream depression D_1/B . The rate of decrement is more in smaller cutoff thickness than in greater one.

Varying D_2/B from 0.02 to 0.15 for the same thickness, u/s depression and cutoff depth it is found that:

- I. The velocity potentials ϕ_D and ϕ_E increase with increase in the downstream depression D_2/B . The rate of increment is more in greater thickness than in smaller one.

5.3 Potentials at the key points for the depressed weir with concrete cutoff at different points of the floor

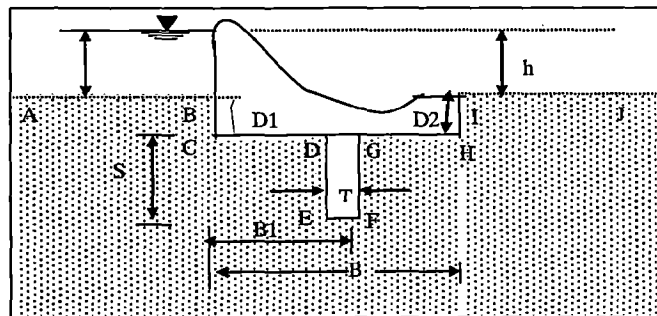


Figure 5.3.1 Variation of concrete cutoff at different point of the horizontal floor

B =Total horizontal floor length, B_1 =Length of u/s floor

B_2 =Length of d/s floor, T =Thickness of concrete cutoff

S = Depth of concrete cutoff, D =Equal depression for upstream and downstream whereas D_1 and D_2 is used for upstream depression and downstream depression respectively.

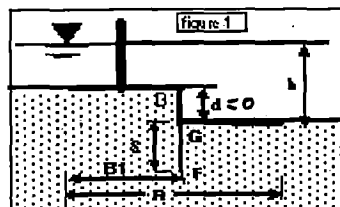


Figure 5.3.2 Variation of sheet pile at different point of the horizontal floor

The difference in exact potential and approximate potential computed by Khosla method is presented in Table 5.3.1. The deviation is computed subtracting the exact value from the approximate value.

Table 5.3.1 Deviation of Φ_D from Khosla's values expressed as percentage

		B/S=5					
		B/T=10			B/T=20		
S.No	B ₁ /B	B/D1=25 B/D2=25	B/D1=10 B/D2=80	B/D1=80 B/D2=10	B/D1=25 B/D2=25	B/D1=10 B/D2=80	B/D1=80 B/D2=10
1	0	0	0	0	0	0	0
2	0.1	-1.3	2.48	-3.71	1.02	2.58	-0.49
3	0.2	-1.67	1.95	-4.19	0.49	2.77	-1.53
4	0.3	-2.17	1.19	-4.67	-0.13	3.2	-2.65
5	0.4	-2.72	0.41	-5.18	-0.76	2.34	-3.25
6	0.5	-3.28	-0.35	-5.72	-1.34	1.57	-3.81
7	0.6	-3.85	-1.09	-6.27	-1.88	0.87	-4.35
8	0.7	-4.46	-1.88	-6.87	-2.41	0.18	-4.88
9	0.8	-5.21	-2.44	-7.56	-3	-0.99	-5.45
10	0.9	-5.72	-3.59	-7.91	-3.27	-1.09	-5.59
11	1	-5.85	-3.66	-8.33	-2.67	-0.56	-5.23
		B/S=30					
		B/T=10			B/T=20		
1	0	0	0	0	0	0	0
2	0.1	-2.71	1.77	-6.01	0.46	2.71	-1.82
3	0.2	-2.29	1.46	-5.19	-0.08	3.56	-2.45
4	0.3	-2.57	0.8	-5.32	-0.68	2.61	-3.43
5	0.4	-2.98	0.13	-5.7	-1.24	1.82	-3.97
6	0.5	-3.51	-0.57	-6.26	-1.92	1.08	-4.6
7	0.6	-4.06	-1.34	-6.98	-2.45	0.33	-5.04
8	0.7	-4.99	-2.25	-7.92	-3.22	-0.51	-6.5
9	0.8	-6.17	-3.37	-9.26	-4.23	-1.62	-7.71
10	0.9	-8.16	-5.51	-11.42	-6.01	-2.99	-9.42
11	1	-13.04	-10.49	-16.48	-10.04	-6.29	-12.49

The cutoff position has been varied from upstream to downstream position. $B_1/B=0$ indicates the upstream cutoff and $B_1/B=1.0$ indicates downstream cutoff. A negative value is the indication of underestimation of ϕ_D by Khosla approximate method. A positive value means over estimation. Mostly Khosla approximate method underestimates. Therefore it is not safe to use Khosla approximate method to design the thickness of floor.

The deviation of true value from that computed using Khosla's approximate method for point G is presented in Table 5.3.2. As seen Khosla's method over estimates for most of the weir. However in some cases, Khosla's method under estimates ϕ_G . As mentioned in the Table 5.3.2 negative sign means under estimation of ϕ_G and positive sign means over estimation of ϕ_G . Under estimations occurs for higher downstream depression

Table 5.3.2 Deviation in % for Φ_G with respect to Khosla's values

		B/S=5					
		B/T=10			B/T=20		
S.No	B1/B	B/D1=25 B/D2=25	B/D1=10 B/D2=80	B/D1=80 B/D2=10	B/D1=25 B/D2=25	B/D1=10 B/D2=80	B/D1=80 B/D2=10
1	0	6.41	8.27	4.53	4.91	6.81	3.07
2	0.1	5.72	7.91	3.79	3.27	5.59	1.09
3	0.2	5.21	7.56	2.82	3.00	5.45	0.59
4	0.3	4.46	6.87	1.88	2.41	4.88	-0.18
5	0.4	3.85	6.27	1.09	1.88	4.35	-0.87
6	0.5	3.28	5.72	0.35	1.34	3.81	-1.57
7	0.6	2.72	5.18	-0.41	0.76	3.25	-2.34
8	0.7	2.17	4.67	-1.19	0.13	2.65	-3.20
9	0.8	1.67	4.94	-1.95	-0.49	1.35	-4.08
10	0.9	1.30	3.71	-2.48	-1.02	1.50	-4.83
11	1	0.00	0.00	0.00	0.00	0.00	0.00
		B/S=30					
		B/T=10			B/T=20		
1	0	13.45	16.33	9.10	10.76	13.77	8.43
2	0.1	8.16	11.42	5.51	5.79	9.21	3.06
3	0.2	6.17	9.26	3.47	4.23	7.41	1.51
4	0.3	4.99	7.92	2.25	3.22	6.22	0.49
5	0.4	4.15	6.98	1.34	2.47	5.32	-0.33
6	0.5	3.51	6.26	0.57	1.73	4.60	-1.08
7	0.6	3.08	5.70	-0.13	1.26	3.97	-1.53
8	0.7	2.57	5.32	-0.80	0.68	3.40	-2.93
9	0.8	2.29	5.33	-1.46	0.08	2.80	-3.92
10	0.9	2.71	6.01	-1.77	-0.83	2.82	-4.52
11	1	0.00	0.00	0.00	0.00	0.00	0.00

Table 5.3.3 Differences in velocity potential Φ_D, Φ_F and Φ_G with changing cutoff position from upstream end of floor to downstream end of floor for B/S=5,30 and B/T=10,20.

S.No.	B1/B	B/D1=25	B/D1=10	B/D1=80	B/D1=25	B/D1=10	B/D1=80
		B/D2=25	B/D2=80	B/D2=10	B/D2=25	B/D2=80	B/D2=10
B/T=10.0				B/T=20.0			
Variation at point 'G'							
1	0	-16.10	-15.08	-18.57	-17.29	-16.18	-17.78
2	0.1	-15.17	-14.10	-15.89	-15.09	-13.99	-15.64
3	0.2	-12.73	-11.99	-13.04	-12.46	-11.73	-12.77
4	0.3	-11.21	-10.69	-11.37	-10.93	-10.40	-11.07
5	0.4	-10.31	-9.90	-10.36	-10.02	-9.64	-10.07
6	0.5	-9.75	-9.44	-9.76	-9.59	-9.19	-9.49
7	0.6	-9.32	-9.16	-9.40	-9.18	-8.96	-8.87
8	0.7	-9.17	-8.92	-9.18	-9.02	-8.82	-9.30
9	0.8	-8.70	-8.93	-8.83	-8.75	-7.87	-9.16
10	0.9	-6.64	-5.75	-7.34	-7.86	-6.73	-7.74
11	1	0.00	0.00	0.00	0.00	0.00	0.00

Variation at point 'D'							
1	0	0	0	0	0	0	0
2	0.1	6.64	7.34	5.75	7.49	8.18	6.72
3	0.2	8.7	8.83	8.32	8.75	10.11	8.4
4	0.3	9.17	9.18	8.92	9.02	8.98	8.79
5	0.4	9.42	9.4	9.16	9.2	9.16	8.96
6	0.5	9.75	9.76	9.44	9.4	9.49	9.19
7	0.6	10.4	10.36	9.9	10.04	10.07	9.92
8	0.7	11.21	11.37	10.69	10.93	11.05	10.12
9	0.8	12.73	12.76	11.99	12.46	13.06	11.43
10	0.9	15.17	15.69	14.1	14.87	15.71	13.78
11	1	15.96	16.30	14.98	15.77	17.41	15.87
Variation at point 'F'							
1	0	-10.54	-9.51	-11.17	-11.76	-10.15	-12.03
2	0.1	-9.24	-8.20	-9.90	-8.56	-7.53	-9.26
3	0.2	-6.48	-5.80	-6.93	-5.68	-5.03	-6.10
4	0.3	-4.75	-4.27	-5.05	-4.01	-3.57	-4.30
5	0.4	-3.58	-3.21	-3.83	-2.92	-2.59	-3.14
6	0.5	-2.63	-2.31	-2.87	-2.16	-1.78	-2.28
7	0.6	-1.56	-1.33	-1.94	-1.18	-0.93	-1.18
8	0.7	-0.34	0.06	-0.77	-0.09	0.22	-0.77
9	0.8	1.96	2.29	1.22	1.79	2.65	0.82
10	0.9	6.91	8.07	5.44	5.47	6.86	4.65
11	1	10.14	11.21	8.47	10.00	11.68	8.96

Table 5.3.3 indicates that the error in Khosla's approximate method is highly dependent on the position of cutoff. The maximum over estimation is 16% and this would lead uneconomical design. The maximum under estimation is of the order of 19% which would lead to unsafe design.

Therefore, the method should be adopted for design of barrage floor with concrete cutoff. The computation of water pressure on concrete cutoff will be useful in designing the cutoff

The value of ϕ_G is reducing marginally as the position of cutoff is transferred toward d/s side and it finally reaches to zero value as shown in the following fig 5.3.3.

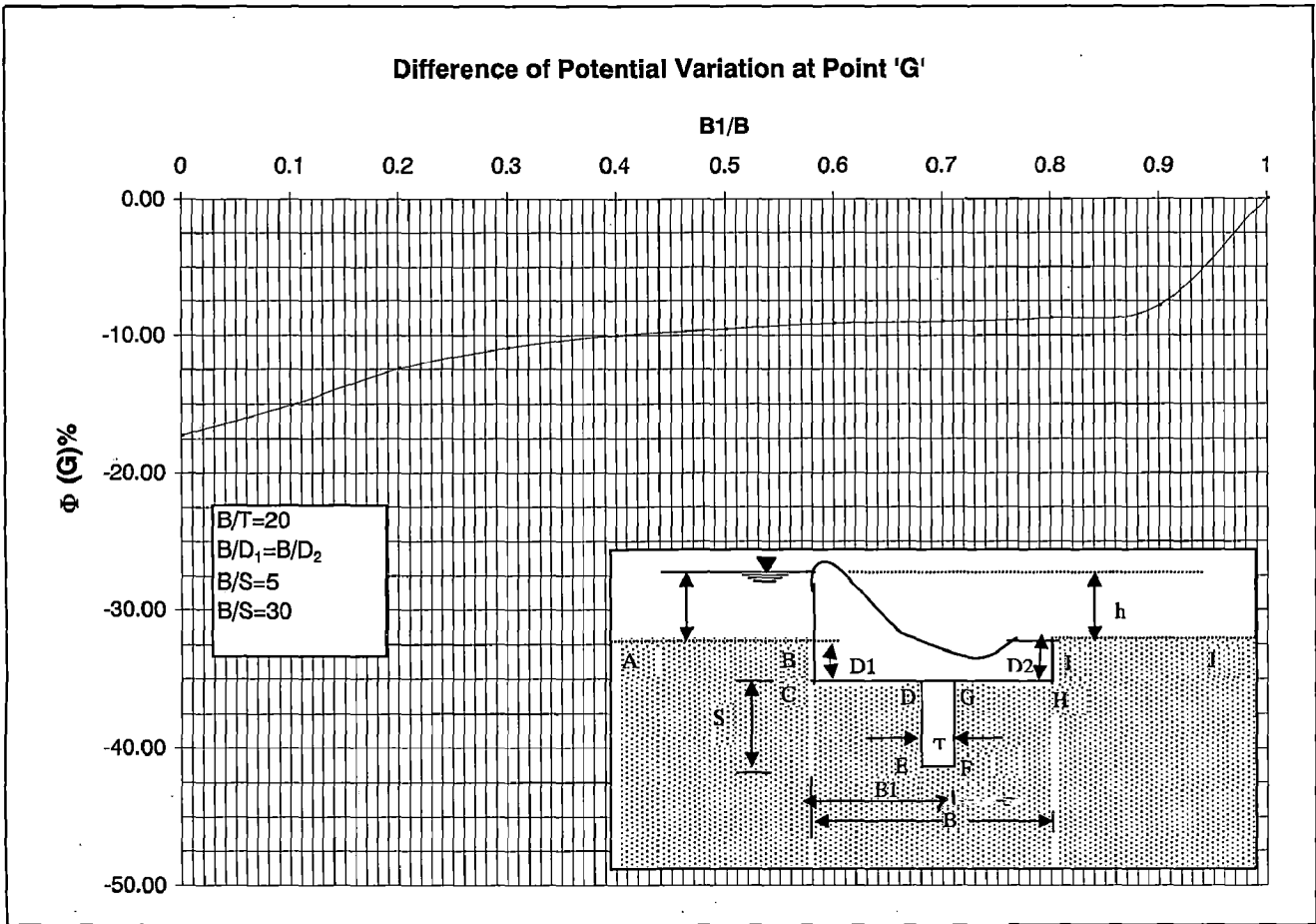


Figure 5.3.3 Variation of Potential difference Φ_G for constant cutoff thickness with variation of cutoff depth

- I. By increasing the cutoff depth from $B/S=30$ to $B/S=5$, ϕ_D value decreases by 15% when the cutoff position arrives at the end of d/s floor. The variation of potential difference is shown in the fig 5.3.4

Difference of Potential Variation at Point 'D'

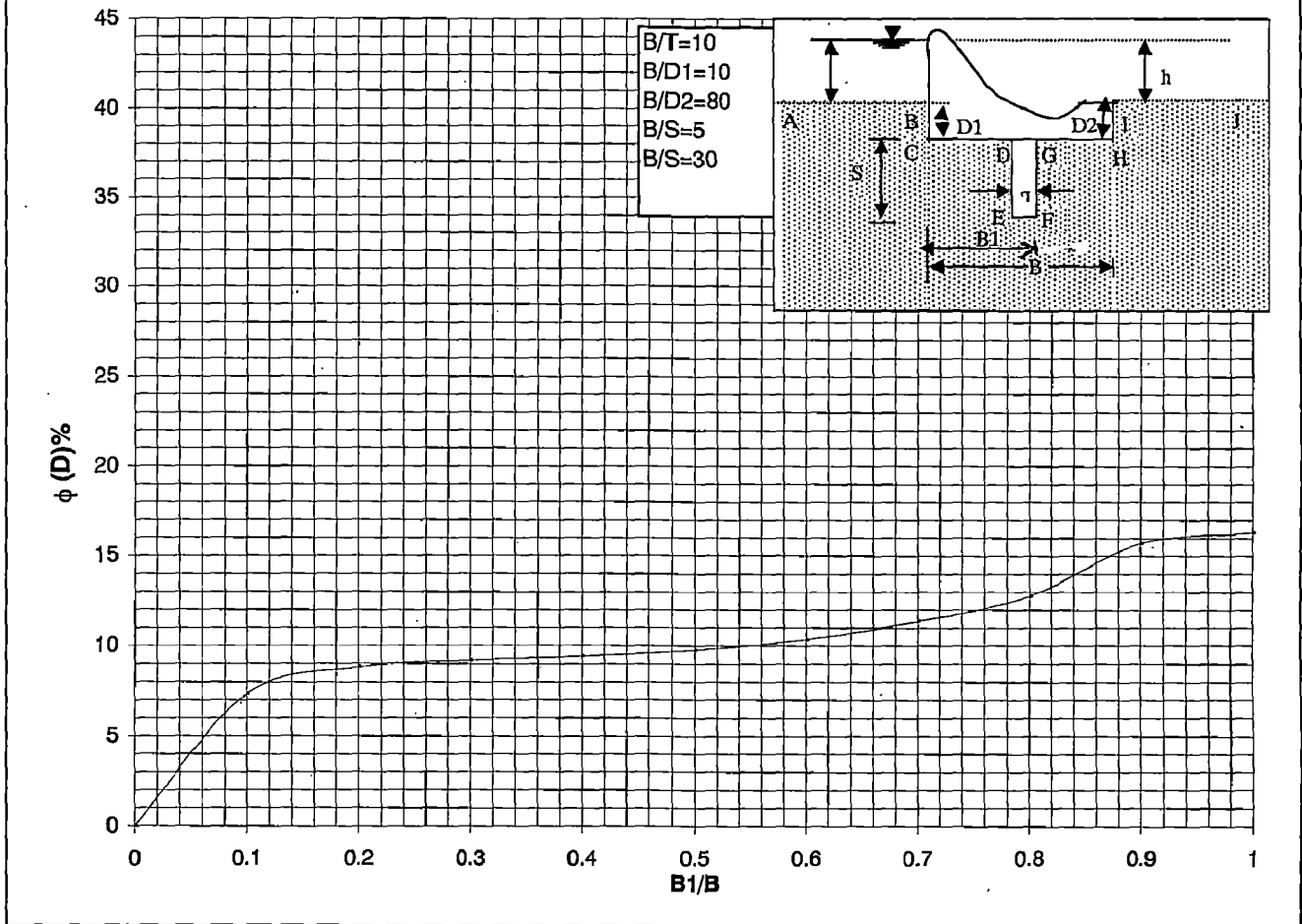


Figure 5.3.4 Variation of Potential difference Φ_D for constant cutoff thickness with variation of cutoff depth

II. As the depth of cutoff increase from $B/S=30$ to 5 , the value of ϕ_F decreases unto 10% for the cutoff position at the u/s end of the floor. ϕ_F goes on decreasing marginally as the cutoff position shifts toward downstream side of the floor. ϕ_F attains zero value when cutoff crosses 0.65 of horizontal floor. Afterward ϕ_F value increases up to 10% for the cutoff position at the downstream end of floor as shown in the fig 5.3.5.

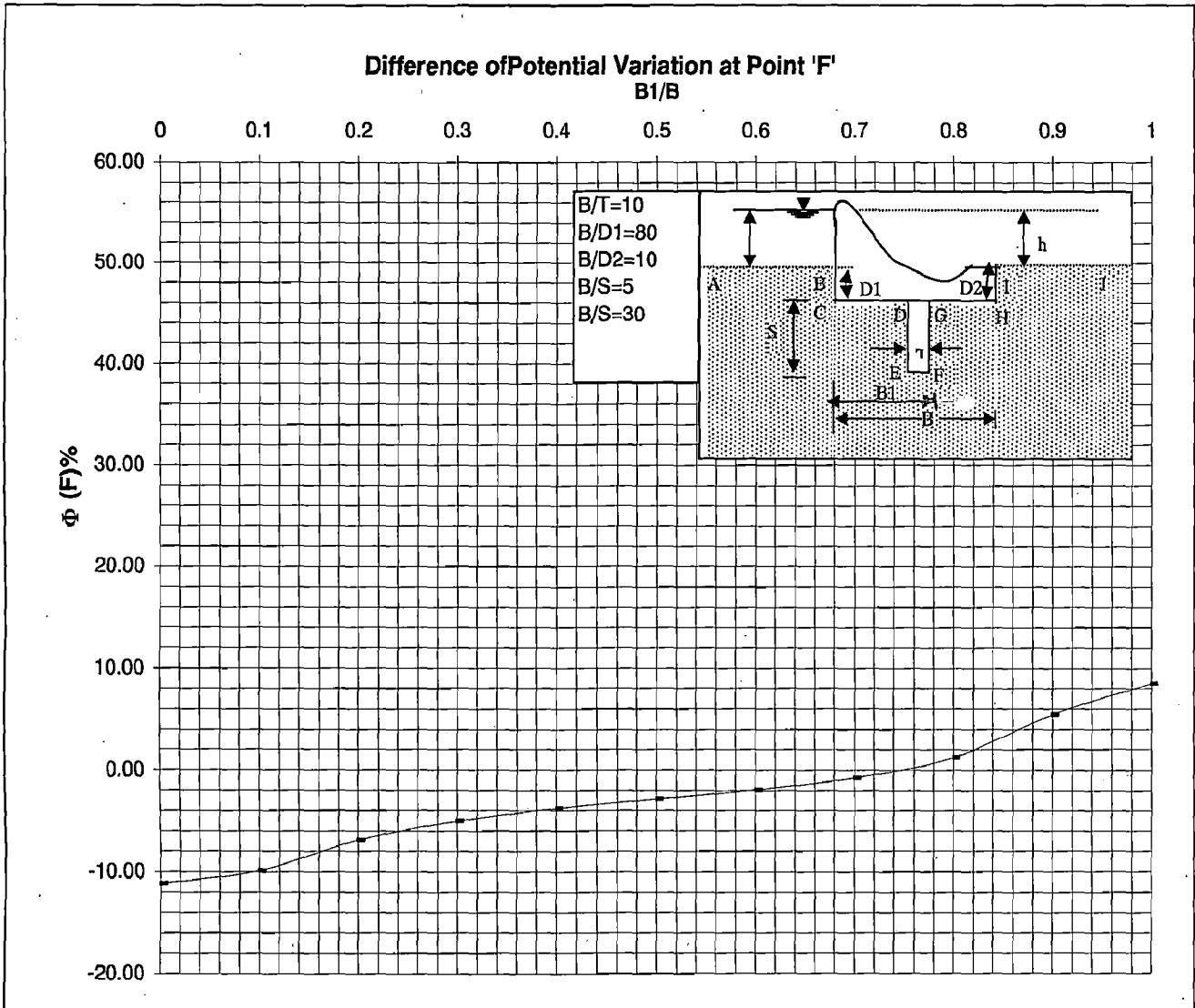


Figure 5.3.5 Variation of Potential difference Φ_F for constant cutoff thickness with variation of cutoff depth

5.4 Exit Gradient

The permissible exit gradient depends on the type of soil below the floor; for sand the permissible exit gradient is higher than for silt. Depending on grain size, it ranges between 0.20 to 0.25 for sand. Values less than 0.2 are for silt and silty clay.

Different cases are considered and results are presented in chapter 4 on Table 4.4.1 and 4.4.2 and variation of maximum exit gradient with B/S are shown from fig 4.4.1(a) to 4.4.1 (f) for equal depression and 4.4.2 (a) to 4.4.2 (e) for unequal depression.

The results are also presented in Table 5.3.4 and 5.3.5. From the study of the curves following table is obtained.

Table 5.3.4 Floor length with respect to equal depression

S.No.	D/S	T/S	I_E	B/S
1	0.2	0.2	0.1	13
2	0.2	0.4	0.1	12.5
3	0.2	0.6	0.1	12
4	0.4	0.2	0.1	10
5	0.4	0.4	0.1	9.75
6	0.4	0.6	0.1	9.5
7	0.6	0.2	0.1	7.8
8	0.6	0.4	0.1	7.5
9	0.8	0.8	0.1	5.6

Table 5.3.5 Floor length with respect to unequal depression

S.No.	D_1/S	D_2/S	T/S	I_E	B/S
1	0.40	0.10	0.20	0.10	14.00
2	0.40	0.10	0.40	0.10	13.50
3	0.60	0.10	0.40	0.10	13.00
4	0.10	0.60	0.40	0.10	8.30
5	0.10	0.60	0.60	0.10	8.00

Incase of sheet pile $I_E = 0.10$ B/S = 19.50

The value of B/S for which $I_E = 0.1$ are shown in Tables 5.3.4 and 5.3.5. Provision of higher depression in the down stream would lead to less floor width. This is because; the depression in down stream side is more effective in reducing the maximum exit gradient. Higher depression on the upstream side is not of much consequence in reducing the maximum exit gradient.

5.5 Conclusion

5.5.1 Effect of downstream cutoff thickness:

- 1) The thickness of cutoff which has been neglected so far has significant impact on the uplift pressure.
- 2) Uplift pressure increase with increase in cutoff depth.
- 3) The variation of thickness of downstream cutoff has more impact on the variation of uplift pressure than for variation in the depth of cutoff.

- 4) The increment rate of potential values decreases marginally for different depth for the same cutoff thickness.
- 5) Equal depressions have less impact on the potential values in comparison to unequal depression. For same cutoff thickness, the variation in depth of cutoff leads to marginal variation in potential.
- 6) The potential values decrease by providing upstream depression greater than downstream one and reverse will be the case on providing downstream depression greater than upstream one.

5.5.2 Effect of upstream cutoff thickness:

- 1) Velocity potential Φ_D and Φ_E decrease as the thickness of cutoff increases; same things happen on increasing the cutoff depth.
- 2) The decrement rate on potential value is minor on increasing cutoff thickness for greater depression.
- 3) The increase in cutoff depth has more impact on Φ_E than on Φ_D .
- 4) There is the difference of impact due to depression on potential values.
- 5) Potential values decrease with increase in upstream depression.

5.5.3 Comparison of Potential on the floor with concrete cutoff, and Khosla's potential values

In the present analysis thickness of concrete cutoff has been considered while Khosla's solution assumes the thickness of cutoff to be negligible.

5.5.4 Exit gradient

- 1) With an increase in the permissible value of exit gradient, the design depth of downstream cutoff and floor length decrease.
- 2) The exit gradient is not controlled by upstream cutoff depth.
- 3) The increase in thickness of cutoff subject to its limitation, to maintain permissible maximum exit gradient, decreases the floor length to some extent but it increases uplift pressure on the floor nominally.

5.5.5 Overall view

It is economical and safer to provide concrete cutoff as it reduces the length of floor and there will be no chance of leakage from the construction joint as in case of sheet pile. The potential values obtained from the present analytical method are on safer side compared to those values obtained by Khosla et al.

General

Most of the analytical method for the solution of two-dimensional ground water problem is concerned with the determination of a function, which will transform a problem from a geometrical domain within which a solution is sought for into one within which the solution is known. This chapter deals with the study of elementary function and the manner in which these functions transform geometric figures from one complex to another.

Conformal mapping technique is a powerful tool for solving two-dimensional Laplace equations. The method is used for solving the problems of flow under hydraulic structures.

Conformal Mapping Technique

An elementary but rather important case of conformal transformation is represented by the formula

$$Z = \frac{b}{2} \cosh \omega \quad \text{where } z = x+iy \text{ and } \omega = u+iv$$

$$x = \frac{b}{2} \cosh u \cos v \quad y = \frac{b}{2} \sinh u \sin v$$

From this general formula (which may be considered as the equation of complex potential), we can obtain two sets of curves, by letting either

$$u = \text{constant, or } v = \text{constant}$$

It is generally known that for a weir with flat base and resting on a surface of ground, the stream lines or lines of flow are confocal ellipses with their foci at 'o' as shown in figure A-1. The equation to these ellipses is given by:

For u const.

$$\frac{x^2}{\left(\frac{b}{2} \cosh u\right)^2} + \frac{y^2}{\left(\frac{b}{2} \sinh u\right)^2} = 1 \quad (1)$$

where u is stream line function.

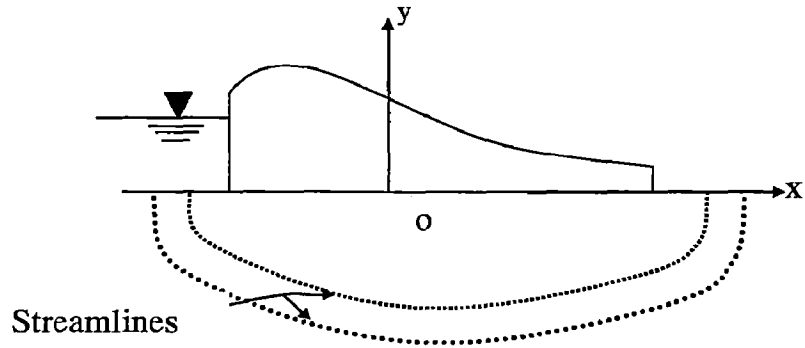


Figure A-1 Streamlines for flat base weirs on surface

For v const. We can obtain we can obtain a family of confocal hyperbola

$$\frac{x^2}{\left(\frac{b}{2} \cos v\right)^2} - \frac{y^2}{\left(\frac{b}{2} \sin v\right)^2} = 1$$

(2)

Either of these two groups may alternatively be taken to represent equipotentials or stream lines

Consider the physical domain in the z -plane Figure A-2 .when a vertical obstruction like as the cutoff is introduced , the configuration of the streamlines or the flow lines are distorted .By applying the Schwartz-Christoffel transformation technique, the distortion can be brought back to the normal configuration as shown in figure A-3.The streamlines that will be formed after the transformation are smooth ellipses with confocal points.

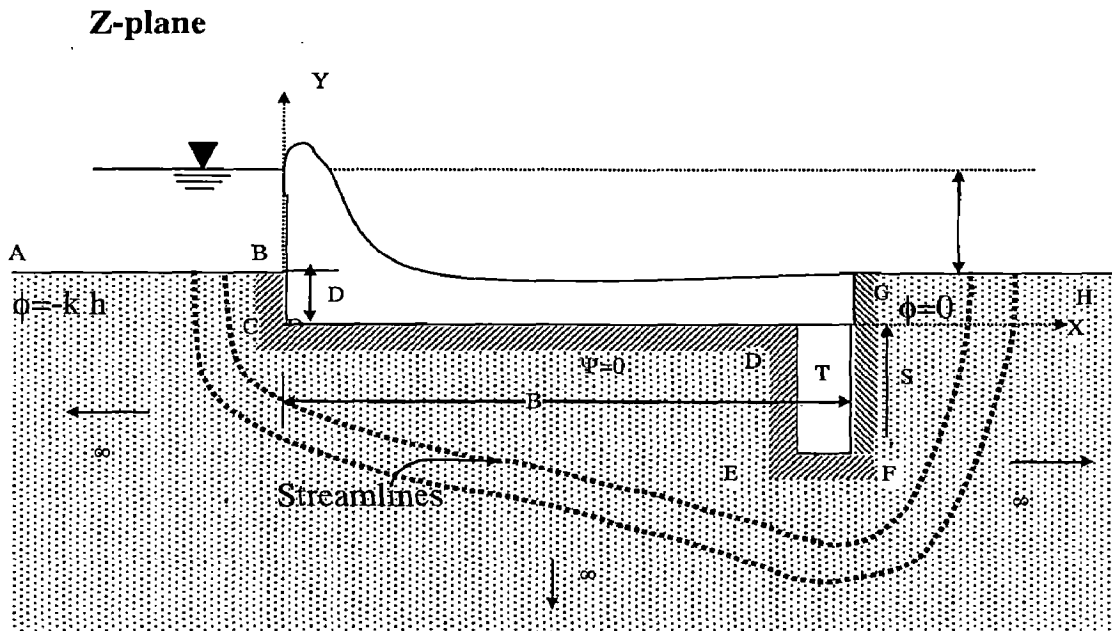


Figure A-2 Physical domain in Z-plane

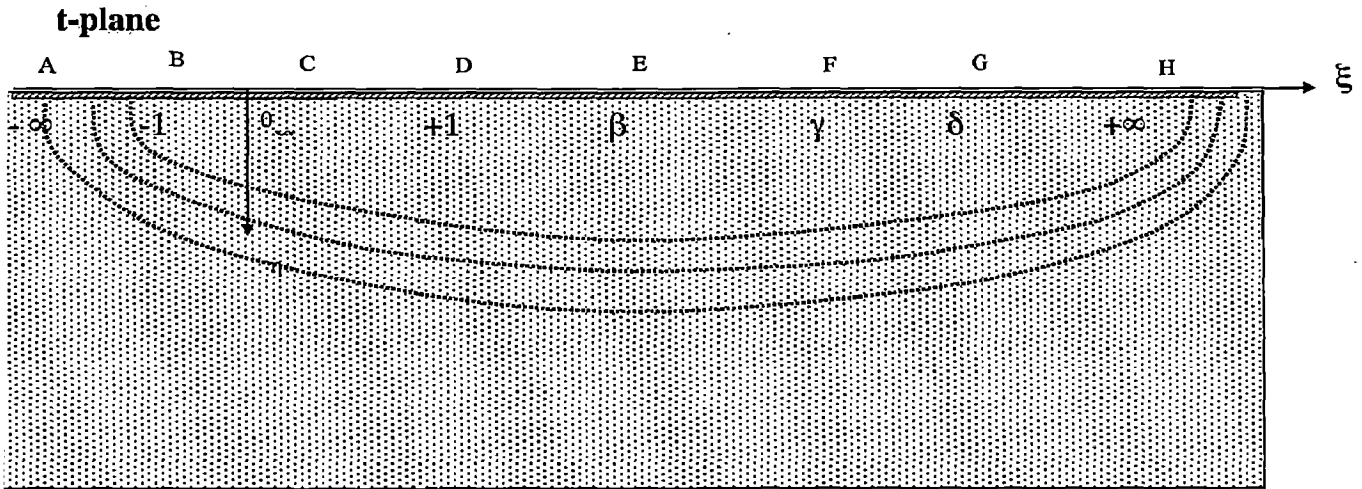


Figure A-3 Physical domain mapped on t-plane

Assuming physical domain to be on the Z-plane, any point on this plane is given by $Z=x+iy$. The transformed plane is known as t-plane, where any point on this plane is described by $\zeta=\xi+i\eta$.

In weir-foundation problems the zones subject to percolating straight lines (or circles of infinite diameter). It therefore follows that the case in which a rectilinear polygon is transformed into a semi-infinite plane is the most significant problem in this method.

So, the physical flow domains in z-plane as well as complex potential domain ω are transformed onto a common platform known as the auxiliary t-plane for which a direct relation between z-plane and ω -plane are obtained. In this process, the flow region in the z-plane is first mapped into the lower half of the auxiliary t-plane. Then the complex potential plane is also mapped into lower half of t-plane. From these two conformal mapping s, the relation between z and ω plane is obtained.

This transformation is given by the relation:

$$z = M \int \frac{dt}{(t - \alpha_1)^{\lambda_1} (t - \alpha_2)^{\lambda_2} (t - \alpha_3)^{\lambda_3} (t - \alpha_4)^{\lambda_4} (t - \alpha_5)^{\lambda_5} (t - \alpha_6)^{\lambda_6}} \quad (3)$$

where $\lambda_1\pi, \lambda_2\pi, \lambda_3\pi, \lambda_4\pi, \lambda_5\pi, \lambda_6\pi$ are the changes in the angles at vertices B,C,D,E,F,G in the positive sense and $\alpha_1, \alpha_2, \alpha_3, \alpha_4, \alpha_5, \alpha_6$ are the ordinates at the points B,C,D,E,F,G in the t-plane on which the points B,C,D,E,F,G of the z-plane are mapped.

As seen in the figure A-2 on the z-plane, the angles of turning at B,C,D,E,F,G are

$\frac{\pi}{2}, -\frac{\pi}{2}, \frac{\pi}{2}, -\frac{\pi}{2}, -\frac{\pi}{2}, \frac{\pi}{2}$ respectively so that

$$\begin{aligned} \lambda_1 \pi &= \frac{\pi}{2} & \text{or} & \quad \lambda_1 = \frac{1}{2} \\ \lambda_2 \pi &= -\frac{\pi}{2} & \text{or} & \quad \lambda_2 = -\frac{1}{2} \\ \lambda_3 \pi &= \frac{\pi}{2} & \text{or} & \quad \lambda_3 = \frac{1}{2} \\ \lambda_4 \pi &= -\frac{\pi}{2} & \text{or} & \quad \lambda_4 = -\frac{1}{2} \quad \text{and so on.} \end{aligned}$$

The origin in figure A-2 is at the point C, while in t-plane it is chosen I between Band C. Assuming, $\alpha_1=-1$, $\alpha_2=\alpha$, $\alpha_3=+1$, $\alpha_4=\beta$, $\alpha_5=\gamma$, $\alpha_6=\delta$ the equation of the transformation reduces to

$$z = M \int \frac{dt}{(\alpha-t)^{\frac{1}{2}}(1+t)^{\frac{1}{2}}(1-t)^{\frac{1}{2}}(\beta-t)^{\frac{1}{2}}(\gamma-t)^{\frac{1}{2}}(\delta-t)^{\frac{1}{2}}} + N$$

$$z = M \int \frac{\sqrt{(\alpha-t)(\beta-t)(\gamma-t)}}{\sqrt{(1-t^2)(\delta-t)}} dt + N \quad (4)$$

The equation (4) is the general equation between z-plane and t-plane obtained by Schwartz Christoffel transformation technique for the physical domain shown in fig A-2.

Similarly by applying the same transformation technique, the relation between ω -plane and t-plane can be obtained as explained in chapter 3 figure 3.3.4(b). The derived equation is:

$$\omega = M_1 \sin^{-1} \left(\frac{2t+1-\delta}{1+\delta} \right) + N_1 \quad (5)$$

By equating equations (4) and (5) t can be eliminated and direct relationship between z and ω -plane can be obtained.

General

Since the mapping steps result in a set of non linear equations, which require a suitable technique to compute the unknown parameters. The implicit nature of the non linear equations restricts the range of its applicability. So such non linear equations are solved by iterative method given by Newton- Rapshon.

The set of non linear equations are derived in Chapter 3. All the sets eg. for downstream cutoff, upstream cutoff and cutoff varying at different position of the floor from u/s to d/s are represented by :

$F_i(X_1, X_2, \dots, X_n) = 0$, where $i=1, 2, \dots, n$ constitute the variables X_1, X_2, \dots, X_n .

Let 'X' and 'F' denote entire values of vector X_i and functions F_i , then in the neighbourhood of X, each of the functions F_i can be expanded in Taylor series.

$$F_i(X + \delta x) = F_i(X) + \sum_{j=1}^n \frac{\partial F_i}{\partial x_j} \Delta x_j + 0. \delta x^2$$

In matrix notation, the above equation can be written as:

$$F_i(X + \delta x) = F_i(X) + J. \Delta x_j + 0. \delta x^2$$

Neglecting the term of the order δx^2 and higher and setting $F_i(X + \delta x) = 0$

We have: $J. \Delta x = -F(X)$ is an equation of matrix of set of non-linear equations. This matrix equation can be solved by LU decomposition and then correction are then added to the solution vector as: $X_{new} = X_{old} + \Delta x$

Where **J** is known as the Jacobian matrix and is represented as:

$$\mathbf{J} = \begin{bmatrix} \frac{\partial F_1}{\partial x_1} & \frac{\partial F_1}{\partial x_2} & \frac{\partial F_1}{\partial x_3} & \dots & \frac{\partial F_1}{\partial x_n} \\ \frac{\partial F_2}{\partial x_1} & \frac{\partial F_2}{\partial x_2} & \frac{\partial F_2}{\partial x_3} & \dots & \frac{\partial F_2}{\partial x_n} \\ \dots & \dots & \dots & & \\ \dots & \dots & \dots & & \\ \frac{\partial F_n}{\partial x_1} & \frac{\partial F_n}{\partial x_2} & \frac{\partial F_n}{\partial x_3} & & \frac{\partial F_n}{\partial x_n} \end{bmatrix}$$

Where,

$$\frac{\partial F_i}{\partial x_i} = \frac{F_i(x_1, x_2, x_3, \dots, x_j + \Delta h, \dots, x_n) - F_i(x_1, x_2, x_3, \dots, x_n)}{\Delta h}$$

$$\text{and } \Delta x_i = -F.[J]^{-1}$$

or $X_i = X_i + \Delta x$ X_i is the variables in the non linear equations.

FORTRAN PROGRAM

```
*****
* This Program is a part of M.Tech Dissertation for W.R.D.T.C,IIT Roorkee *
* Developed by Gir Bahadur K.C.M.Tech WRD (Civil) 2002-2004. *
* This source code is intended as a supplement to the Dissertation *
*“Design of Depressed Weir on Permeable Foundation with *
*downstream Concrete Cutoff” *
*****
```

C PROGRAM FOR DEPRESSED WEIR WITH DOWNSTREAM CONCRETE CUTOFF

C B=TOTAL FLOOR LENGTH,T=CUTOFF THICKNESS,D1=U/S DEPRESSION,
C D2 =D/S DEPRESSION,S=CUTOFF DEPTH

DIMENSION WW(96),XX(96)

```
open(1,file='weirp.dat',status='old')
open(2,file='weirp.out',status='unknown')
open(3,file='gauss.dat',status='old')
```

READ(3,*)N

READ (3,*)(WW(I),I=1,N)

READ (3,*)(XX(I),I=1,N)

READ (1,*)B,T,S,D1,D2

```
WRITE (2,*)'Program Result for Velocity Potential'
WRITE (2,*)'*****'
WRITE (2,*)' B T S D1 D2'
WRITE (2,5)B,T,S,D1,D2
5 FORMAT(5F5.2)
WRITE (2,*)' '
```

6 FORMAT(4F7.2)

INDEX=1

```
ALPHA0=.01
BETA0=1.+ALPHA0
GAMA0=BETA0+.01
```

DETA0=GAMA0+.01

```
WRITE(2,*)' INITIALLY GUESSED VALUES'
WRITE (2,*)' '
```

```
WRITE(2,*)'ALPHA0 BETA0 GAMA0 DETA0 '
WRITE(2,6)ALPHA0,BETA0,GAMA0,DETA0
```

```
CALL MAIN(N,WW,XX,ALPHA0,BETA0,GAMA0,DETA0,
1 ENT1,ENT2,ENT3,ENT4,ENT5,B,T,D1,D2,S,
2 FA,FB,FC,FD,FF1,FF2,FF3,FF4,
3 DALPHA0,DBETA0,DGAMA0,DDETA0)
```



```

Write(2,*)'Value of ENT2=',ENT2
WRITE(2,*)'*****'
CALL PRESS(ENT2,ALPHA0,BETA0,GAMA0,DETA0,PC,PD,PE,PF,ZIE)
WRITE(2,*)' RESULTS'
WRITE(2,*)'*****'
WRITE (2,*)' VELOCITY POTENTIALS IN %'
WRITE (2,*)' '
WRITE (2,*)' PC PD PE PF'
WRITE (2,*)' '
WRITE (2,6)PC,PD,PE,PF
WRITE(2,*)'*****'
WRITE (2,*)' EXIT GRADIENT'
WRITE (2,*)' '
WRITE(2,*)' B/S IE'
109 WRITE(2,109)B/S,ZIE
FORMAT(2(F9.5,2X))
WRITE (2,*)' '
WRITE(2,*)' B/S D1/S D2/S T/S'
110 WRITE(2,110)B/S, D1/S,D2/S,T/S
FORMAT(4(F7.3,2X))
WRITE (*,*)' B/S IE'
111 WRITE (*,111) B/S,ZIE
FORMAT(2(F8.5,2X))

WRITE(2,*)'*****END OF RESULTS*****'
STOP
END

```

```

c *****
C SUBROUTINE MAIN (SOLUTION OF JACOBIAN MATRIX)
c *****
SUBROUTINE MAIN(N,WW,XX,ALPHA0,BETA0,GAMA0,DETA0,
1 ENT1,ENT2,ENT3,ENT4,ENT5,B,T,D1,D2,S,
2 FA,FB,FC,FD,FF1,FF2,FF3,FF4,
3 DALPHA0,DBETA0,DGAMA0,DDETA0)
DIMENSION WW(96),XX(96)
DIMENSION AA(4,4),CC(4)

EPSILON=0.00001
10 CONTINUE
CALL BX(N,WW,XX,ALPHA0,BETA0,GAMA0,DETA0,
1 ENT1,ENT2,ENT3,ENT4,ENT5,B,T,D1,D2,S,
2 FA,FB,FC,FD,FF1,FF2,FF3,FF4)
CC(1)=-FF1
CC(2)=-FF2
CC(3)=-FF3
CC(4)=-FF4

C *****
DALPHA=EPSILON
DBETA=EPSILON
DGAMA=EPSILON
DDETA=EPSILON

C *****
ALPHA1=ALPHA0+DALPHA
CALL BX(N,WW,XX,ALPHA1,BETA0,GAMA0,DETA0,
1 ENT1,ENT2,ENT3,ENT4,ENT5,B,T,D1,D2,S,
2 FA,FB,FC,FD,FF11,FF22,FF33,FF44)

```

```

AA(1,1)=(FF11-FF1)/DALPHA
AA(2,1)=(FF22-FF2)/DALPHA
AA(3,1)=(FF33-FF3)/DALPHA
AA(4,1)=(FF44-FF4)/DALPHA
C *****
BETA1=BETA0+DBETA
CALL BX(N,WW,XX,ALPHA0,BETA1,GAMA0,DETA0,
1 ENT1,ENT2,ENT3,ENT4,ENT5,B,T,D1,D2,S,
2 FA,FB,FC,FD,FF11,FF22,FF33,FF44)

AA(1,2)=(FF11-FF1)/DBETA
AA(2,2)=(FF22-FF2)/DBETA
AA(3,2)=(FF33-FF3)/DBETA
AA(4,2)=(FF44-FF4)/DBETA
C *****
GAMA1=GAMA0+DGAMA
CALL BX(N,WW,XX,ALPHA0,BETA0,GAMA1,DETA0,
1 ENT1,ENT2,ENT3,ENT4,ENT5,B,T,D1,D2,S,
2 FA,FB,FC,FD,FF11,FF22,FF33,FF44)

AA(1,3)=(FF11-FF1)/DGAMA
AA(2,3)=(FF22-FF2)/DGAMA
AA(3,3)=(FF33-FF3)/DGAMA
AA(4,3)=(FF44-FF4)/DGAMA
C *****
DETA1=DETA0+DDETA
CALL BX(N,WW,XX,ALPHA0,BETA0,GAMA0,DETA1,
1 ENT1,ENT2,ENT3,ENT4,ENT5,B,T,D1,D2,S,
2 FA,FB,FC,FD,FF11,FF22,FF33,FF44)

AA(1,4)=(FF11-FF1)/DDETA
AA(2,4)=(FF22-FF2)/DDETA
AA(3,4)=(FF33-FF3)/DDETA
AA(4,4)=(FF44-FF4)/DDETA
C *****
WRITE(*,*)'*****'
WRITE(*,*)'MATRIX AA'
DO 9 I=1,4
WRITE(*,21) (AA(I,J),J=1,4)
21 FORMAT (16F8.5,8X)
9 CONTINUE
C *****
MM=4
CALL MATRIXIN(AA,MM)
C *****
SUM=0
DO J=1,4
SUM=SUM+AA(1,J)*CC(J)
ENDDO
DALPHA0=SUM
SUM=0
DO J=1,4
SUM=SUM+AA(2,J)*CC(J)
ENDDO
DBETA0=SUM
SUM=0
DO J=1,4
SUM=SUM+AA(3,J)*CC(J)
ENDDO
DGAMA0=SUM

```

```

SUM=0
DO J=1,4
SUM=SUM+AA(4,J)*CC(J)
ENDDO
DDETA0=SUM

C      *****
      ALPHA0=DALPHA0+ALPHA0
      BETA0=DBETA0+BETA0
      GAMA0=DGAMA0+GAMA0
      DETA0=DDETA0+DETA0

C      *****
      INDEX=INDEX+1
      IF(INDEX.GT.1500)GOTO 20
      IF(ABS(DALPHA0).GT.0.00001)GOTO 10
      IF(ABS(DBETA0).GT.0.00001) GOTO 10
      IF(ABS(DGAMA0).GT.0.00001) GOTO 10
      IF(ABS(DDETA0).GT.0.00001) GOTO 10
      GOTO 30
20     CONTINUE
      WRITE(2,*)'ITERATRION HAS FAILED'
      GOTO 40
30     CONTINUE
      WRITE(2,*)'*****'
      WRITE(2,*)'NUMBER OF ITERATIONS =',INDEX
400    FORMAT(I3)
      WRITE(2,*)'*****'
      WRITE(2,*)'VALUES OF THE FUNCTIONS AFTER ITERATIONS'
      WRITE(2,500)cc(1),cc(2),cc(3),cc(4)
      WRITE(2,*)'*****'
500    FORMAT(4F7.5)
      WRITE(*,*)'*****'
      WRITE(2,*)'  VALUES COMPUTED'
      WRITE(2,*)'ALPHA  BETA  GAMA  DETA'
      WRITE(2,600)ALPHA0,BETA0,GAMA0,DETA0
600    FORMAT(4(F8.5,2X))
      WRITE(2,*)'
40     CONTINUE
      RETURN
      END

C      *****
C      SUBROUTINE MATRIXINV (LU DECOMPOSITION)
C      *****

      SUBROUTINE MATRIXIN (AA,MM)
      DIMENSION AA(4,4),B(4),C(4)

      NN=MM-1
      AA(1,1)=1./AA(1,1)
      DO 8 M=1,NN
      K=M+1
      DO 3 I=1,M
      B(I)=0.0
      DO 3 J=1,M
3       B(I)=B(I)+AA(I,J)*AA(J,K)
      D=0.0
      DO 4 I=1,M
4       D=D+AA(K,I)*B(I)
      D=-D+AA(K,K)

```

```

      AA(K,K)=1./D
      DO 5 I=1,M
5      AA(I,K)=-B(I)*AA(K,K)
      DO 6 J=1,M
      C(J)=0.0

      DO 6 I=1,M
6      C(J)=C(J)+AA(K,I)*AA(I,J)
      DO 7 J=1,M
7      AA(K,J)=-C(J)*AA(K,K)
      DO 8 I=1,M
      DO 8 J=1,M
8      AA(I,J)=AA(I,J)-B(I)*AA(K,J)
      WRITE(*,*)'*****'
      WRITE(*,*)'INV MATRIX'
      DO 17 I=1,4
      WRITE(*,29) (AA(I,J),J=1,4)
29      FORMAT (16F8.5,5X)
17      CONTINUE
C
      RETURN
      END

C      *****
C      SUBROUTINE PRESSURE(CALCULATES UPLIFT PRESSURE)
C      *****
SUBROUTINE PRESS(ENT2,ALPHA0,BETA0,GAMA0,DETA0,PC,PD,PE,PF,
1      ZIE)
      PI=3.141592654
      PC=(-.5-1./PI*ASIN((2*ALPHA0+1-DETA0)/(DETA0+1.))) *
1      100.

      PD=(-.5-1./PI*ASIN((3.-DETA0)/(DETA0+1.))) *
1      100.
      PE=(-.5-1./PI*ASIN((2.*BETA0+1.-DETA0)/(DETA0+1.))) *
1      100.
      PF=(-.5-1./PI*ASIN((2*GAMA0+1.-DETA0)/(DETA0+1.))) *
1      100.

      X1=SQRT(DETA0-1.)
      X2=SQRT((DETA0-ALPHA0)*(DETA0-BETA0)*(DETA0-GAMA0))
      X3=(1./PI)*ENT2

      ZIE=X3*(X1/X2)

      RETURN
      END
C      *****
C      SUBROUTINE BX(GROUPING OF SUBROUTINES)
C      *****
SUBROUTINE BX(N,WW,XX,ALPHA0,BETA0,GAMA0,DETA0,
1      ENT1,ENT2,ENT3,ENT4,ENT5,B,T,D1,D2,S,
2      FA,FB,FC,FD,FF1,FF2,FF3,FF4)
      DIMENSION WW(96),XX(96)

      CALL Fx1(N,WW,XX,ALPHA0,BETA0,GAMA0,DETA0,ENT 1)
      CALL Fx2(N,WW,XX,ALPHA0,BETA0,GAMA0,DETA0,ENT 2)
      CALL Fx3(N,WW,XX,ALPHA0,BETA0,GAMA0,DETA0,ENT 3)
      CALL Fx4(N,WW,XX,ALPHA0,BETA0,GAMA0,DETA0,ENT 4)

```

```
CALL Fx5(N,WW,XX,ALPHA0,BETA0,GAMA0,DETA0,ENT 5)
```

```
FA=ENT2/ENT1  
FB=ENT3/ENT1  
FC=ENT4/ENT1  
FD=ENT5/ENT1
```

```
FF1=(S/(B-T))-FA  
FF2=(T/(B-T))-FB  
FF3=((D2+S)/(B-T))-FC  
FF4=(D1/(B-T))-FD
```

```
RETURN  
END
```

```
C SUBROUTINE Fx1  
SUBROUTINE Fx1(N,WW,XX,ALPHA0,BETA0,GAMA0,DETA0,ENT1 )  
DIMENSION WW(96),XX(96)
```

```
SUM=0  
DO I=1,N  
U=XX(I)  
Y =((U+1.)/2.)*(SQRT(1.-ALPHA0))
```

```
F1N=SQRT((1.-ALPHA0-Y**2.)*(BETA0-1.+Y**2.))*  
1 (GAMA0-1.+Y**2.)
```

```
F1D=SQRT((2.-Y**2.)*(DETA0-1.+Y**2.))
```

```
F1=F1N/F1D  
SUM=SUM+WW(I)*F1
```

```
ENDDO  
ENT1=SUM*(SQRT(1.-ALPHA0))  
RETURN  
END
```

```
! SUBROUTINE Fx2  
SUBROUTINE Fx2(N,WW,XX,ALPHA0,BETA0,GAMA0,DETA0,ENT2 )  
DIMENSION WW(96),XX(96)
```

```
SUM=0  
DO I=1,N  
U=XX(I)  
Y =((U+1.)/2.)*(SQRT(BETA0-1.))  
F2N=SQRT((1.+Y**2.-ALPHA0)*(BETA0-1.-Y**2.))*  
1 (GAMA0-1.-Y**2.)
```

```
F2D=SQRT((DETA0-1.-Y**2.)*(2.+Y**2.))
```

```
F2=F2N/F2D
```

```
SUM=SUM+WW(I)*F2  
ENDDO  
ENT2=SUM*SQRT(BETA0-1.)  
RETURN  
END
```

```
! SUBROUTINE Fx3  
SUBROUTINE Fx3(N,WW,XX,ALPHA0,BETA0,GAMA0,DETA0,ENT3)
```

```

        DIMENSION WW(96),XX(96)
        SUM=0
        DO I=1,N
        U=XX(I)
        Y=((U+1.)/2.)*(SQRT(GAMA0-BETA0))

        F3N=(Y**2.)*(SQRT((BETA0+Y**2.-ALPHA0)*(GAMA0-BETA0-Y**2.)))

        F3D=SQRT((BETA0+1.+Y**2.)*(BETA0+Y**2.-1.)*
1      (DETA0-BETA0-Y**2.))
        F3=F3N/F3D

SUM=SUM+WW(I)*F3

```

```

        ENDDO
        ENT3=SUM*(SQRT(GAMA0-BETA0))
RETURN
        END

```

```

!      SUBROUTINE Fx4
        SUBROUTINE Fx4(N,WW,XX,ALPHA0,BETA0,GAMA0,DETA0,ENT4)
        DIMENSION WW(96),XX(96)
        SUM=0
        DO I=1,N
        U=XX(I)
        Y=((U+1.)/2.)*(SQRT(DETA0-GAMA0))

        F4N=SQRT((DETA0-Y**2.-ALPHA0)*(DETA0-Y**2.-BETA0)
1      *(DETA0-Y**2.-GAMA0))
        F4D=SQRT((DETA0-Y**2.+1.)*(DETA0-Y**2.-1.))
        F4=F4N/F4D
        SUM=SUM+WW(I)*F4
        ENDDO
        ENT4=SUM*(SQRT(DETA0-GAMA0))
RETURN
        END

```

```

C      SUBROUTINE Fx5
        SUBROUTINE Fx5(N,WW,XX,ALPHA0,BETA0,GAMA0,DETA0,ENT5)
        DIMENSION WW(96),XX(96)
        SUM=0
        DO I=1,N
        U=XX(I)
        Y=((U+1.)/2.)*(SQRT(1.+ALPHA0))
        F5N=SQRT((ALPHA0+1.-Y**2.)*(BETA0+1.-Y**2.)*
1      (GAMA0+1.-Y**2.))

        F5D=SQRT((2.-Y**2.)*(DETA0+1.-Y**2.))

        F5=F5N/F5D
        SUM=SUM+WW(I)*F5
        ENDDO
        ENT5=SUM*(1.+ALPHA0)
RETURN
        END

```

Sample result output

Data Entry Procedure:(Weir parameters to be entered as per below)
B T S D1 D2
50. 0.10 1.0 0.2 0.8

SAMPLE RESULT OUTPUT

Program Result for Velocity Potential

B T S D1 D2
50.00 .10 1.00 .20 .80

INITIALLY GUESSED VALUES

ALPHA0 BETA0 GAMA0 DETA0
.01 1.01 1.02 1.03

NUMBER OF ITERATIONS = 9

VALUES OF THE FUNCTIONS AFTER ITERATIONS
.00000 .00000 .00000 .00000

VALUES COMPUTED
ALPHA BETA GAMA DETA
-.97110 1.03592 1.05949 1.11511

Value of ENT2= 3.841983E-02

RESULTS

VELOCITY POTENTIALS IN %

PC PD PE PF

92.54 14.99 12.40 10.37

EXIT GRADIENT

B/S IE

50.00000 .04329

B/S D1/S D2/S T/S
50.000 .200 .800 .100
*****END OF RESULTS*****

! DEPRESSED FLOOR WITH CONCRETE CUTOFF VARYING FROM U/S END TO D/S
END OF FLOOR

! B1=BASE1,T=CUTOFF THICKNESS,B2=BASE2,D1=U/S DEPRESSION,
C D2=D/S DEPRESSION,S=DEPTH OF CUTOFF

C *****

DIMENSION WW(96),XX(96)

open(1,file='weirp.dat',status='old')
open(2,file='weirp.out',status='unknown')
open(3,file='gauss.dat',status='old')

READ(3,*)N

READ (3,*)(WW(I),I=1,N)

READ (3,*)(XX(I),I=1,N)

READ (1,*)B1,B2,D1,D2,S,T

6

FORMAT(6F7.3)

INDEX=1

B=B1+B2

GAMA0=.1

DETA0=.25

SIGMA0=1.1

CMU0=SIGMA0+.1

BETA0=1.1

ALPHA0=BETA0+.15

WRITE(2,*)' B1 T B2 D1 D2 S '

WRITE(2,6)B1,T,B2,D1,D2,S

write (2,*)' INITIALLY GUESSED VALUES'

WRITE(2,*)' '

WRITE(2,*)'ALPHA0, BETA0, GAMA0, DETA0, SIGMA0, MU0 '

WRITE(2,7)ALPHA0,BETA0,GAMA0,DETA0,SIGMA0,CMU0

7

FORMAT(6F7.3)

1 CALL MAIN(N,WW,XX,ALPHA0,BETA0,GAMA0,DETA0,SIGMA0,CMU0,
ENT1,ENT2,ENT3,ENT4,ENT5,ENT6,ENT7,B1,T,B2,D1,D2,S,

2 FA,FB,FC,FD,FE,FF,FF1,FF2,FF3,FF4,FF5,FF6,

3 DALPHA0,DBETA0,DGAMA0,DDETA0,DSIGMA0,DCMU0)

Write(2,*)'Value of ENT1=',ENT1

WRITE(2,*)'*****'

CALL PRESS(ALPHA0,GAMA0,DETA0,CMU0,PD,PE,PF,PG)

WRITE(2,*)' RESULTS'

WRITE(2,*)'*****'

WRITE(2,*)' B/T B/S B/D1 B/D2'

WRITE(2,109)B/T,B/S,B/D1,B/D2

109

FORMAT(4(F7.2,2X))

WRITE(2,*)' '

WRITE(2,*)'B1/B B2/B PD% PE% PF% PG%'

WRITE(2,110)B1/B,B2/B,PD,PE,PF,PG

110

FORMAT(6(F5.2,2X))

WRITE(2,*)'*****END OF RESULTS*****'

STOP

END

```
c *****
C SUBROUTINE MAIN (SOLUTION OF JACOBIAN MATRIX)
c *****
  SUBROUTINE MAIN(N,WW,XX,ALPHA0,BETA0,GAMA0,DETA0,SIGMA0,CMU0,
1   ENT1,ENT2,ENT3,ENT4,ENT5,ENT6,ENT7,B1,T,B2,D1,D2,S,
2   FA,FB,FC,FD,FE,FF,FF1,FF2,FF3,FF4,FF5,FF6,
3   DALPHA0,DBETA0,DGAMA0,DDETA0,DSIGMA0,DCMU0)
    DIMENSION WW(96),XX(96)
    DIMENSION AA(6,6),CC(6)
    DELTA=0.0001
10  CONTINUE
    CALL BX(N,WW,XX,ALPHA0,BETA0,GAMA0,DETA0,SIGMA0,CMU0,
1   ENT1,ENT2,ENT3,ENT4,ENT5,ENT6,ENT7,B1,T,B2,D1,D2,S,
2   FA,FB,FC,FD,FE,FF,FF1,FF2,FF3,FF4,FF5,FF6)
    CC(1)=-FF1
    CC(2)=-FF2
    CC(3)=-FF3
    CC(4)=-FF4
    CC(5)=-FF5
    CC(6)=-FF6
C   *****
    DALPHA=DELTA
    DBETA =DELTA
    DGAMA =DELTA
    DDETA =DELTA
    DSIGMA=DELTA
    DCMU =DELTA
C   *****
    ALPHA1=ALPHA0+DALPHA
    CALL BX(N,WW,XX,ALPHA1,BETA0,GAMA0,DETA0,SIGMA0,CMU0,
1   ENT1,ENT2,ENT3,ENT4,ENT5,ENT6,ENT7,B1,T,B2,D1,D2,S,
2   FA,FB,FC,FD,FE,FF,FF11,FF22,FF33,FF44,FF55,FF66)

    AA(1,1)=(FF11-FF1)/DALPHA
    AA(2,1)=(FF22-FF2)/DALPHA
    AA(3,1)=(FF33-FF3)/DALPHA
    AA(4,1)=(FF44-FF4)/DALPHA
    AA(5,1)=(FF55-FF5)/DALPHA
    AA(6,1)=(FF66-FF6)/DALPHA

C   *****
    BETA1=BETA0+DBETA
    CALL BX(N,WW,XX,ALPHA0,BETA1,GAMA0,DETA0,SIGMA0,CMU0,
1   ENT1,ENT2,ENT3,ENT4,ENT5,ENT6,ENT7,B1,T,B2,D1,D2,S,
2   FA,FB,FC,FD,FE,FF,FF11,FF22,FF33,FF44,FF55,FF66)

    AA(1,2)=(FF11-FF1)/DBETA
    AA(2,2)=(FF22-FF2)/DBETA
    AA(3,2)=(FF33-FF3)/DBETA
    AA(4,2)=(FF44-FF4)/DBETA
    AA(5,2)=(FF55-FF5)/DBETA
    AA(6,2)=(FF66-FF6)/DBETA

C   *****
    GAMA1=GAMA0+DGAMA
    CALL BX(N,WW,XX,ALPHA0,BETA0,GAMA1,DETA0,SIGMA0,CMU0,
1   ENT1,ENT2,ENT3,ENT4,ENT5,ENT6,ENT7,B1,T,B2,D1,D2,S,
2   FA,FB,FC,FD,FE,FF,FF11,FF22,FF33,FF44,FF55,FF66)
```

```

AA(1,3)=(FF11-FF1)/DGAMA
AA(2,3)=(FF22-FF2)/DGAMA
AA(3,3)=(FF33-FF3)/DGAMA
AA(4,3)=(FF44-FF4)/DGAMA
AA(5,3)=(FF55-FF5)/DGAMA
AA(6,3)=(FF66-FF6)/DGAMA

```

C

```

*****

```

```

DETA1=DETA0+DDETA

```

```

1 CALL BX(N,WW,XX,ALPHA0,BETA0,GAMA0,DETA1,SIGMA0,CMU0,
2 ENT1,ENT2,ENT3,ENT4,ENT5,ENT6,ENT7,B1,T,B2,D1,D2,S,
FA,FB,FC,FD,FE,FF,FF11,FF22,FF33,FF44,FF55,FF66)

```

```

AA(1,4)=(FF11-FF1)/DDETA
AA(2,4)=(FF22-FF2)/DDETA
AA(3,4)=(FF33-FF3)/DDETA
AA(4,4)=(FF44-FF4)/DDETA
AA(5,4)=(FF55-FF5)/DDETA
AA(6,4)=(FF66-FF6)/DDETA

```

C

```

*****

```

```

SIGMA1=SIGMA0+DSIGMA

```

```

1 CALL BX(N,WW,XX,ALPHA0,BETA0,GAMA0,DETA0,SIGMA1,CMU0,
2 ENT1,ENT2,ENT3,ENT4,ENT5,ENT6,ENT7,B1,T,B2,D1,D2,S,
FA,FB,FC,FD,FE,FF,FF11,FF22,FF33,FF44,FF55,FF66)

```

```

AA(1,5)=(FF11-FF1)/DSIGMA
AA(2,5)=(FF22-FF2)/DSIGMA
AA(3,5)=(FF33-FF3)/DSIGMA
AA(4,5)=(FF44-FF4)/DSIGMA
AA(5,5)=(FF55-FF5)/DSIGMA
AA(6,5)=(FF66-FF6)/DSIGMA

```

C

```

*****

```

```

CMU1=CMU0+DCMU

```

```

1 CALL BX(N,WW,XX,ALPHA0,BETA0,GAMA0,DETA0,SIGMA0,CMU1,
2 ENT1,ENT2,ENT3,ENT4,ENT5,ENT6,ENT7,B1,T,B2,D1,D2,S,
FA,FB,FC,FD,FE,FF,FF11,FF22,FF33,FF44,FF55,FF66)

```

```

AA(1,6)=(FF11-FF1)/DCMU
AA(2,6)=(FF22-FF2)/DCMU
AA(3,6)=(FF33-FF3)/DCMU
AA(4,6)=(FF44-FF4)/DCMU
AA(5,6)=(FF55-FF5)/DCMU
AA(6,6)=(FF66-FF6)/DCMU

```

```

MM=6

```

```

CALL MATRIXIN(AA,MM)

```

```

*****

```

```

SUM=0

```

```

DO J=1,6

```

```

SUM=SUM+AA(1,J)*CC(J)

```

```

ENDDO

```

```

DALPHA0=SUM

```

```

SUM=0

```

```

DO J=1,6

```

```

SUM=SUM+AA(2,J)*CC(J)

```

```

ENDDO

```

C

```

DBETA0=SUM

SUM=0
DO J=1,6
SUM=SUM+AA(3,J)*CC(J)
ENDDO
DGAMA0=SUM

SUM=0
DO J=1,6
SUM=SUM+AA(4,J)*CC(J)
ENDDO
DDETA0=SUM

SUM=0
DO J=1,6
SUM=SUM+AA(5,J)*CC(J)
ENDDO
DSIGMA0=SUM
SUM=0
DO J=1,6
SUM=SUM+AA(6,J)*CC(J)
ENDDO
DCMU0=SUM

C *****
ALPHA0=DALPHA0+ALPHA0
BETA0=DBETA0+BETA0
GAMA0=DGAMA0+GAMA0

DETA0=DDETA0+DETA0
SIGMA0=DSIGMA0+SIGMA0
CMU0=DCMU0+CMU0
WRITE(*,*)'*****!'
WRITE(*,*)'ALPHA0,BETA0,GAMA0,DETA0,SIGMA0,CMU0'
WRITE(*,*) ALPHA0,BETA0,GAMA0,DETA0,SIGMA0,CMU0

C *****
INDEX=INDEX+1
IF(INDEX.GT.1500)GOTO 20

IF(ABS(DALPHA0).GT.0.00001)GOTO 10
IF(ABS(DBETA0).GT.0.00001)GOTO 10
IF(ABS(DGAMA0).GT.0.00001)GOTO 10
IF(ABS(DDETA0).GT.0.00001)GOTO 10
IF(ABS(DSIGMA0).GT.0.00001)GOTO 10
IF(ABS(DCMU0).GT.0.00001)GOTO 10

GOTO 30
20 CONTINUE
WRITE(2,*)'ITERATRION HAS FAILED'
GOTO 40
30 CONTINUE

WRITE(2,*)
WRITE(2,*)'NUMBER OF ITERATIONS =', INDEX
WRITE(2,400)
400 FORMAT(I3)
WRITE(2,*)'

```

```

WRITE(2,*)'VALUES OF THE FUNCTIONS AFTER ITERATIONS'
WRITE(2,*)'
WRITE(2,500)cc(1),cc(2),cc(3),cc(4),cc(5),cc(6)
500  FORMAT(6F7.4)
WRITE(2,*)'*****'
WRITE(2,*)' Final Values Computed'
WRITE(2,*)' ALPHA  BETA  GAMA  DETA  SIGMA
1  MU'
WRITE(2,600)ALPHA0, BETA0,GAMA0,DETA0,SIGMA0,CMU0

600  FORMAT(6(F10.4,2X))
WRITE(2,*)'*****'
40   CONTINUE

RETURN
END

C   *****
C   SUBROUTINE MATRIXINV (LU DECOMPOSITION)
C   *****

SUBROUTINE MATRIXIN (AA,MM)
DIMENSION AA(6,6),B(6),C(6)
NN=MM-1
AA(1,1)=1./AA(1,1)
DO 8 M=1,NN
K=M+1
DO 3 I=1,M
B(I)=0.0
DO 3 J=1,M
3   B(I)=B(I)+AA(I,J)*AA(J,K)
D=0.0
DO 4 I=1,M
4   D=D+AA(K,I)*B(I)
D=-D+AA(K,K)
AA(K,K)=1./D
DO 5 I=1,M
5   AA(I,K)=-B(I)*AA(K,K)
DO 6 J=1,M
C(J)=0.0

DO 6 I=1,M
6   C(J)=C(J)+AA(K,I)*AA(I,J)
DO 7 J=1,M
7   AA(K,J)=-C(J)*AA(K,K)
DO 8 I=1,M
DO 8 J=1,M
8   AA(I,J)=AA(I,J)-B(I)*AA(K,J)
WRITE(*,*)'*****'
WRITE(*,*)'INV MATRIX'
DO 17 I=1,5
WRITE(*,29) (AA(I,J),J=1,5)
29  FORMAT (25F8.5,5X)
17  CONTINUE
C

RETURN
END

C   *****
C   SUBROUTINE PRESS(CALCULATION OF PRESSURE AT KEY PONTS)
C   *****
SUBROUTINE PRESS(ALPHA0,GAMA0,DETA0,CMU0,PD,PE,PF,PG)

```

PI=3.141592654

PD=(.5-1./PI*ASIN((-2.+ALPHA0-CMU0)/(ALPHA0+CMU0)))*100.

PE=(.5-1./PI*ASIN((2.*GAMA0+ALPHA0-CMU0)/(ALPHA0+CMU0)))*100.

PF=(.5-1./PI*ASIN((2.*DETA0+ALPHA0-CMU0)/(ALPHA0+CMU0)))*100.

PG=(.5-1./PI*ASIN((2.+ALPHA0-CMU0)/(ALPHA0+CMU0)))*100.

RETURN

END

C
C
C

SUBROUTINE BX(GROUPING OF SUBROUTINES)

1 SUBROUTINE BX(N,WW,XX,ALPHA0,BETA0,GAMA0,DETA0,SIGMA0,CMU0,
2 ENT1,ENT2,ENT3,ENT4,ENT5,ENT6,ENT7,B1,T,B2,D1,D2,S,
FA,FB,FC,FD,FE,FF,FF1,FF2,FF3,FF4,FF5,FF6)
DIMENSION WW(96),XX(96)

CALL Fx1(N,WW,XX,ALPHA0,BETA0,GAMA0,DETA0,SIGMA0,CMU0,ENT1)
CALL Fx2(N,WW,XX,ALPHA0,BETA0,GAMA0,DETA0,SIGMA0,CMU0,ENT2)
CALL Fx3(N,WW,XX,ALPHA0,BETA0,GAMA0,DETA0,SIGMA0,CMU0,ENT3)
CALL Fx4(N,WW,XX,ALPHA0,BETA0,GAMA0,DETA0,SIGMA0,CMU0,ENT4)
CALL Fx5(N,WW,XX,ALPHA0,BETA0,GAMA0,DETA0,SIGMA0,CMU0,ENT5)
CALL Fx6(N,WW,XX,ALPHA0,BETA0,GAMA0,DETA0,SIGMA0,CMU0,ENT6)
CALL Fx7(N,WW,XX,ALPHA0,BETA0,GAMA0,DETA0,SIGMA0,CMU0,ENT7)

FA=ENT2/ENT1
FB=ENT3/ENT1
FC=ENT4/ENT1
FD=ENT5/ENT1
FE=ENT6/ENT1
FF=ENT7/ENT1

FF1=(S/T)-FA
FF2=(B2/T)-0.5-FB
FF3=(D2/T)-FC
FF4=(S/T)-FD
FF5=(B1/T)-0.5-FE
FF6=(D1/T)-FF

RETURN

END

C

SUBROUTINE Fx1

1 SUBROUTINE Fx1(N,WW,XX,ALPHA0,BETA0,GAMA0,DETA0,SIGMA0,
CMU0,ENT1)
DIMENSION WW(96),XX(96)

SUM=0
DO I=1,N
U=XX(I)
Y=(U+1.)/2.*SQRT(DETA0-GAMA0)
F1N=(Y**2.)*(SQRT((BETA0+GAMA0+Y**2.)*(DETA0-GAMA0-Y**2.))
1 *(SIGMA0-GAMA0-Y**2.))
F1D=SQRT((ALPHA0+GAMA0+Y**2.)*(CMU0-GAMA0-Y**2.))*
1 (1.+GAMA0+Y**2.)*(1.-GAMA0-Y**2.))

F1=F1N/F1D

SUM=SUM+WW(I)*F1

ENDDO

ENT1=SUM*SQRT(DETA0-GAMA0)

RETURN

END

!

SUBROUTINE Fx2

SUBROUTINE Fx2(N,WW,XX,ALPHA0,BETA0,GAMA0,DETA0,SIGMA0,

1 CMU0,ENT2)

DIMENSION WW(96),XX(96)

SUM=0

DO I=1,N

U=XX(I)

Y=(U+1.)/2.*SQRT(1.-DETA0)

F2N=SQRT((1.-Y**2.-GAMA0)*(BETA0+1.-Y**2.)

1 *(1.-DETA0-Y**2.)*(SIGMA0-1.+Y**2.))

F2D=SQRT((2.-Y**2.)*(ALPHA0+1.-Y**2.)*(CMU0-1.+Y**2.))

F2=F2N/F2D

SUM=SUM+WW(I)*F2

ENDDO

ENT2=SUM*SQRT(1.-DETA0)

RETURN

END

!

SUBROUTINE Fx3

SUBROUTINE Fx3(N,WW,XX,ALPHA0,BETA0,GAMA0,DETA0,SIGMA0,

1 CMU0,ENT3)

DIMENSION WW(96),XX(96)

SUM=0

DO I=1,N

U=XX(I)

Y=(U+1.)/2.*SQRT(SIGMA0-1.)

F3N=SQRT((BETA0+Y**2.+1.)*(1.-GAMA0+Y**2.)*(1.-DETA0+Y**2.)*

1 (SIGMA0-1.-Y**2.))

F3D=SQRT((ALPHA0+Y**2.+1.)*(CMU0-Y**2.-1.)*

1 (2.+Y**2.))

F3=F3N/F3D

SUM=SUM+WW(I)*F3

ENDDO

ENT3=SUM*SQRT(SIGMA0-1.)

RETURN

END

!

SUBROUTINE Fx4

SUBROUTINE Fx4(N,WW,XX,ALPHA0,BETA0,GAMA0,DETA0,SIGMA0,

1 CMU0,ENT4)

DIMENSION WW(96),XX(96)

SUM=0

DO I=1,N

```

      U=XX(I)
      Y=(U+1.)/2.*SQRT(CMU0-SIGMA0)

      F4N=(Y**2.)*(SQRT((BETA0+SIGMA0+Y**2.)*(SIGMA0-GAMA0+Y**2.)
1      *(SIGMA0-DETA0+Y**2.)))

      F4D=SQRT((ALPHA0+SIGMA0+Y**2.)*(CMU0-SIGMA0-Y**2.)*
1      (SIGMA0+Y**2.+1.)*(SIGMA0+Y**2.-1.))
      F4=F4N/F4D
      SUM=SUM+WW(I)*F4
      ENDDO
      ENT4=SUM*SQRT(CMU0-SIGMA0)
      RETURN
      END

!      SUBROUTINE Fx5
      SUBROUTINE Fx5(N,WW,XX,ALPHA0,BETA0,GAMA0,DETA0,SIGMA0,
1      CMU0,ENT5)
      DIMENSION WW(96),XX(96)
      SUM=0
      DO I=1,N
      U=XX(I)
      Y=(U+1.)/2.*SQRT(1.+GAMA0)
      F5N=SQRT((BETA0-1.+Y**2.)*(GAMA0+1.-Y**2.)
1      *(DETA0+1.-Y**2.)*(SIGMA0+1.-Y**2.))

      F5D=SQRT((ALPHA0-1.+Y**2.)*(2.-Y**2.)*
1      (CMU0+1.-Y**2.))
      F5=F5N/F5D
      SUM=SUM+WW(I)*F5
      ENDDO
      ENT5=SUM*SQRT(1.+GAMA0)
      RETURN
      END

!      SUBROUTINE Fx6
      SUBROUTINE Fx6(N,WW,XX,ALPHA0,BETA0,GAMA0,DETA0,SIGMA0,
1      CMU0,ENT6)
      DIMENSION WW(96),XX(96)
      SUM=0
      DO I=1,N
      U=XX(I)
      Y=(U+1.)/2.*SQRT(BETA0-1.)

      F6N=(SQRT((BETA0-1.-Y**2.)*(GAMA0+1.+Y**2.)
1      *(DETA0+1.+Y**2.)*(SIGMA0+1.+Y**2.)))

      F6D=SQRT((ALPHA0-1.-Y**2.)*(2.+Y**2.)*
1      (CMU0+1.+Y**2.))

      F6=F6N/F6D
      SUM=SUM+WW(I)*F6

      ENDDO
      ENT6=SUM*SQRT(BETA0-1.)
      RETURN
      END
!      SUBROUTINE Fx7

      SUBROUTINE Fx7(N,WW,XX,ALPHA0,BETA0,GAMA0,DETA0,SIGMA0,

```

```

1      CMU0,ENT7)
      DIMENSION WW(96),XX(96)
      SUM=0
      DO I=1,N

          U=XX(I)
          Y=(U+1.)/.2.*SQRT(ALPHA0-BETA0)

          F7N=(Y**2.)*(SQRT(((GAMA0+BETA0+Y**2.)*(DETA0+BETA0+Y**2.)
1      *(SIGMA0+BETA0+Y**2.)))

          F7D=SQRT((ALPHA0-BETA0-Y**2.)*(BETA0+Y**2.+1.)*
1      (BETA0+Y**2.-1.)*(CMU0+BETA0+Y**2.))

          F7=F7N/F7D
          SUM=SUM+WW(I)*F7
          ENDDO
          ENT7=SUM*SQRT(ALPHA0-BETA0)
          WRITE(3,*)'ENT7=',ENT7
          RETURN
      END

```

Sample Out Put

```

B1   T   B2   D1  D2   S
27.000 3.000 3.000 .200 1.200 1.000

```

INITIALLY GUESSED VALUES

```

ALPHA0 BETA0 GAMA0 DETA0 SIGMA0 MU0
1.250   1.100 .100   .250   1.100   1.200

```

NUMBER OF ITERATIONS = 12

VALUES OF THE FUNCTIONS AFTER ITERATIONS

```

.0000 .0000 .0000 .0000 .0000 .0000

```

Final Values Computed

```

ALPHA  BETA  GAMA  DETA  SIGMA  MU
8.7637 8.7237 -.7795 .7445  1.3562 1.5593

```

Value of ENT1= 9.260363E-01

RESULTS

```

B/T  B/S  B/D1  B/D2
10.00 30.00 150.00 25.00

```

```

B1/B  B2/B  PD%  PE%    PF%  PG%
.90 .10  33.18 31.58 18.13 14.96

```

*****END OF RESULTS*****

REFERENCES

1. Khosla.R.B.A.N.,Bose.N.K., Taylor.E.Mck,"Design of Weirs on Permeable Foundations"CBIP, India, Publication No.12.(1962)
2. William .H.P., William.T.V., Saul.A.T., brain.C.F."Numerical Recipes in FORTRAN, The art of science computing",Cmbridge University Press (1933).,pp-372.
3. Harr.M.E.,"Ground Water and Seepage"McGraw-Hill Book Company (1962).
4. Garg N.K.,Bhagat S.K.,Asthana B.N.,"optimum Barrage Design based on Sub-surface Flow Considerations", Journal of Irrigation and Drainage Engineering,ASCE(July/Aug.2002).pp-253
5. Polubarinova-Kochina P.Ya.,"Theory of Ground Water Movement",Princeton University Press (1962).pp-(93-105)
6. Leliavsky S., "Irrigation and Hydraulic Design", Vol.I,Chapman & Hall Ltd,London (1959).pp-90
7. Byrd Paul F., Friedman Morris D.,"Hand Book of Elliptic Integrals for Engineers and Scientists" Spriger-Verlag,Newyork (1971)
8. Bowman F. "Introduction to Elliptic Functions", English University Press London(1953).
9. Kavier C."Fortran 77 and Numerical Methods"